5-1-2009

Role of MMPs and TIMP-3 in neuronal death and white matter injury following transient global ischemia.

Espen Walker

Espen Jacob Walker
Candidate

Biomedical Sciences
Department

This dissertation is approved, and it is acceptable in quality and form for publication:

Approved by the Dissertation Committee:

Dr. Gary Rosenberg, MD, Chairperson

Dr. LeeAnna Cunningham, PhD

Dr. Oscar Bizzozero, PhD

Dr. R. Ross Reichard, MD

ROLE OF MMPS AND TIMP-3 IN NEURONAL DEATH AND WHITE MATTER INJURY FOLLOWING TRANSIENT GLOBAL ISCHEMIA

BY

ESPEN JACOB WALKER

B.A. Psychobiology, University of California, Santa Cruz, 1999

DISSERTATION

Submitted in Partial Fulfillment of the
Requirements for the Degree of

Doctor of Philosophy
Biomedical Sciences

The University of New Mexico
Albuquerque, New Mexico

May, 2009

●●●●●○○○○○●●●●●

For my wife, Katherine, with her continuous support

and

For my father, Lawrence, with guidance on the path of science

●●●●●○○○○○●●●●●

Acknowledgements

I would like to express my sincere gratitude to my advisor, Dr. Gary Rosenberg for his ideas, guidance, and support during our work together. His excitement about the potential application of this research has kept me going. I would also like to thank my committee including Dr. LeeAnna Cunningham, Dr. Oscar Bizzozero, and Dr. Ross Reichard for their perspective and input on this project. It was essential to get various viewpoints throughout this process to help guide me towards a broader understanding of science.

I want to thank Jeffrey Thompson for his daily support and training in the lab. Having him there to teach me, exchange ideas, and help with experiments has been very important in completion of this work. I am thankful for the assistance of Dr. Eduardo Candelario-Jalil in training me on various technical lab assays, helping me with writing, and his extensive input on what experiment would best help answer the questions that came up. Eduardo Estrada was very helpful in training me in surgical techniques that have proven to be invaluable skills. His knowledge of physiology has been very useful. Dr. Yi Yang's expertise in immunological analysis of cells and molecular analysis of cellular proteins has been very helpful in my scientific training. I would like to thank Dr. Mark Grossetete for his daily exchanges on experimental planning and his good nature, bringing some humor into the lab.

The Departments of Neurology and Neurosciences have been essential in providing support throughout this process and I am grateful to all who have assisted me. I would like to thank the Biomedical Sciences Graduate Program for all of the education and training that has helped me become a critical scientist. I am thankful for the Biomedical Sciences Student Society for facilitating fun interactions and discussions between students of all departments.

Finally, I would like to express immense gratitude to my wife, Katherine, my son, Finn, and my daughter, Siri for their complete dedication and support throughout this process. This would not have been possible without their understanding, patience, and love.

ROLE OF MMPS AND TIMP-3 IN NEURONAL DEATH AND WHITE MATTER INJURY FOLLOWING TRANSIENT GLOBAL ISCHEMIA

BY

ESPEN JACOB WALKER

ABSTRACT OF DISSERTATION

Submitted in Partial Fulfillment of the
Requirements for the Degree of

Doctor of Philosophy
Biomedical Sciences

The University of New Mexico
Albuquerque, New Mexico

May, 2009

ROLE OF MMPs AND TIMP-3 IN NEURONAL DEATH AND WHITE MATTER INJURY FOLLOWING TRANSIENT GLOBAL ISCHEMIA

by
Espen Jacob Walker

B.A. Psychobiology, University of California, Santa Cruz, 1999
Ph.D. Biomedical Sciences, University of New Mexico, 2009

ABSTRACT

Transient global ischemia to the mouse results in hypoxic hypoperfusion to the brain and can lead to regional vulnerability, inflammation, and cell death. Characterization of this model with varying occlusion and reperfusion times allowed us to provide evidence for a consistent injury to the hippocampus and white matter regions of the brain. Following 30 minutes of bilateral carotid artery occlusion (BCAO) and 7 days of reperfusion, hippocampal injury to the CA2 region was consistently identified with neuronal loss and fluorojade positive cells. Three days following reperfusion, white matter injury was demonstrated by increased astrocyte reactivity and oligodendrocyte loss. With a consistent reduction in blood flow following BCAO and reliable cell loss, we confirmed this model for further investigation.

In the hippocampus, we provide evidence for increased reactivity of astrocytes and microglia. With tissue inhibitor of metalloproteinase-3 (TIMP-3) expression in the astrocytes, we demonstrate a role for TIMP-3 in delayed neuronal death using a *Timp-3* knockout (T3KO) mouse following 7 days of reperfusion. The increased activity of tumor necrosis factor (TNFα) activating enzyme (TACE) at 3 days correlated with reduced expression of the death receptor TNFR1 on the surface of the T3KO mouse neurons, leading to neuronal protection. Increased matrix metalloproteinase-3 (MMP-3) activity was observed and neuronal stereology in the CA2 region shows neuronal protection in

the *Mmp-3* KO mice. Increased reactive microglia and TNFα expression in the *Mmp-3* WT was also observed. Delayed treatment with the broad-spectrum MMP inhibitor BB-94 led to neuronal protection in both the T3WT and T3KO mice, implicating TIMP-3 and MMP independent mechanisms of neuronal injury following global ischemia.

The white matter has also shown sensitivity to global ischemia and reperfusion. To quantify oligodendrocyte (OLG) cell loss we have developed a method using a combination of morphology and immunohistochemistry to identify oligodendrocytes and apply it towards ischemic injury. We provide evidence for increased reactivity of astrocytes and microglia, with MMP-2 expression in the astrocytes. MMP-2 protein is increased at 1 day of reperfusion, with MMP-2 activity occurring at 3 days of reperfusion. This timing correlated with a breakdown in myelin basic protein (MBP). OLG loss also occurred at 3 days of reperfusion along with increased caspase-3 expression in the white matter. Treatment with BB-94 led to reduced astrocyte reactivity, less MMP-2 activity, and reduced MBP loss. Drug treatment did not result in changes in OLG loss or caspase-3 expression. These findings suggest a role for MMPs in the loss of myelin, with OLG loss occurring by an MMP-independent mechanism.

We provide evidence of a role for TIMP-3 and MMP-3 in delayed neuronal loss as well as a potential role for MMP-2 in myelin degradation, but not OLG loss. We were able to inhibit the detrimental effect of these MMPs with BB-94 following BCAO induced global ischemia. With varying timelines of injury to the gray and white matter, it appears MMPs have cell specific expression that leads to regional sensitivity. Further investigation into the use of MMP inhibitors may allow for potential therapeutic uses as we investigate these delayed mechanisms of injury to the brain.

TABLE OF CONTENTS

LIST OF FIGURES and TABLE

CHAPTER 1:

Introduction and Literature Review

1.1 Global Ischemia

Global ischemia is the reduction in blood flow to the brain through the occlusion or blockage of the arterial blood supply. This results in delayed cell death to both the gray and white matter. Global ischemia is one of the many types of vascular injuries classified as stroke. Stroke is the third leading cause of death in the Western world (Lo, et al., 2003). With millions of people dying each year, and a growing number of survivors with severe disabilities as a result of the various types of stroke, working towards a better understanding of the cell death mechanisms involved with this injury is a worthwhile effort.

Strokes are classified as thrombotic, embolic, or hemorrhagic. Occlusion or hemorrhage of blood vessels supplying the brain can occur from a blocked single blood vessel which causes focal ischemia or a global restriction in blood flow as occurs during cardiac arrest, near-drowning, or hypotension during a surgical procedure (Back, et al., 2004, Harukuni and Bhardwaj, 2006, Lo, et al., 2003). Both types of blood flow restriction result in the death of brain cells. Transient global ischemia is a model to represent cardiac arrest or other temporary restrictions in blood flow. Much work has been done with the focal ischemia model of vessel occlusion, but less is known about global ischemia and the delayed mechanisms of cell death that occur following this injury. With cardiac arrest

leading to many types of potential brain injuries, it is essential to get a better understanding of the mechanisms of cell death that occur.

Global ischemia leads to delayed injury of the rodent hippocampus with neuronal death to the CA1 and CA2 regions occurring at 3 to 5 days (Oguro, et al., 2001). The oligodendrocytes, making up the myelin sheath in the white matter, also have delayed cell death (Tomimoto, et al., 2003). The mechanism of cell death in each of these brain regions has not yet been determined.

With an insult that leads to an injury mechanism representative of apoptosis, not necrosis (Back, et al., 2004, Bottiger, et al., 1998), the delayed injury and cell death following global ischemia and reperfusion becomes more pronounced days after the initial insult (Bottiger, et al., 1998, Harukuni and Bhardwaj, 2006). The white matter appears to be affected first, with glial activation and oligodendrocyte death following 3 days of reperfusion, and hippocampal death occurring at 7 days of reperfusion.

1.2 White and Gray Matter Injury

Certain areas of the brain, such as the CA1 and CA2 regions of the hippocampus, are more vulnerable to transient global ischemia in the mouse (Kelly, et al., 2001, Lee, et al., 2004, Magnoni, et al., 2004) The pyramidal neurons of the hippocampus are easily distinguished and have long been identified as a region with high sensitivity to ischemia (Pulsinelli, 1985, Yang, et al., 1997). A majority of the studies on global ischemia have

focused on death mechanisms occurring in the hippocampus and have shown delayed damage to these neurons (Kelly, et al., 2001, Lee, et al., 2004, Magnoni, et al., 2004, Oguro, et al., 2001, Zalewska, et al., 2002). However, the mechanism of this delayed damage is not completely understood.

Strokes restricted to the white matter have been identified as a major class of neurological injury, comprising 25% of strokes seen clinically (Petty and Wettstein, 1999). The white matter is sensitive to global ischemia, leading to degenerative changes similar to what occurs in the elderly population with cognitive impairments, gait disorders, and vascular dementia. The mouse model of transient global ischemia also shows injury to the white matter, represented by reactive gliosis (Magnoni, et al., 2004).

The cell population in the white matter is different than the gray matter; consisting of fibrous astrocytes, oligodendrocytes, microglia, and the myelinated axons of neurons. The pyramidal neurons of the hippocampus are surrounded by other cell types, such as astrocytes and microglia that may be involved in their survival or death. With different vascular supply, cell types, proteins, and enzymes, the white and gray matter display different patterns of delayed cell death. Understanding the different ways in which these cell populations are affected by an ischemic insult will help target therapeutics to the right region and timeframe.

1.3 Rodent Models of Global Ischemia

There are various models of global ischemia, representing different clinical injuries. Some of the more commonly studied models of global ischemia include the transient bilateral common carotid artery occlusion in the gerbil (Zalewska, et al., 2002), the permanent carotid occlusion in the rat (Schmidt-Kastner, et al., 2005), and the transient carotid occlusion in the mouse (Kelly, et al., 2001). Each of these models has their own distinct characteristic, and all are referred to as global ischemia (Ginsberg and Busto, 1989, Traystman, 2003).

Bilateral Carotid Artery Occlusion (BCAO) is the rodent surgery model more commonly used to represent global ischemia. In the rat, a permanent occlusion of both common carotid arteries leads to delayed cell death in the hippocampus at 3 days (Sugawara, et al., 2002) and white matter injury that increases up to 30 days (Farkas, et al., 2004, Lee, et al., 2006, Masumura, et al., 2001, Wakita, et al., 2002). Another model in the rat involves electro-coagulation of the vertebral arteries and clamps on both carotid arteries for 20 minutes (Pulsinelli and Brierley, 1979). This leads to glial reactivity and CA1 hippocampal injury 3 days after injury (Rivera, et al., 2002).

With increasing prevalence of mouse knockouts for gene-specific analysis, a mouse model of global ischemia has been developed. Isolation and occlusion of both common carotid arteries of the mouse for 10 to 40 minutes leads to reduced blood flow to the brain, as may occur in cardiac arrest or carotid stenosis. Although there have been various times of occlusion and reperfusion, a consistent injury to the CA1 region of the

hippocampus is seen (Kelly, et al., 2001, Lee, et al., 2004). In addition, glial reactivity and white matter damage occurs (Magnoni, et al., 2004). Various reperfusion times have also led to different time points of injury, with some groups demonstrating hippocampal injury at 3 days (Lee, et al., 2004) , with others showing that it takes 7 days for neuronal injury to occur (Oguro, et al., 2001). Another model of global ischemia has used a microcoil to permanently reduce blood flow through the carotid arteries of the mouse and found white matter lesion formation (Nakaji, et al., 2006, Shibata, et al., 2004).

1.4 Matrix Metalloproteinases (MMPs) and their role in ischemic injury

MMPs are part of a family of zinc-dependent metalloproteinases called metazincins that require activation through cleavage of the propeptide domain. They are involved in extracellular matrix (ECM) breakdown, death receptor cleavage and angiogenesis (Cauwe, et al., 2007, Nagase, 1997). The current 24 members of the MMPs are classified as to their substrate specificity and organized into subgroups that include gelatinases, stromelysins, collagenases, membrane-type (MT)-MMPs, and 'other MMPs' (Nagase and Woessner, 1999, Yong, 2005, Yong, et al., 2001). Another group of enzymes falls within the more general heading of metalloproteinases. These are proteins with a disintegrin and metalloproteinase (ADAM). There are several identified ADAMS, but for only a few has a role in the brain been identified (Rosenberg, 2009). One of these, ADAM-17, or TNFα converting enzyme (TACE), is involved in regulation of cell surface death receptors and ligands (Gearing, et al., 1994). MMPs are involved in ECM degradation (Gu, et al., 2002), myelin basic protein (MBP) degradation (Chandler, et al., 1995), cleavage and

activation of other MMPs, as well as shedding of death receptor ligands, such as FasL (Wetzel, et al., 2003).

MMPs are rapidly up regulated after cerebral ischemia in rats, mice, nonhuman primates, and humans. They are involved in both injury and survival pathways (Cunningham, et al., 2005, Rosenberg, 2002). Stromelysin (MMP-3) is involved in inhibition of apoptotic cell death through cleavage of FasL (Wetzel, et al., 2004), as well as blood brain barrier (BBB) breakdown and inflammatory mechanisms (Gurney, et al., 2006, Kim, et al., 2005). Gelatinase A (MMP-2) causes degradation of myelin basic protein (MBP) and basal lamina in white matter during ischemia (Asahi, et al., 2001, Chandler, et al., 1995). Increased MMP-9 expression during global ischemia has been shown to lead to increased neuronal death via disruption of the ECM, resulting in anoikis-like cell death (Gu, et al., 2002, Lee, et al., 2004).

Matrix metalloproteinases (MMPs) are known to have both detrimental and beneficial roles at various time points following ischemic events: MMP-9 has been shown to be involved in neuronal injury, while MMP-3 may lead to either neuronal survival or injury, and MMP-2 appears to play a role in white matter damage. MMPs have emerged as players in various injury mechanisms to the brain, including multiple sclerosis (MS) (Rosenberg, 2002) and neurodegenerative mechanisms (Rosenberg, 2009). However, the role for MMPs in repair pathways such as myelin formation (Larsen, et al., 2006) and angiogenesis (Zhao, et al., 2006) cannot be overlooked. Getting a better understanding of

the role for MMPs in the injury and repair pathways (Yong, 2005) in the central nervous system (CNS) will allow us to develop therapeutics to target their modulation.

1.5 Tissue Inhibitors of Metalloproteinases (TIMPs)

MMPs are inhibited by tissue inhibitors of metalloproteinases (TIMPs). There are currently 4 known TIMPs (TIMPs 1-4). TIMPs inhibit the active forms of MMPs through high affinity, non-covalent binding of the MMP catalytic domain (Brew, et al., 2000). TIMP-3 appears to have many roles in ischemic cell death through inhibition of membrane-type MMP (MT-MMP), MMP-2, MMP-3, and MMP-9 (Wallace, et al., 2002, Wetzel, et al., 2003, Will, et al., 1996). By inhibiting the sheddase activity of MMP-3 in vivo, TIMP-3 allows FasL to remain on the cell surface and apoptosis results. This has been shown in various models including doxorubicin-induced injury *in vitro* (Wetzel, et al., 2003, Wetzel, et al., 2004), as well as OGD models in cell culture and mild ischemia in the TIMP-3 KO mouse (Wetzel, et al., 2007). Each of these studies supports the role for TIMP-3 in neuronal death.

TIMP-3 also inhibits another sheddase, TACE. TACE is involved in cleavage of tumor necrosis factor α receptor-1 (TNFR-1). With increased TACE activity, TNFR1 is removed from the cell surface and there is a reduction in apoptotic death. Upon inhibition of TACE by TIMP-3, TNFR1 is stabilized and there is increased cell death (Smith, et al., 1997, Smookler, et al., 2006). However, TACE also cleaves latent TNFα from the cell surface to produce active TNFα. The active TNFα can then bind to TNFR1, promoting

apoptosis (Rosenberg, 2009). With the various potential effects of TACE inhibition, further studies of TIMP-3 in disorders of the CNS are warranted.

TIMP-3 also inhibits the gelatinases MMP-2 and MMP-9, which have been shown to play a role in cell death and ECM disruption following ischemia (Gu, et al., 2002, Lee, et al., 2004, Magnoni, et al., 2004). Reducing the activation of MMP-2 and MMP-9 (via MT-MMP and MMP-3 inhibition, respectively), myelin basic protein remains intact and there is a reduction in cell death following ischemia (Asahi, et al., 2001). In this pathway it would seem TIMP-3 plays a role in cell survival. TIMP-3 seems to have a variety of roles following cerebral ischemia, which may include both cell death and survival (Fig. 1.1). By looking at the role of this enzyme inhibitor more closely, its role in ischemic cell death may be better understood.

1.6 Pharmacological MMP Inhibition

As MMPs appear to play a role in cell death and survival pathways following ischemia, MMP inhibitors have been considered for use in therapeutic applications. Testing these in rodent models has shown some promise, but the diverse role of MMPs at different times after ischemia has made it difficult to determine the optimal time to administer these drugs. Use of a broad-spectrum MMP inhibitor, BB-94, reduced hippocampal neuronal cell death 3 days following reperfusion from global ischemia (Lee, et al., 2004), this was proposed to be due to MMP-9 inhibition. Another drug, quercetin, decreased neuronal damage at 3 days following global ischemia through MMP inhibition (Cho, et al., 2006).

As quercetin has anti-inflammatory effects, neuronal protection could also have been due to reduced inflammation. An MMP-2 specific inhibitor, AG3340, reduced the amount of white matter lesions and activated astroglia in the rat model of permanent BCAO (Nakaji, et al., 2006).

However, there is evidence to support a beneficial role of MMPs in certain circumstances (Wetzel, et al., 2003). Inhibition of the beneficial effects, such as angiogenesis and neurogenesis, may cause increased injury (Larsen, et al., 2006, Oh, et al., 1999). In addition, the timeframe of administration of the MMP inhibitor may affect its role. One study started treatment with a broad-spectrum MMP inhibitor, FN-439 at 7 days following focal ischemic injury. By 14 days there was a reduction in MMP activity, decreased neurovascular remodeling, and increased ischemic brain injury compared to control treatment (Zhao, et al., 2006). This shows that MMPs may have a protective effect at later times after reperfusion compared to the early damaging effects.

There are many different models of cerebral ischemia, each with their own mechanism of insult and cascade of molecular effects. Transient global ischemia, especially in the white matter, has not been as extensively investigated as other models such as focal ischemia. However, there are significant clinical examples in the human which represent this type of insult, including cardiac arrest, sleep apnea, arteriosclerosis, and more. Metalloproteinases clearly play a role in some of the death pathways in this injury. Getting a better understanding of the endogenous inhibitors (TIMPs) that affect the activity of the MMPs following global ischemia will help researchers get a clearer picture

of the damage pathways in this injury. Testing the practical use and timing of when to administer exogenous MMP inhibitors will help clinicians plan when and how to use these drugs. Clarifying the distinct anatomical regions of the brain and how they respond to global ischemia will help researchers to map out the damage pathways and work towards developing therapeutic interventions in a regional and time dependent manner.

1.7 Specific Aims and Hypotheses

Specific Aim 1: Determine effect and mechanism of global ischemia on hippocampal neuronal injury.

Hypothesis: Global ischemia leads to delayed neuronal death in the hippocampus via metalloproteinase inhibition. With both TIMP-3 and MMP-3 involved in inflammation and ischemic injury, there will be decreased inflammation and neuronal death in both the *Timp-3* and *Mmp-3* knockout mice.

- Aim 1a: Investigate timeline and location of hippocampal injury
- Aim 1b: Determine role of TIMP-3 in delayed neuronal death
- Aim 1c: Analyze contribution of MMP-3 in delayed hippocampal injury
- Aim 1d: Measure effect of MMP inhibitor in hippocampal cell death

Specific Aim 2: Determine effect and mechanism of global ischemia on oligodendrocyte injury and myelin breakdown.

Hypothesis: Global ischemia leads to delayed oligodendrocyte death and myelin breakdown via metalloproteinase activity. Oligodendrocyte death and myelin damage will be decreased following MMP inhibition.

- Aim 2a: Investigate effect of global ischemia on delayed oligodendrocyte death
- Aim 2b: Determine mechanism and timeline of myelin breakdown
- Aim 2c: Measure effect of MMP inhibitor on oligodendrocyte death and myelin breakdown

1.8 Animal Studies

The use of the mouse to investigate global cerebral ischemia is crucial to understanding the mechanism of injury in a whole organism. Use of an *in vitro* model would not show the interactions of all proteins and enzymes responsible for this damage. The C57BL/6 mouse was chosen for the ability to knockout certain genes to understand how the animal reacts without a certain gene present. This strain is the background for many genetic knockouts. Previous studies have used these species and found them to be the most sensitive to BCAO induced injury. The use of animals has been approved by the Office of Animal Care and Compliance, Protocol #06HSC009, and conforms to NIH guidelines for animal research. All animals will be housed in the Animal Care Facility and will receive veterinary care as necessary. Animal number has been kept to a minimum with extensive data being collected from each mouse.

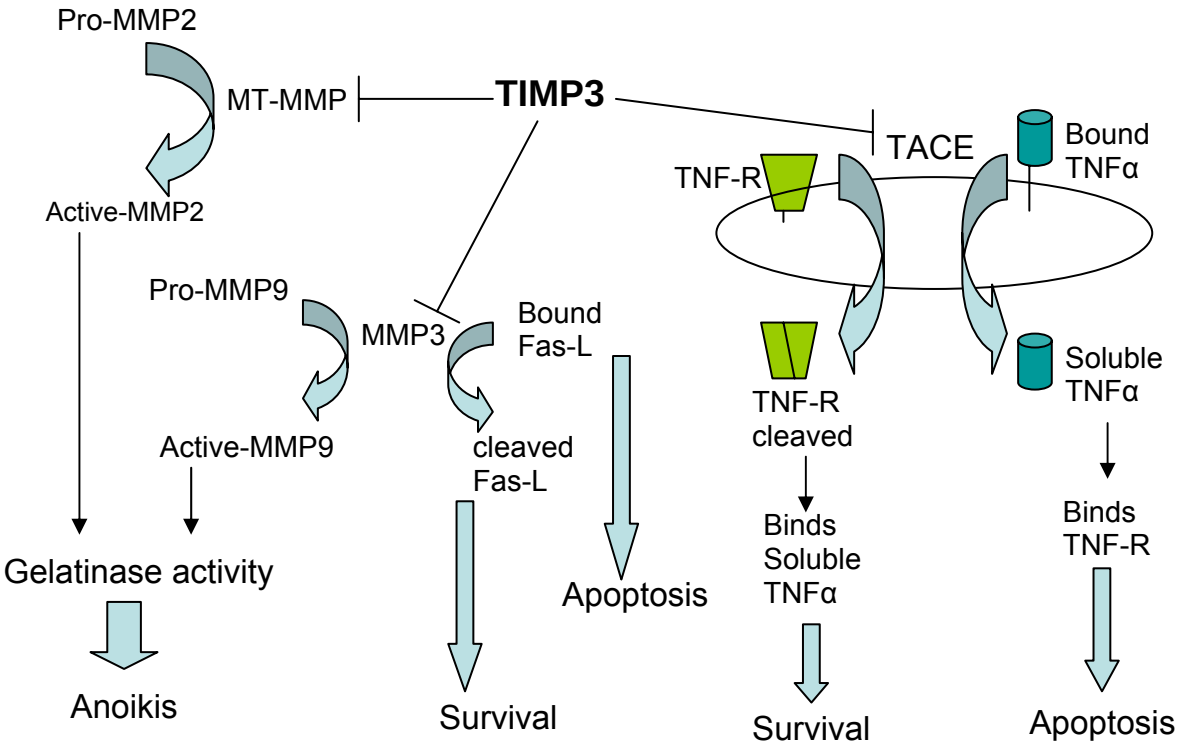

Figure 1.1: Potential TIMP-3 pathways of cell death and survival.

CHAPTER 2:

BCAO Mouse Model Development

2.1 Abstract

Global ischemia is an emerging model of cerebral injury that represents injuries such as cardiac arrest, near-drowning, or hypotension following surgery. With various representations of global ischemia in different types of animals we chose to develop the mouse model of transient global ischemia in order to utilize knockout mice and better represent brain injury following an acute reduction in cerebral blood flow. Our data describes patent blood vessels and 11.2% original blood flow following occlusion of both common carotid arteries. Times tested include 12, 18, and 30 minutes of occlusion with 1, 3, 7, and 30 days of reperfusion. Bilateral common carotid artery occlusion (BCAO) for 30 minutes led to oligodendrocyte loss from 1-3 days and neuronal loss at 7 days of reperfusion. Astrocytes became reactive at 3 days of reperfusion and 30 minutes of occlusion. We conclude that 30 minutes of BCAO, followed by reperfusions from 3-7 days leads to a consistent injury to both the gray and white matter in the brain.

2.2 Introduction

Much of the work done in cerebral ischemia has been done using the middle cerebral artery occlusion (MCAO) model to produce a focal ischemic insult. However, the global model of transient ischemia is less well understood. With a mechanism of injury differing from the focal model, including minimal BBB opening and decreased inflammation, the

bilateral carotid artery occlusion (BCAO) may be a good model to isolate injury to certain areas and cell types, such as the hippocampus (Kelly, et al., 2001) or white matter (Tomimoto, et al., 2003). While there is preliminary data on the mechanism of neuronal death, the death mechanism of cell types of the white matter, such as astrocytes and oligodendrocytes also need further investigation.

The majority of the experiments performed using the BCAO have been done with the rat (Farkas, et al., 2004, Tomimoto, et al., 2003). While the rat is a good model to perform immunohistochemistry and other techniques requiring a larger brain, such as imaging with MRI, the mouse model provides the opportunity to use genetic knockouts to isolate mechanisms of damage. We were interested in the role of TIMP-3 and MMP-3 in delayed cell death and could study the knockout mice available in the University of New Mexico Animal Facility.

Correlating an animal model with a human injury is ideal when attempting to create treatments for humans. Global ischemia has been shown to be a model of cardiac arrest or hypotension following surgery (Back, et al., 2004, Harukuni and Bhardwaj, 2006). These episodes of blood flow reduction to the brain lead to behavioral deficits such as vascular dementia or vascular cognitive impairment (VCI). With a current human study of MMP expression changes in the cerebrospinal fluid (CSF) of VCI patients occurring in the Rosenberg lab, the need for an animal model was desired.

2.3 Materials and Methods

Transient Global Cerebral Ischemia

All experiments were approved by the University of New Mexico (UNM) Animal Care Committee and conformed to the National Institutes of Health Guide for the Care and Use of Animals in research. Transient bilateral common carotid artery occlusion (BCAO) was conducted on the C57BL/6 mouse. The animals were anesthetized in an incubation chamber via 2% isoflurane by inhalation and injected with 0.1 mg/kg of analgesic (buprenorphine) IP with animal temperature constantly maintained. The skull was exposed and cerebral blood flow measured with a Laser Doppler blood flow monitor (Moore Instruments Limited, Devon, UK) 3 mm caudal and 3 mm lateral to Bregma. Both common carotid arteries were exposed, isolated, and clipped with metal aneurysm clips for 12, 18, or 30 minutes to determine optimal occlusion time. Animals were allowed to recover in their cage for 1-2 hours with a heating lamp. Following reperfusion, the animals were anaesthetized with 2% isoflurane by inhalation and injected IP with 30 mg/kg of sodium pentobarbital at 3, 7, or 30 days. Perfusion with PBS/0.1% Procaine followed by 2% PLP (2% paraformaldehyde, 0.1 M sodium periodate, 0.075 M lysine in 100 mM phosphate buffer at pH 7.4) was conducted intracardially. Brains were removed and immersed in 2% PLP overnight. The brains were cryoprotected with 30% sucrose in PBS, and frozen in OCT. They were stored at -80^{o} C until sectioned.

Cresyl Violet and Fluorojade Staining

To assess neuronal injury following transient global ischemia, 20 μm sections taken every 100 μm were rehydrated through alcohols, rinsed in PBS and water, and stained

with cresyl violet acetate (CVA). Slides were rinsed in tap water, dehydrated through alcohols and xylene, then coverslipped using DPX (Sigma-Aldrich). Fluoro-Jade C staining (HistoChem Inc., Jefferson, AZ) of 10 μm sections was performed per company protocol.

Immunohistochemistry (IHC)

For fluorescence IHC, 10 μm sections were rehydrated through alcohols and PBS containing 0.1% Tween-20 (PBT). Nonspecific binding sites were blocked with PBT containing 1% bovine serum albumin (BSA), and 5% normal serum. Slides were incubated overnight at 4°C with primary antibodies. Slides were washed in PBT and incubated for 90 min at room temperature with secondary antibodies conjugated with Cy-3. All IHC slides were viewed on an Olympus BX-51 bright field and fluorescence microscope (Olympus America Inc., Center Valley, PA) equipped with an Optronics digital camera and Picture Frame image capture software (Optronics, Goleta, CA). The antibody used for IHC was glial fibrillary acidic protein (GFAP) for astrocytes (1:400; Sigma-Aldrich, St. Louis, MO).

Oligodendrocyte Stereology

Oligodendrocytes were identified morphologically and counted with stereology according to the method described in detail in Chapter 4.

2.4 Results

Cerebral Vasculature and Blood Flow

Initial studies were performed to confirm blood flow reduction following occlusion of both common carotid arteries. Cerebral blood flow was measured over the exposed skull with a Laser Doppler blood flow monitor before, during, and following carotid occlusion with 11.2 +/- 1.1% of original flow during the occlusion period, and flow returning to 44.9 +/- 6.3% following clip removal (n=30) (Fig. 2.1). In addition, India Ink staining of mouse blood vessels by Eduardo Estrada showed no qualitative differences between TIMP-3 WT and TIMP-3 KO mice, as well as the MMP-3 WT and MMP-3 KO mice. With patent blood vessels and consistent blood flow reduction, we continued to pursue the model.

Timeline of Occlusion and Reperfusion

To determine the optimal time to measure cell death, a variety of occlusion and reperfusion time points were compared. The BCAO surgery was performed on the C57BL/6 mouse; showing neuronal damage at various time points and verifying the damage regions to be consistent with published data. The following time points were looked at: 12, 18, and 30 min occlusion with 1, 3, 7, and 30 days reperfusion. Sections were stained with cresyl violet (CV) and the pyramidal neurons of the hippocampus were visualized (Fig. 2.2). Damage specific to the CA2 region was consistent with published work (Magnoni, et al., 2004) with damage more apparent at 30 minutes of occlusion and longer periods of reperfusion. Focusing on the 30 minute occlusion time, we compared

hippocampal injury bilaterally. With CV positive cell loss in the CA1 and CA2 regions correlating with Fluorojade positive staining (Fig. 2.3), there was a consistent injury.

Astrocyte Reactivity

To characterize the injury to the cell types of the white matter, reactive astrocytes were stained for GFAP at various time points of occlusion and reperfusion (Fig. 2.4). This showed greater astrocytosis at 30 minutes of occlusion, peaking around 3 days of reperfusion. This indicates a temporal reactivity of the astrocytes in the corpus callosum and suggests a potential time point of reperfusion for further investigation.

Oligodendrocyte Loss Timeline

These qualitative data give a general idea of the timescale of damage that is occurring, but quantitation of cell death gives a more comprehensive result of what is happening in the BCAO model of ischemic white matter injury. Oligodendrocytes were stained using a comprehensive stain technique developed in our laboratory (see Chapter 4 for complete description). These preliminary findings showed oligodendrocyte cell loss in the external capsule at 1 and 3 days of reperfusion after an occlusion time of 30 min (Fig. 2.5). Cell death was not as extensive at 7 and 30 days of reperfusion or shorter occlusion times.

2.5 Discussion

Various ischemia models have been used to represent different components of stroke injury to the brain. Much of the work has focused on the focal ischemia model of

complete restriction of blood flow to a distinct region of the brain, representing ischemic stroke. With reduction in blood flow leading to various clinical injuries, a model for transient reduction in cerebral blood flow is warranted. Transient global ischemia in the mouse has been shown to lead to consistent injury to the hippocampus (Lee, et al., 2004) as well as glial reactivity (Magnoni, et al., 2004). However, the timing of occlusion and reperfusion has varied between labs (Kelly, et al., 2001, Oguro, et al., 2001), requiring us to perform our own investigation of this model.

Other models of global ischemia have provided some valuable insight into the mechanisms of brain injury following hypoxia. The rat model of permanent bilateral carotid occlusion describes a chronic hypoxic hypoperfusion with both hippocampal neuronal death (Farkas, et al., 2007), as well as white matter injury (Wakita, et al., 2002). In an attempt to model the permanent reduction of blood flow that occurs in the rat, a model of bilateral carotid artery stenosis (BCAS) was developed with a microcoil around the carotid arteries, permanently placed to reduce blood flow to the brain (Shibata, et al., 2004). This allowed for further investigations into mechanisms of chronic vessel disease (Nakaji, et al., 2006) and comparisons of the rat and mouse models.

In the transient model of mouse global ischemia there is earlier inflammation and cell death than the permanent models. With limited studies on the effect of this injury to the white matter, we needed to develop this model in our lab. Using the C57BL/6 mouse allowed us to continue these studies in the TIMP-3 KO mice which are housed in the UNM Animal Facility.

One concern that arose when developing this model was the consistency of the bilateral injury. Using various assays of injury, including fluorojade staining, GFAP immunohistochemistry, OLG and neuronal stereology, and blood flow analysis it was determined there were no overall differences between hemispheres. With bilateral occlusion of the carotid arteries, there was a bilateral injury in the mouse gray and white matter regions.

By analyzing occlusion times of 12, 18, and 30 minutes and reperfusion times of 1, 3, 7, and 30 days, we found consistent death in both the white and gray matter occurs following 30 minutes of occlusion. There appears to be different timing of cell type injury, with white matter injury occurring from 1-3 days, and neuronal injury following 7 days of reperfusion. In conclusion, the data collected supports the utility of the BCAO mouse model of transient global ischemia for further studies into the mechanisms of cell death to the gray and white matter of the brain.

2.6 Figures and Legends

A

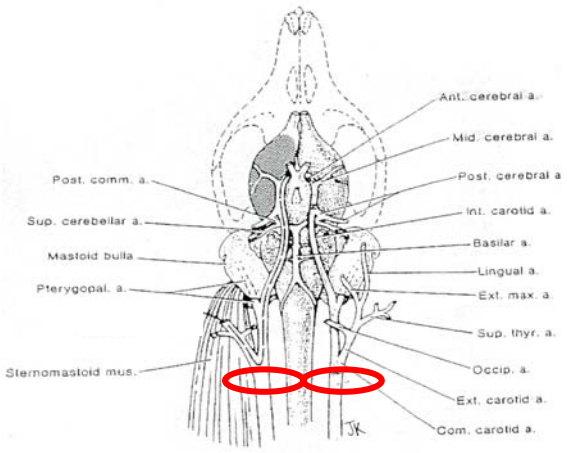

B

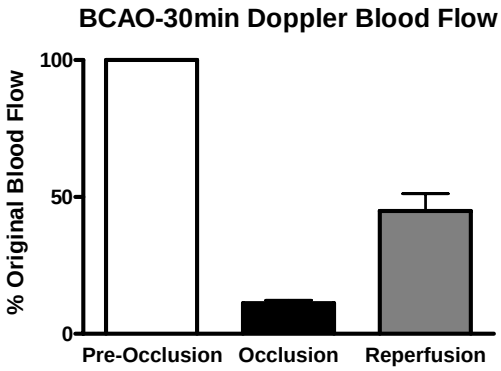

Figure 2.1: Bilateral Carotid Artery Occlusion (BCAO) vessel description and blood flow monitoring. Results given as percentage of original blood flow (n=30).

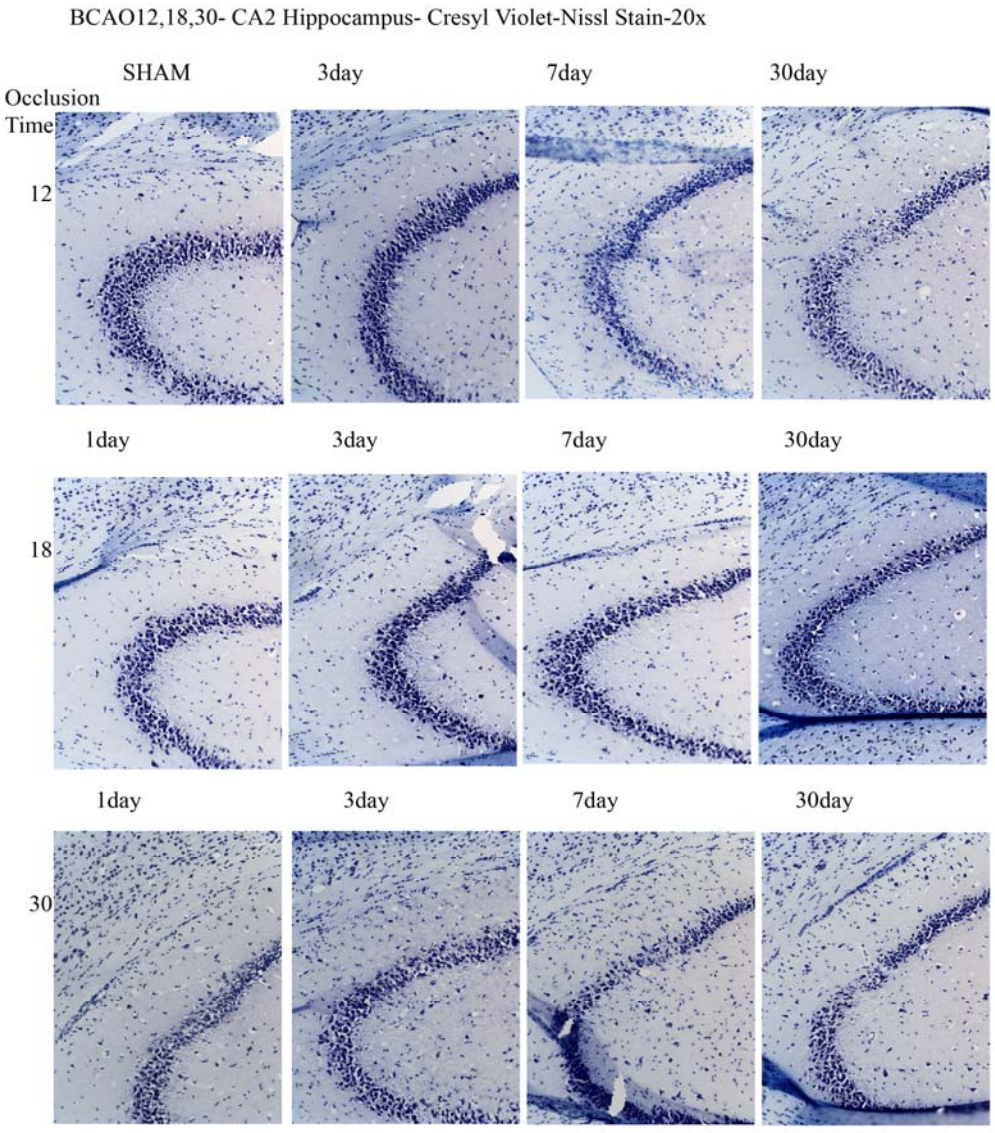

Figure 2.2: Hippocampal CA2 neuronal damage found to be consistent with previously published results (Magnoni, et al., 2004). Greater damage was apparent at 30 minutes of occlusion and longer reperfusion times.

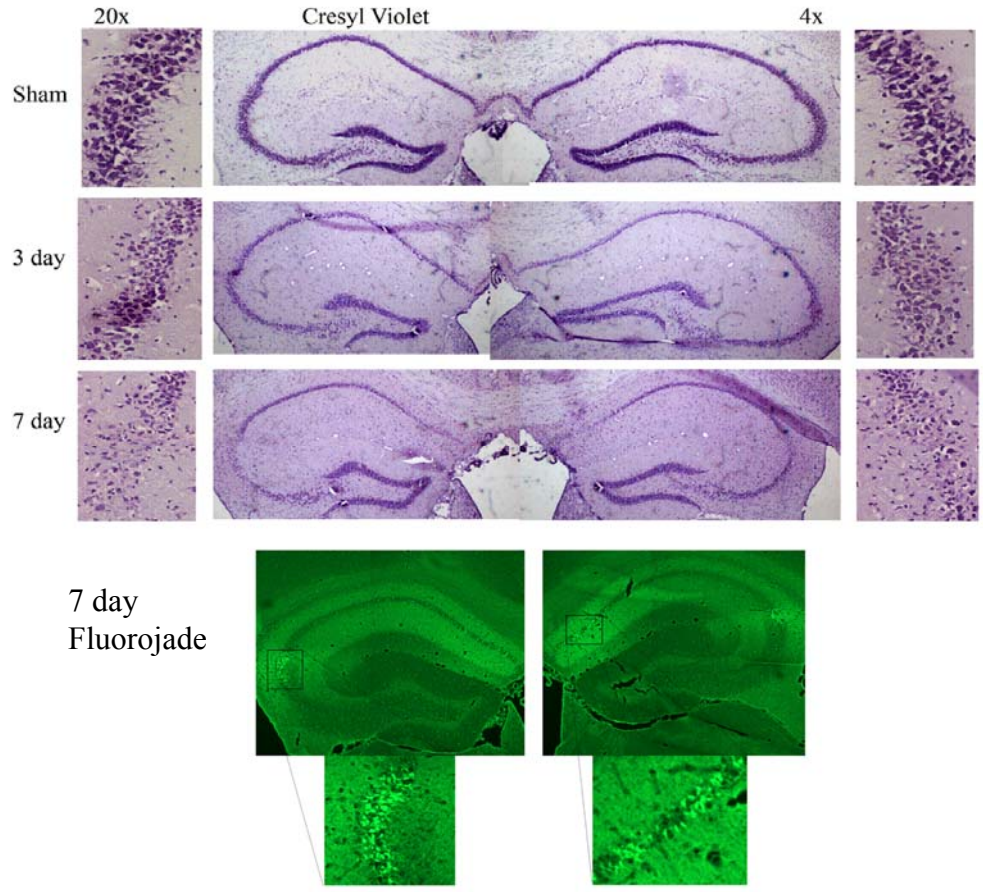

Figure 2.3: Hippocampal injury following 30 min BCAO localized to CA1 and CA2. Loss of CV positive neurons correlated with Fluorojade positive regions at 7 days of reperfusion Fluorojade staining 4x, inset 20x.

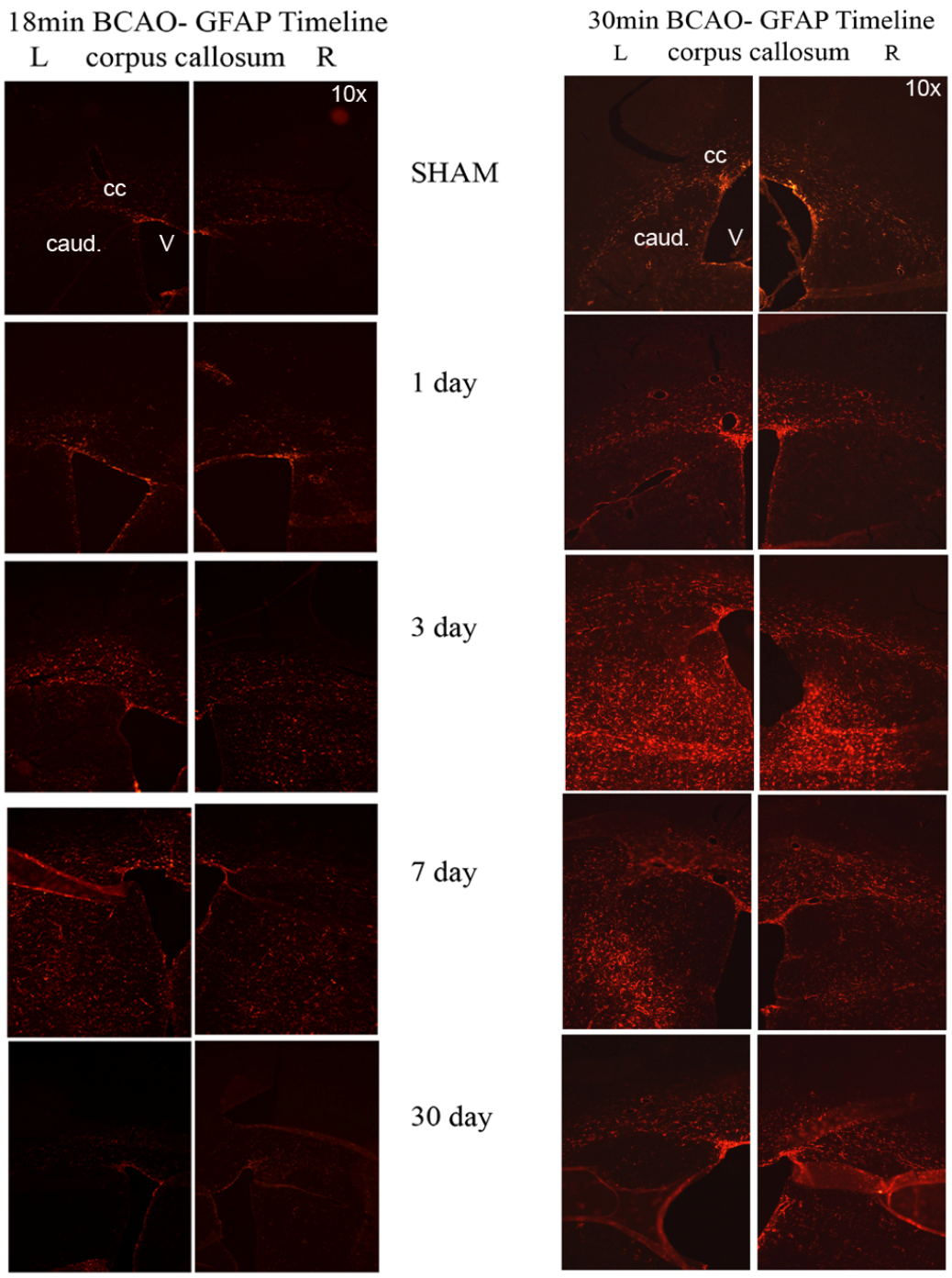

Figure 2.4: GFAP staining of astrocytes in coronal Bregma sections following 18 and 30 minutes of BCAO and 1, 3, 7, and 30 days of reperfusion. There was increased astrocyte reactivity in the caudate and corpus callosum following 30 minutes of occlusion and 3-7 days of reperfusion.

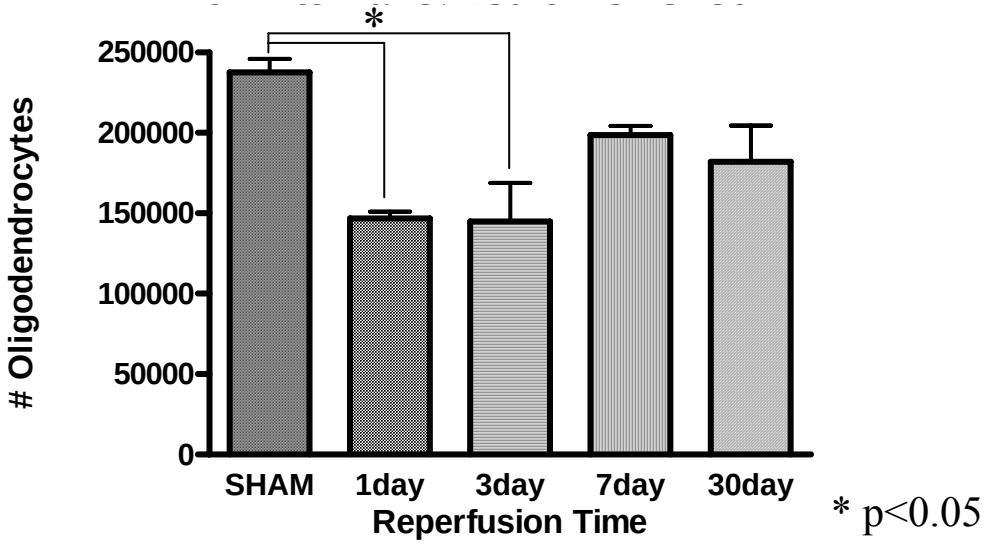

Figure 2.5: Preliminary data of BCAO oligodendrocyte stereology. Data shows early oligodendrocyte loss at 1 and 3 days of reperfusion (n=4). Additional animals will need to be counted to confirm findings. See Chapter 4 for complete methods discussion.

CHAPTER 3:

TIMP-3 and MMP-3 contribute to delayed inflammation and hippocampal neuronal death following global ischemia

Espen J. Walker [a,b] and Gary A. Rosenberg [a,b,c*]

Departments of Neurology [a], Neurosciences [b], and Cell Biology and Physiology [c],

University of New Mexico Health Sciences Center, Albuquerque, NM 87131

Walker, E.J. and Rosenberg, G.A., Experimental Neurology, published March 2009

3.1 Abstract

Hippocampal neuronal death following transient global ischemia in the mouse takes days to occur, providing a potential timeframe for therapeutic intervention. Since matrix metalloproteinase-3 (MMP-3) enhances inflammation and tissue inhibitor of metalloproteinases-3 (TIMP-3) promotes apoptosis in ischemia, we hypothesized that they are involved in neuronal death secondary to transient global ischemia. *Timp-3* knockout (T3KO) and wild type (T3WT) mice underwent 30 min bilateral carotid artery occlusion (BCAO), which causes hippocampal neuronal death 7 days after reperfusion. Mice lacking the *Timp-3* gene have significantly less astrocytosis, microglial reactivity, MMP-3 activity and neuronal cell death. In addition, T3KO mice had decreased tumor necrosis factor (TNF) receptor-1 (TNFR1) expression and increased TNF-α converting enzyme (TACE) activity. *Mmp-3* KO mice with a similar BCAO showed significantly fewer microglial cells, reduced TNF-α expression, and less neuronal death than the *Mmp-3* WT. To see if TIMP-3 and MMP-3 cell death pathways were independent, we blocked MMPs with the broad-spectrum MMP inhibitor, BB-94, on days 3 through 6 of reperfusion in T3WT and T3KO mice. BB-94 rescued hippocampal neurons at 7 days in both T3WT and T3KO mice, but significantly fewer neurons died in T3KO mice treated with BB-94. Our results indicate a novel additive role for TIMP-3 and MMP-3 in delayed neuronal death, and show that MMP inhibitors can be used to reduce delayed hippocampal death.

3.2 Introduction

Global ischemia reduces blood flow to the brain, causing hypoxic hypoperfusion injury to vulnerable, poorly perfused areas as would occur with cardiac arrest or hypotension during a surgical procedure (Back, et al., 2004, Harukuni and Bhardwaj, 2006, Lo, et al., 2003). During global ischemia neurons in the CA1 and CA2 regions of the hippocampus, which are selectively vulnerable, undergo apoptosis after 3 to 7 days (Chen, et al., 1998, Magnoni, et al., 2004, Oguro, et al., 2001). Various acute mechanisms have been proposed for this type of injury, including intracellular mitochondrial dysfunction and DNA degradation (Deierborg, et al., 2008, Kumaran, et al., 2008). The proteases, extracellular tissue plasminogen activator (tPA) and matrix metalloproteinases (MMPs), also play an important role (Lee, et al., 2007, Lee, et al., 2004, Zalewska, et al., 2002). There is evidence that MMP-9 causes early cell death in hippocampal neurons after global ischemia (Lee, et al., 2004). However, the mechanisms involved in the delayed cell death seen after 3 days (Oguro, et al., 2001) remain to be established.

MMPs are involved in neuroinflammation (Rosenberg, 2002), extracellular matrix (ECM) degradation (Gu, et al., 2002), cleavage and activation of other MMPs (Rosenberg, et al., 2001), as well as shedding of death receptors (Wetzel, et al., 2003). They are rapidly upregulated after cerebral ischemia in rats, mice, nonhuman primates, and humans. Research in our lab has previously shown that stromelysin-1 (MMP-3) is involved in blood brain barrier (BBB) breakdown (Gurney, et al., 2006) with expression preceding inflammatory mediator tumor necrosis factor-α (TNF-α) expression in an LPS model of inflammation (Mun-Bryce, et al., 2002). MMP-3 has also been implicated in

microglial activation and inflammation in a Parkinson's disease model (Kim, et al., 2005).

Tissue inhibitor of metalloproteinases-3 (TIMP-3) has many roles in ischemic cell death through inhibition of membrane-type 1-MMP (MT1-MMP), MMP-3, and TNF-α converting enzyme (TACE) (Wei, et al., 2005, Wetzel, et al., 2003, Will, et al., 1996). MMP-3 and TACE act as sheddases on the cell surface, releasing death receptors and ligands in the TNF superfamily. By inhibiting sheddase activity, TIMP-3 allows stabilization of death receptors and subsequent apoptosis in a variety of models, including focal ischemia (Wallace, et al., 2002), doxorubicin-induced injury *in vitro* (Wetzel, et al., 2003), and more recently in oxygen-glucose deprivation (OGD) models in cell culture and mild focal ischemia in the *Timp-3* KO (T3KO) mouse (Wetzel, et al., 2008). Tumor necrosis factor α receptor-1 (TNFR1) stabilization on the cell surface is regulated by TACE. TACE activity leads to TNFR1 cleavage and reduced apoptosis (Smith, et al., 1997). TIMP-3 regulates the activity of TACE (Amour, et al., 1998) and can lead to reduced TNFR1 cleavage.

As MMP-3 and TIMP-3 both appear to play a role in cell death and inflammation, we hypothesized that both were involved in delayed hippocampal neuronal death following global ischemia. We demonstrate a delayed inflammatory response and regional selective neuronal death following global ischemia in the mouse. Utilizing both *Mmp-3* KO (M3KO) and T3KO mice, we investigated cell-specific inflammation, death receptor expression, enzyme activation, and neuronal loss in the hippocampus. Using a

combination of genetic and pharmacological interventions, we inhibited both TIMP-3 and MMP-3 by genetic knockout and delayed drug treatment in the same animal and were able to prevent hippocampal neuronal death.

3.3 Materials and Methods

Transient Global Cerebral Ischemia

All experiments were approved by the University of New Mexico (UNM) Animal Care Committee and conformed to the National Institutes of Health Guide for the Care and Use of Animals in research. Transient bilateral common carotid artery occlusion (BCAO) was conducted on the C57BL/6 mouse, T3KO, M3KO and corresponding wild-types from colonies maintained in the Animal Research Facility at UNM. The T3KO mice were backcrossed seven times or more then bred on a C57BL/6 background and were a generous gift from R. Khokha. The M3KO mice were backcrossed three times then bred on a B10RIII.H2 background from Taconic with the kind permission of J. Mudgett. The animals were anaesthetized in an incubation chamber via 2% isoflurane by inhalation and injected with 0.1 mg/kg of analgesic (buprenorphine) IP with animal temperature constantly maintained. The skull was exposed and cerebral blood flow measured with a Laser Doppler blood flow monitor (Moore Instruments Limited, Devon, UK) 3 mm caudal and 3 mm lateral to Bregma. Both common carotid arteries were exposed, isolated, and clipped with metal aneurysm clips for 12, 18, or 30 minutes to determine optimal occlusion time. Animals were allowed to recover in their cage for 1-2 hours with a heating lamp. Following reperfusion, the animals were anaesthetized with 2%

isoflurane by inhalation and injected IP with 30 mg/kg of sodium pentobarbital at 3, 7, or 30 days. Perfusion with PBS/0.1% Procaine followed by 2% PLP (2% paraformaldehyde, 0.1 M sodium periodate, 0.075 M lysine in 100 mM phosphate buffer at pH 7.4) was conducted intracardially. Brains were removed and immersed in 2% PLP overnight. The brains were cryoprotected with 30% sucrose in PBS, and frozen in OCT. They were stored at -80^{o} C until sectioned. For activity assays and immunoblotting, brains were removed and quickly frozen in 2-methylbutane.

Immunohistochemistry (IHC)

For fluorescence IHC, 10 μm sections were rehydrated through alcohols and PBS containing 0.1% Tween-20 (PBT). Nonspecific binding sites were blocked with PBT containing 1% bovine serum albumin (BSA), and 5% normal serum. Slides were incubated overnight at 4°C with primary antibodies. Slides were washed in PBT and incubated for 90 min at room temperature with secondary antibodies conjugated with FITC and Cy-3. Slides were incubated with 4'-6-diamidino-2-phenylinidole (DAPI) (Molecular Probes, Inc., Carlsbad, CA) prior to coverslipping to label cell nuclei. All IHC slides were viewed on an Olympus BX-51 bright field and fluorescence microscope (Olympus America Inc., Center Valley, PA) equipped with an Optronics digital camera and Picture Frame image capture software (Optronics, Goleta, CA). Antibodies used for IHC included TIMP-3 (1:1000; Chemicon, Temecula, CA), glial fibrillary acidic protein (GFAP) for astrocytes (1:400; Sigma-Aldrich, St. Louis, MO), Iba-1 for microglia/ macrophages (1:400; Wako Pure Chemical Industries, Richmond, VA), neuron specific nuclear protein (NeuN) (1:400 mouse; Chemicon), p55TNF Receptor 1 (1:1000 Abcam,

Cambridge, MA), MMP-3 (1:200 R&D Systems Inc., Minneapolis, MN), TNF-α (10μg/ml; R&D Systems). Fluoro-Jade C staining (HistoChem Inc., Jefferson, AZ) of 10 μm sections was performed per company protocol.

Fluorescence Intensity Analysis

To compare various reperfusion time points and regions of interest, slides stained with IHC were analyzed for fluorescence staining intensity. All slides to be compared were stained together. Images were taken at the same exposure time for each section and changed to grayscale. Using NIH Image J software, the region of interest was outlined and the total mean fluorescence intensity of each region was recorded and compared to control staining and other reperfusion time points. Values are reported as fluorescence intensity.

Hippocampal Neuronal Stereology

To assess neuronal injury following transient global ischemia, 20 μm sections taken every 100 μm were rehydrated through alcohols, rinsed in PBS and water, and stained with cresyl violet acetate (CVA). Slides were rinsed in tap water, dehydrated through alcohols and xylene, then coverslipped using DPX (Sigma-Aldrich). Stereology was performed using the optical fractionator function of StereoInvestigator software (Version 6, MicroBrightField Inc., Williston, VT) controlling a motorized stage equipped Olympus BX-51 microscope. Viable neurons in the CA2 region of the hippocampus over a total distance of 3.0 mm were counted as this was the area determined most sensitive to injury. The region of interest was delineated and overlaid with a grid size of 120 x 60 μm and

counting frame set at 35 x 35 μm for stereological quantification of cells. Histological sections were blinded to the investigator as to animal identity and reperfusion time.

Immunoblotting for TNFR1

Hippocampus regions of freshly isolated non-fixed brain homogenate were collected by punch biopsy at -20°C and analyzed for protein expression of TNFR1 by Western blot. 50 μg of total protein was separated on 10% acrylamide gels. Proteins were transferred to polyvinylidene fluoride (PVDF) membranes, blocked, and incubated overnight at 4°C with primary antibodies against TNFR1 (1:1400 Abcam). Membranes were incubated with HRP conjugated secondary antibodies (1:10,000; Jackson ImmunoResearch Laboratories Inc., West Grove, PA) and blots developed using chemiluminescent detection with the West Pico Kit (Pierce Biotechnology, Inc., Rockford, IL). Protein bands were visualized on X-ray film and densitometric analysis was used for semiquantitation of band intensities with AlphaEase image software (Alpha Innotech Corp., San Leandro, CA). Actin staining (1:7500 Sigma-Aldrich) on the same PVDF membranes was used to normalize protein loading and transfer. Results are reported as normalized band intensity for quantifying relative protein expression.

TACE Activity Assay

TNF-α converting enzyme (TACE) activity was measured using a fluorimetric assay with a SensoLyte™ 520 TACE (α-Secretase) Activity Assay Kit (AnaSpec Inc., San Jose, CA) according to the operation manual. The SensoLyte™ 520 TACE Activity Assay Kit used a 5-carboxyfluorescein (5-FAM) (fluorophore) and QXL™ 520 (quencher) labeled

fluorescence resonance energy transfer (FRET) peptide substrate for continuous measurement of enzyme activity. In the intact FRET peptide, the fluorescence of 5-FAM was quenched by QXL™ 520. Upon cleavage of the FRET peptide by the active enzyme, the fluorescence of 5-FAM was recovered, and continuously monitored at excitation / emission = 490 nm / 520 nm. Fresh hippocampus tissue punches were homogenized in lysis buffer containing 50 mM Tris-HCl pH 7.6, 150 mM NaCl, 5 mM $CaCl_2$, 0.05% Brij-35, 0.02% NaN_3, and 1% Triton X-100, and centrifuged at 12,000 x g for 10 min at 4°C. Equal amount of total protein (100 µg) was mixed with assay buffer and TACE substrate to a final volume of 100 µl. The change in fluorescence was monitored for 60 min at room temperature with a luminescence spectrometer (model LS55; PerkinElmer Instruments, Buckinghamshire, UK). FL WinLab software was used to express data as relative fluorescence units.

MMP-3 Activity Assay

MMP-3 enzymatic activity was measured with a fluorimetric assay using a 5-FAM/QXL™520 FRET peptide (Anaspec). In the intact FRET peptide, the fluorescence of 5-FAM was quenched by QXL™ 520. Upon cleavage into two separate fragments by the MMP-3 present in the sample, the fluorescence of 5-FAM was recovered and monitored at excitation / emission = 490 nm / 520 nm for 60 min at room temperature using a luminescence spectrometer (PerkinElmer LS55). Homogenized hippocampus tissue samples with 100 µg protein (the same ones used for the TACE activity assay above) were mixed with assay buffer (50 mM Tris-HCl, pH 7.6, 200 mM NaCl, 5 mM $CaCl_2$, 20 µM $ZnSO_4$, and 0.05% Brij-35) and fluorogenic substrate (1 µM final

concentration) to a final volume of 200 µl. FL WinLab software was used to express data as relative fluorescence units.

Statistical Analysis

Statistical comparisons among groups were done using ANOVA with post-hoc analysis for multiple *t*- tests (Prism 4.0, GraphPad Software Incorporated). All data were presented as mean ± standard error of the mean (SEM). Statistical significance was set at $p<0.05$.

3.4 Results

Delayed hippocampal neuronal injury

Global ischemia was induced in the C57BL/6 mouse by 12, 18, and 30 min occlusion with 3, 7, and 30 days of reperfusion. Blood flow was monitored before, during, and following carotid occlusion with 11.2 +/- 1.1% of original flow during the occlusion period, and flow returning to 44.9 +/- 6.3% following clip removal. Neuronal loss after different occlusion times was compared at 7 days (Fig. 3.1A). CVA and Fluoro-Jade C staining of the hippocampus at various time points showed that damage was predominantly in the hippocampal CA2 region 7 days after BCAO (Fig. 3.1B). The 7 day time point with 30 min occlusion was selected for further investigation.

TIMP-3 involved in hippocampal neuronal death

Previous studies have shown TIMP-3 to be involved in neuronal death in the cortex following focal ischemia (Wallace, et al., 2002), and with increased expression in the astrocytes (Liu, et al., 2007). To determine the cellular source of TIMP-3 in our model, we used immunohistochemistry (IHC) and found co-localization of TIMP-3 with the astrocyte marker, GFAP at 7 days reperfusion (Fig. 3.2A). Quantification of TIMP-3 fluorescence intensity in the hippocampus showed a significant rise in TIMP-3 at 7 days of reperfusion as compared to sham values (Fig. 3.2B).

To determine the effect of TIMP-3 on cellular injury, we used T3KO and T3WT mice to compare neuronal survival following global ischemia. Stereological analysis of viable hippocampal neurons of the CA2 region showed no cell death at 3 days reperfusion in either genotype. Following 7 days reperfusion, both genotypes showed significant neuronal loss ($p<0.001$) as compared to sham. More importantly, there was attenuated cell death in the T3KO mice as compared to the T3WT ($p<0.01$) (Fig. 3.3).

Inflammation and death receptor stabilization in the T3WT hippocampus

To better understand the role of TIMP-3 in neuronal death, we analyzed hippocampal tissue in the T3KO and T3WT mice for signs of inflammation and death receptor expression. Astrocytes were stained with GFAP at various time points in both the T3KO and T3WT mice and analyzed for fluorescence intensity. There was an increase in astrocytosis in the T3WT as compared to the T3KO at 3 days ($p<0.01$) and 7 days ($p<0.001$) of reperfusion (Fig. 3.4A,B). There was also a significant increase in the Iba-1

microglial staining in the T3WT mice at 3 days ($p<0.05$) and 7 days ($p<0.001$) reperfusion as compared to the T3KO (Fig. 3.4C,D).

We then investigated the expression of TNFR1 in the T3WT and T3KO mice to determine the involvement of this death receptor. With TNFR1 expression on the cell surface, TNF-α can bind and lead to apoptotic cell death. Following 3 days reperfusion, there was co-localization of TNFR1 with NeuN-positive neurons (Fig. 3.5A), with the T3WT mice having significantly higher TNFR1 protein expression ($p<0.05$) as compared to the T3KO (Fig. 3.5B). This correlated at the same time point with decreased TNF-α converting enzyme (TACE) activity in the T3WT as compared to the T3KO (Fig. 3.5C).

MMP-3 involved in inflammation and neuronal loss

With neuronal loss occurring in both the T3WT and T3KO mice at 7 days reperfusion, we hypothesized an additional mechanism contributed to the observed hippocampal injury. Using IHC, we found increased MMP-3 staining in both the T3WT and T3KO mice at 3 days, co-localized with Iba-1 positive microglia (Fig. 3.6A). In addition, we performed a fluorometric enzymatic activity assay and found significantly increased MMP-3 activity at 3 days in both T3WT and T3KO mice ($p<0.01$ and $p<0.001$) with T3WT mice having more MMP-3 activity than the T3KO mice at all time points (Fig. 3.6B).

To determine the role of MMP-3 in the delayed death of neurons in the hippocampus, we then compared global ischemic injury in the M3KO and M3WT mice. Neuronal

stereology of the CA2 region of the hippocampus showed significant protection in the M3KO mice at 7 days reperfusion ($p<0.001$), implicating a role for MMP-3 in neuronal loss (Fig. 3.7A). In addition, there was a decrease in the microglial staining intensity (Fig. 3.7C) and TNF-α expression in the M3KO as compared to the M3WT (Fig. 3.7B).

Pharmaceutical MMP inhibition in T3WT and KO mice

To determine if this delayed neuronal loss could be reduced through pharmacological intervention, we tested the effect of administering a broad-spectrum MMP inhibitor, BB-94, as a selective MMP-3 inhibitor is not available. Since we were interested in the delayed neuronal death with inflammation, we administered the drug 3 through 6 days after reperfusion. Staining the T3WT and T3KO mice tissue with CVA, we performed neuronal stereology at 7 days of reperfusion and saw a dramatic increase in cellular survival in both genotypes ($p<0.001$) (Fig. 3.8), further implicating a delayed MMP contribution to hippocampal neuronal death. T3KO mice treated with BB94 had neuronal counts equivalent to those seen in the sham mice.

3.5 Discussion

Our data show that TIMP-3 and MMP-3 contribute independently to delayed hippocampal neuronal loss following transient global ischemia with reperfusion injury in the mouse. Neuronal cell death was reduced in both the T3KO and M3KO mice, suggesting that the presence of TIMP-3 and MMP-3 promote cell death at 7 days. With TIMP-3 affecting TACE activity and TNFR1 expression, and MMP-3 affecting

inflammation and TNF-α expression in microglia, the regulation of this death receptor pathway by both TIMP-3 and MMP-3 may be an important mechanism in delayed apoptotic cell death in global ischemia. An inhibitor to MMPs might be anticipated to mimic a TIMP-3 pro-apoptotic effect. However, we found the opposite; BB-94, a broad-spectrum MMP inhibitor, had an additive effect, increasing protection of neurons in the T3KO mice that already had partial protection. With neuronal rescue occurring through TIMP-3 knockout in addition to MMP inhibition, these two pathways appear to be independent and additive mechanisms of delayed neuronal death.

With increased neuronal survival and decreased inflammation in the T3KO mice, we demonstrate TIMP-3 involvement in delayed death. This finding supports earlier studies, implicating TIMP-3 in cell death in the rat with focal ischemia induced by middle cerebral artery occlusion and in neuronal cell cultures (Wallace, et al., 2002, Wetzel, et al., 2003). TIMP-3 inhibits the sheddase activity of TACE (Amour, et al., 1998, Drynda, et al., 2005). By a mechanism distinct from MMP inhibition (Wei, et al., 2005), TIMP-3 blocks removal of TNFR1 from the cell surface by TACE, leading to cell death in human colon carcinoma cells (Smith, et al., 1997). Our data agree with these findings showing increased TACE and decreased TNFR1 expression in the neurons of the T3KO mice. The loss of TNFR1 has been shown to decrease inflammation using a TNFR1 knockout mouse (Smookler, et al., 2006) and increase immune hyperreactivity in a TNFR1 knock-in mouse (Xanthoulea, et al., 2004). Our results support the role of TIMP-3 inhibiting TACE and stabilizing TNFR1 in the ischemic mouse hippocampus. In addition, our data

further implicate a role for TIMP-3 in the increased reactivity of astrocytes and microglia, exacerbating the delayed inflammatory response.

In an earlier study with doxorubicin treated neuronal cultures, TIMP-3 facilitated cell death through inhibition of MMP-3, which blocked the cleavage of Fas ligand from the cell surface (Wetzel, et al., 2003). TIMP-3 also facilitates neuronal death via death receptor stabilization in ischemia (Wetzel, et al., 2008), arthritic fibroblasts (Drynda, et al., 2005) and in a transgenic model of amyotrophic lateral sclerosis (Lee, et al., 2008). With an inhibitory domain distinct for TACE as compared to other MMPs (Wei, et al., 2005), TIMP-3 can stabilize death receptors such as TNFR1 on the cell membrane, leading to apoptotic cell death.

The interaction of TIMPs with MMPs can influence various pathways that regulate cell death and survival (Crocker, et al., 2004, Cunningham, et al., 2005). TIMP-3 inhibits several MMPs in addition to TACE. *In vitro* studies demonstrate TIMP-3 can promote cell death through inhibiting the protective effect of MMP-3 cleavage of the death receptor ligand, Fas-L (Wetzel, et al., 2003) and through stabilization of the TNFR1 receptor (Smookler, et al., 2006). Increased TNFR1 stabilization may be the mechanism whereby TIMP-3 promotes neuronal death as MMP-3 appears to be detrimental in our *in vivo* BCAO model.

Recent evidence has implicated MMP-3 as a key modulator of inflammation and cell death in various disease models. Intracellular expression of MMP-3 triggers a

neuroinflammatory cascade in a Parkinson's model with microglial induction of TNF-α and other cytokines (Choi, et al., 2008, Kim, et al., 2005). MMP-3 upregulation precedes the onset of disease in a demyelinating transgenic mouse (D'Souza, et al., 2002) and LPS-induced inflammation leads to increased IL1β stimulation and astrocyte expression of MMP-3 (Crocker, et al., 2006). Previous findings from our lab support a role for MMP-3 in the inflammatory cascade and BBB opening following LPS-induced injury (Gurney, et al., 2006) with MMP-3 upregulation preceding TNF-α expression in reactive microglia (Mun-Bryce, et al., 2002). We therefore hypothesized a role for MMP-3 expression in microglial inflammation and ischemic injury to the mouse neurons following global ischemia. Our data demonstrate an increase in the activity of MMP-3 parallel with increased microglial reactivity, TNF-α expression, and eventual neuronal death in the M3WT compared to M3KO mice. In addition, the T3WT mice had significantly higher MMP-3 activity levels than T3KO mice, suggesting the absence of TIMP-3 may lead to a compensatory increase in MMP-3.

MMP inhibitors have been considered for use in therapeutic applications. Testing these agents in rodent models has shown some promise in reducing injury following ischemia. However, determining the optimal time to administer these drugs is difficult as early inhibition (0-3 days) has shown protection (Cho, et al., 2006, Lee, et al., 2004), but later inhibition in the rat following focal ischemia (7-14 days) reduced recovery through inhibition of neurovascular remodeling (Zhao, et al., 2006). We are unable to determine from our data whether the MMPs in this model are involved in repair processes at the 7 day time point. As inhibition of MMPs has led to reduced inflammation and decreased

death, it seems the MMPs are playing a detrimental role in this delayed death. Finding the appropriate time for MMP inhibition is essential to inhibit cell death. The broad-spectrum MMP inhibitor, BB-94, showed neuroprotection in the mouse hippocampus when given from 0-3 days following global ischemia (Lee, et al., 2004), so we chose to investigate the delayed effect of MMPs and administered BB-94 from 3-6 days of reperfusion. Our results show significant attenuation of neuronal loss in the hippocampus, demonstrating that delayed MMP inhibition can still protect neurons and extend the therapeutic window for treatment of injury.

Inhibiting MMPs in the T3KO mouse allowed us to alter two potential mechanisms of injury in the same animal. With cellular survival increasing additively in the T3KO mice with BB-94, it appears that MMPs and TIMP-3 are independently involved in delayed neuronal loss (Fig. 3.9). The effect of BB-94 protection may also be due to other MMPs, with BB-94 showing acute neuronal protection through MMP-9 inhibition in both focal ischemia (Asahi, et al., 2000) and global ischemia from 0-3 days reperfusion (Lee, et al., 2004). MMP-9 did not appear to be involved in our observed delayed death as we found no difference in MMP-9 expression between experimental and controls at 7 days when neuronal loss was observed (data not shown). Our data has implicated MMP-3 in the observed delayed inflammation and neuronal death, demonstrating that multiple MMPs appear to be involved in neuronal injury.

In conclusion, using a combination of genetic and pharmacological approaches, we provide evidence for the novel role of both TIMP-3 and MMP-3 in delayed hippocampal

injury following global ischemia. With decreased inflammation in both the T3KO and M3KO mice, we demonstrate neuronal protection. Further investigation uncovered a role of the TNF death receptor pathway, with both TIMP-3 and MMP-3 contributing independently. Delayed inhibition of MMPs also shows neuroprotection and supports the use of MMP inhibitors for clinical treatment of delayed injury following hypoxic hypoperfusion from cardiac arrest or hypotension following surgery.

Acknowledgements:

Funding for this work was provided by the National Institutes of Health grants NIH 5RO1NS04547 and R01NS052305.

3.6 Figure Legends

Figure 3.1: Delayed hippocampal injury. A) Cresyl violet staining of hippocampal neurons at various occlusion times with 7 days reperfusion. Compared to sham, 12 and 18 min occlusion had minor injury, with 30 min showing significant hippocampal damage. B) Reperfusion time points showed minimal CA2 injury at 3 days, with marked neuronal loss by 7 days. Fluorojade staining (right column inset) labeled degenerating neurons at 7 days reperfusion. Scale Bars: all 50μm, except B) left column: 300 μm.

Figure 3.2: TIMP-3 delayed expression in astrocytes. A) GFAP-positive astrocytes (FITC, green) do not express TIMP-3 (Cy3, red) in the hippocampus of Sham animals (top row), but show co-localization at 7 days reperfusion (bottom row). DAPI (blue)

stained nuclei become disrupted at 7 days. Scale Bar: 50µm. B) TIMP-3 quantification of fluorescence intensity by immunohistochemistry using Image J software shows significant increase of TIMP-3 expression at 7 days reperfusion (**p<0.01)(n=8 for Sham, 7d, 30d; n=10 for 3d).

Figure 3.3: Stereology of hippocampal neurons in T3WT and T3KO mice. Cresyl violet stained viable neurons of the CA2 region of the hippocampus were counted with stereology. 3 days reperfusion showed no significant cell death or difference between T3WT and T3KO. 7 days reperfusion showed significant death in both groups as compared to sham (***p<0.001), with T3KO mice having significantly less neuronal loss than the T3WT (**p<0.01) (n=12 for WT Sham, n=10 for KO Sham, n=10 for both 3d, n=8 for WT 7d, n=9 for KO 7d).

Figure 3.4: Inflammation of astrocytes and microglia in T3WT mice. A) GFAP-positive astrocytes (green) at 7 days reperfusion. B) Quantification of fluorescence intensity demonstrates T3WT mice had more GFAP reactivity than Sham values at 7 days (***p<0.001) and compared to T3KO mice at 3 days (**p<0.01) and 7 days reperfusion (***p<0.001) (n=8 for WT Sham and WT 30d; n=9 for KO 3d, KO 7d, and KO 30d; n=10 for KO Sham, WT 3d, and WT 7d). C) Iba-1 positive microglia/macrophages at 7 days reperfusion. D) Quantification of fluorescence intensity demonstrates T3WT mice had more Iba-1 reactivity than Sham values at 3 days (**p<0.01) and 7 days reperfusion (***p<0.001) and compared to the T3KO mice at 3 days (*p<0.05) and 7 days reperfusion (***p<0.001) (n=8 / group). Scale Bars: 50 µm.

Figure 3.5: TNFR1 expression and TACE activity. A) NeuN-positive neurons (green) co-localize with TNFR1 (red) more in the T3WT than T3KO in the hippocampus at 3 days reperfusion. DAPI counterstain for nuclei. Scale Bar: 50 µm. B) Western blot quantification of TNFR1 protein at 55kDa confirms increased expression at 3 days reperfusion in the T3WT vs. T3KO (*p<0.05) (n=6 / group). Protein loading normalized with actin. C) TACE activity measured with a fluorometric assay shows increased activity in the T3KO hippocampus at 3 days reperfusion (*p<0.05) (n=7 for Shams, n=9 for 3d, n=5 for 7d).

Figure 3.6: MMP-3 activity in microglia. A) Iba-1 positive microglia/ macrophages (green) co-localize with MMP-3 (red) in both T3WT and T3KO hippocampi at 3 days reperfusion. DAPI counterstain for nuclei. Scale Bar: 50 µm. B) MMP-3 activity assessed with a fluorometric assay shows increased activity in the T3WT hippocampus, with both T3WT and T3KO having increased activation at 3 days reperfusion (**p<0.01, ***p<0.001). T3WT mice had constitutively greater MMP-3 activity than T3KO mice (###p<0.001) (n=10 / group for WT, n=8 for KO Sham, n=10 for KO 3d and KO 7d).

Figure 3.7: M3KO vs. M3WT inflammation and cell loss at 7 days. A) Cresyl violet stained neurons were counted by stereology with the M3KO having attenuated cell loss in the CA2 region of the hippocampus (***p<0.001) (n=4 for Shams, n=8 for 7d). B) Iba-1 positive microglia/macrophages (green) co-localize with TNF-α (red) in the M3WT hippocampus. DAPI counterstain for nuclei. Scale Bars: 50 µm. C) Increased Iba-1

microglial fluorescence intensity in the M3WT vs. M3KO (*p<0.05) (n=4 for Shams, n=8 for WT 7d, n=7 for KO 7d).

Figure 3.8: Delayed BB-94 inhibition of MMPs 3-6 days after reperfusion significantly rescued neuronal loss in the hippocampus of both T3WT and T3KO compared to the original cell death observed in Figure 3, with T3KO plus BB-94 neuronal counts returning to sham levels (***p<0.001) (n=8 for T3WT, n=11 for T3WT+BB94, n=9 for T3KO, n=10 for T3KO+BB94).

Figure 3.9: Proposed mechanism of MMP-3 and TIMP-3 induced neuronal death. Inflammation is induced by two pathways in this model: MMP-3 leads to reactive microglia releasing TNF-α, while TIMP-3 inhibits TNR1 removal by TACE. TNF-α can then bind to TNFR1 on the cell surface leading to neuronal cell death.

3.7 Figures

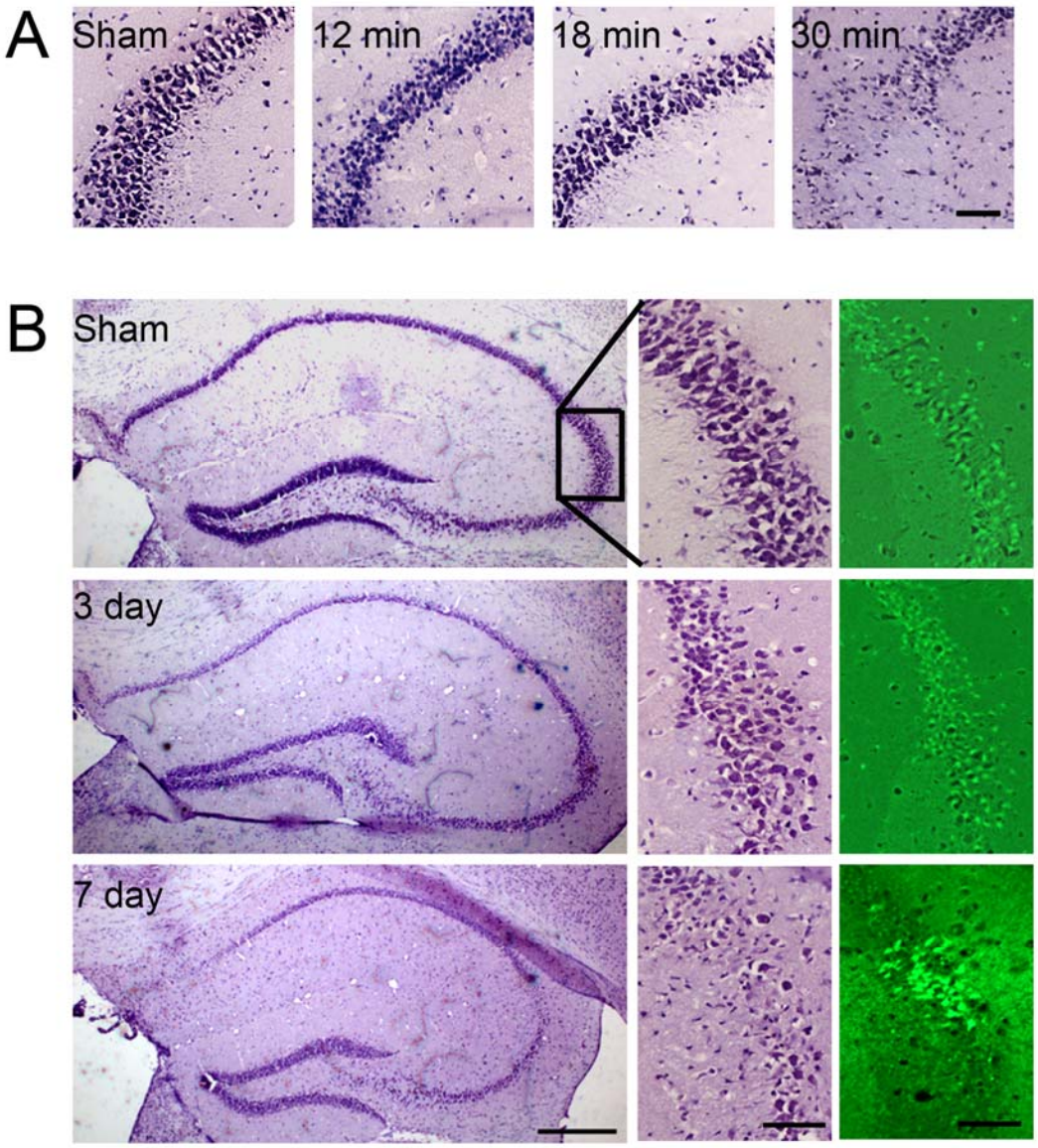

Figure 3.1: Delayed hippocampal injury following BCAO.

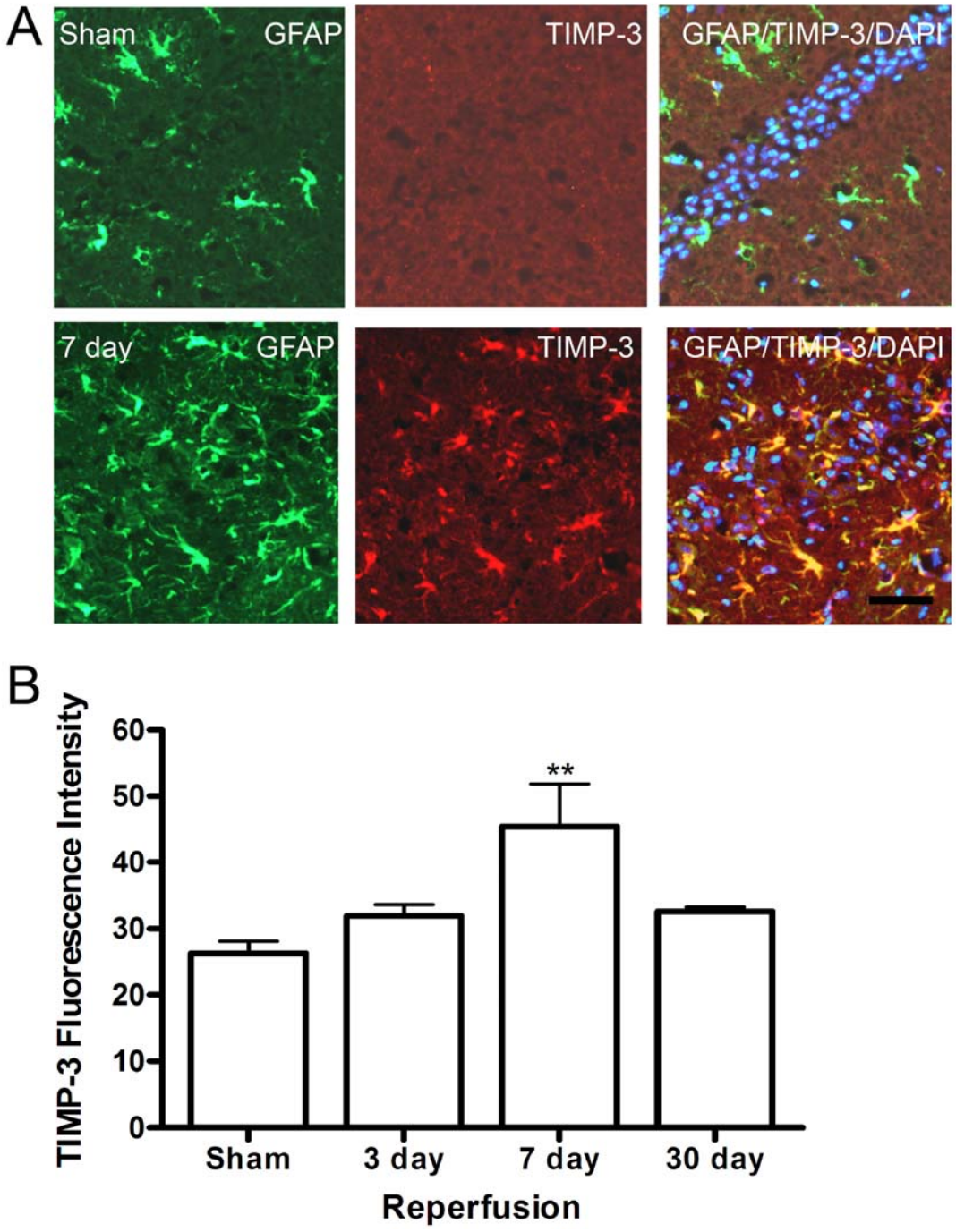

Figure 3.2: Delayed TIMP-3 expression in astrocytes.

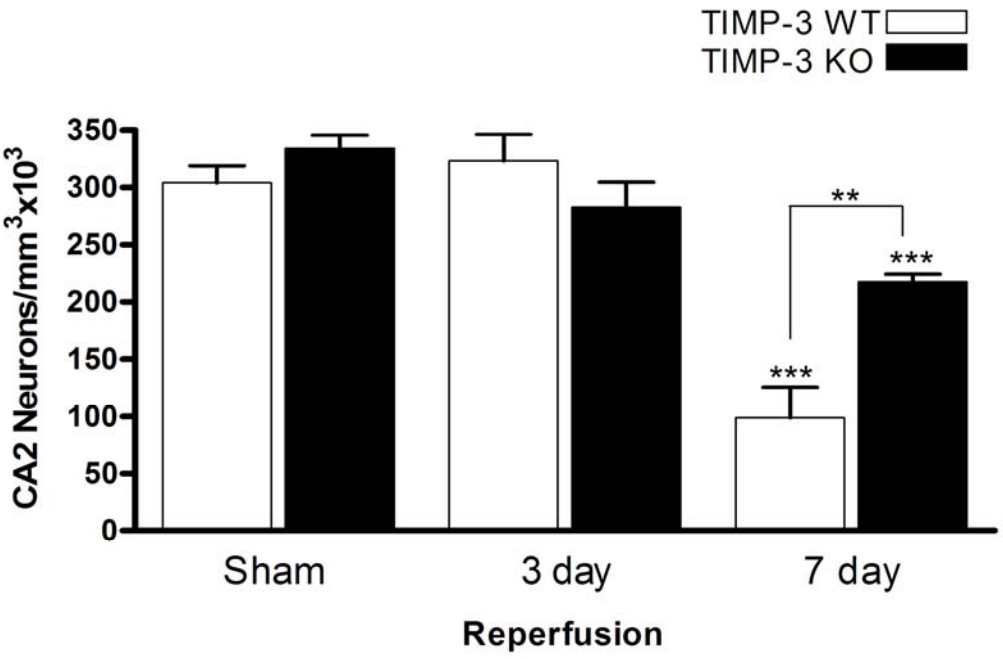

Figure 3.3: Stereology of hippocampal neurons in T3WT and T3KO mice.

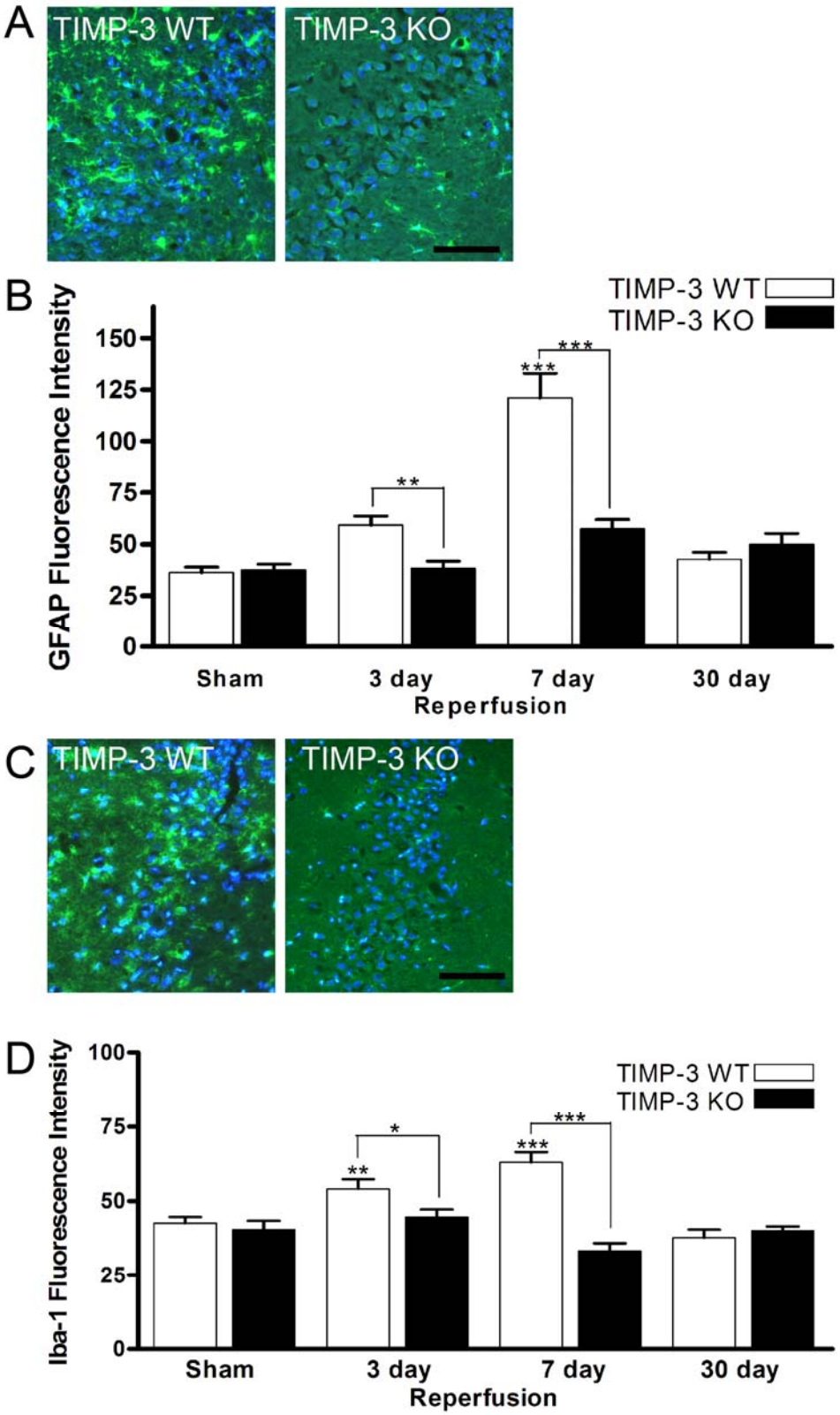

Figure 3.4: Inflammation of astrocytes and microglia in T3WT mice.

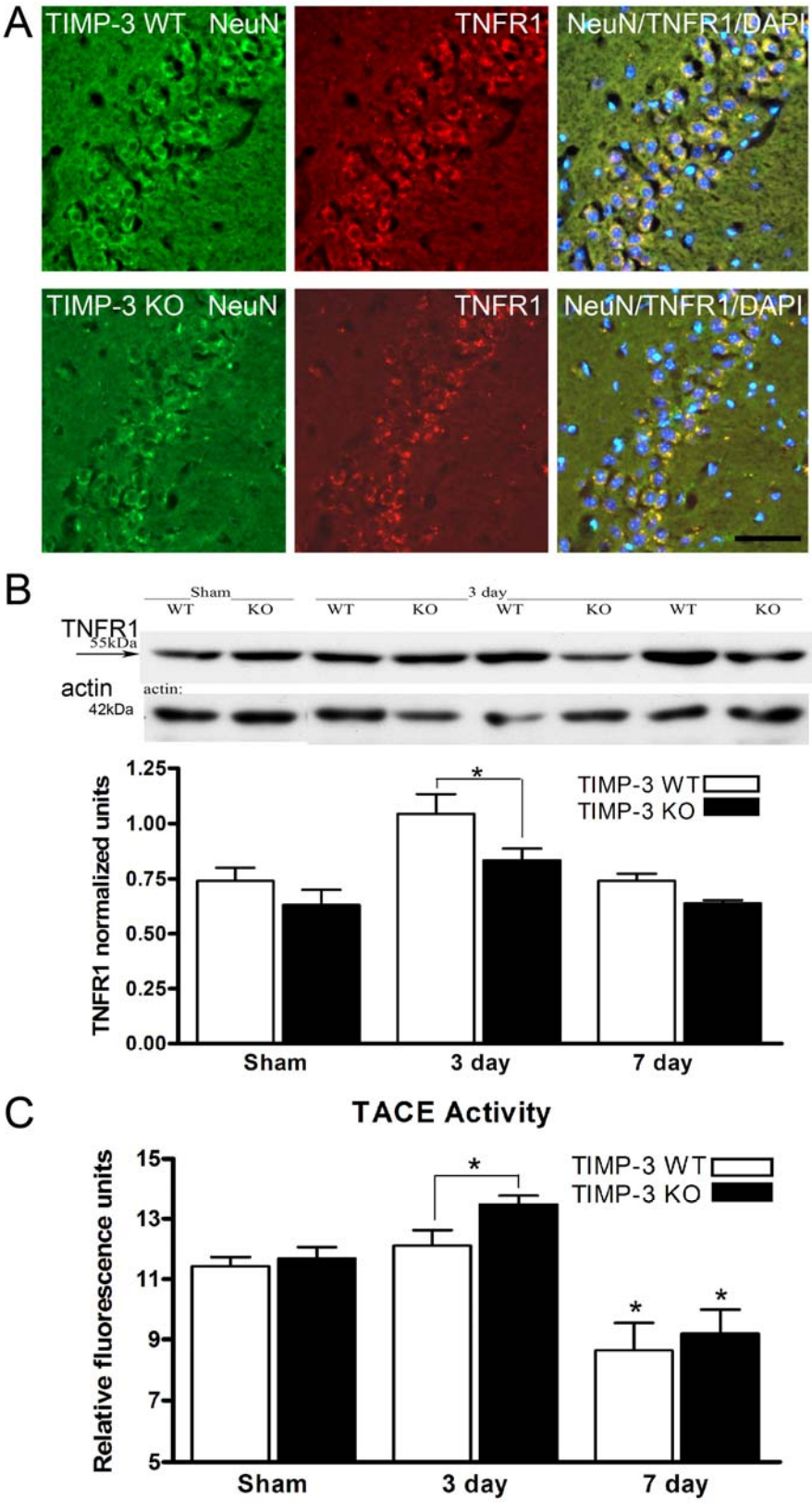

Figure 3.5: TNFR1 expression and TACE activity.

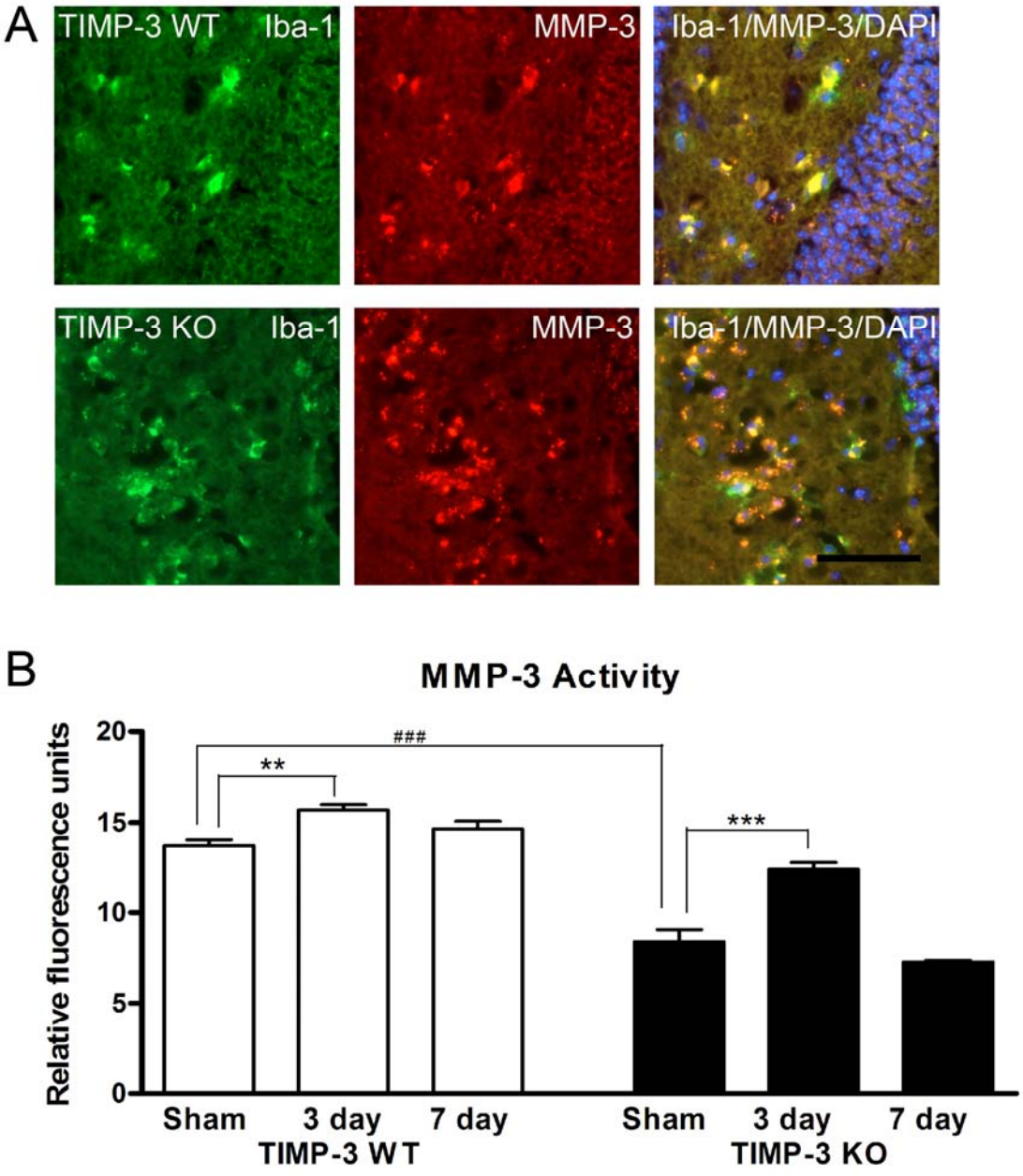

Figure 3.6: MMP-3 activity in microglia in both T3WT and T3KO.

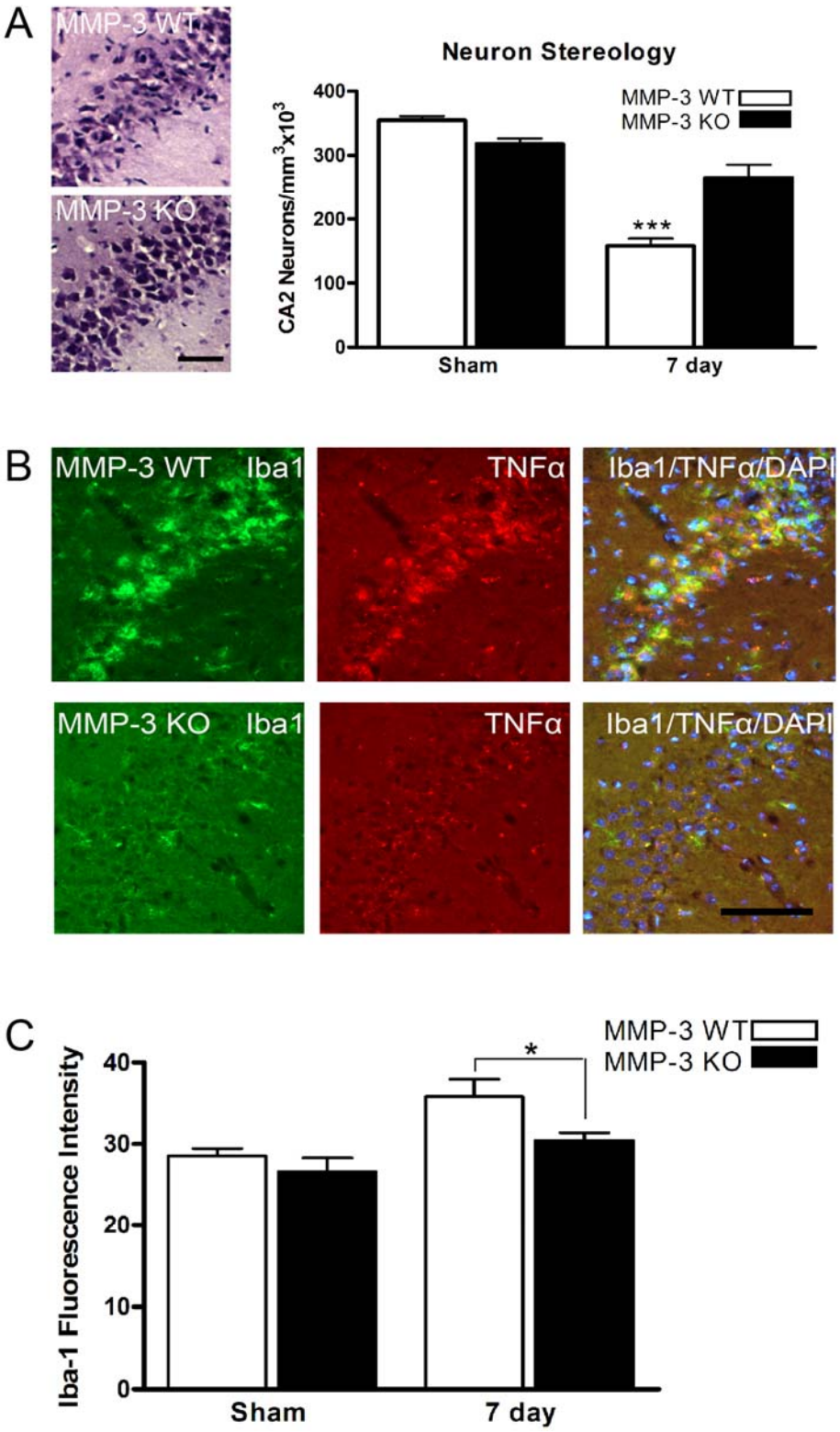

Figure 3.7: M3KO vs. M3WT inflammation and cell loss at 7 days.

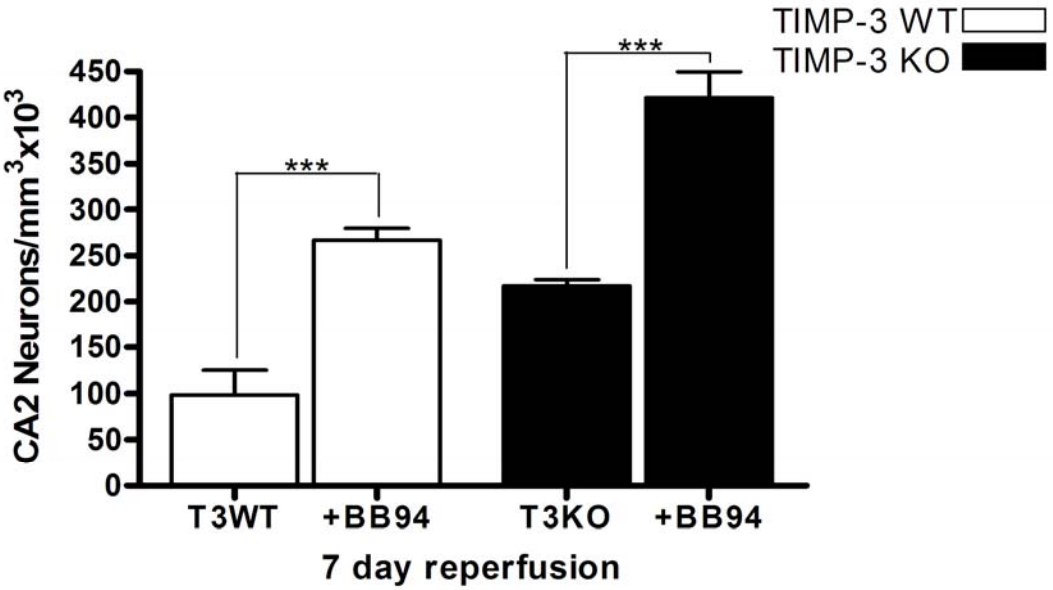

Figure 3.8: Delayed BB-94 inhibition of MMPs in T3WT and T3KO.

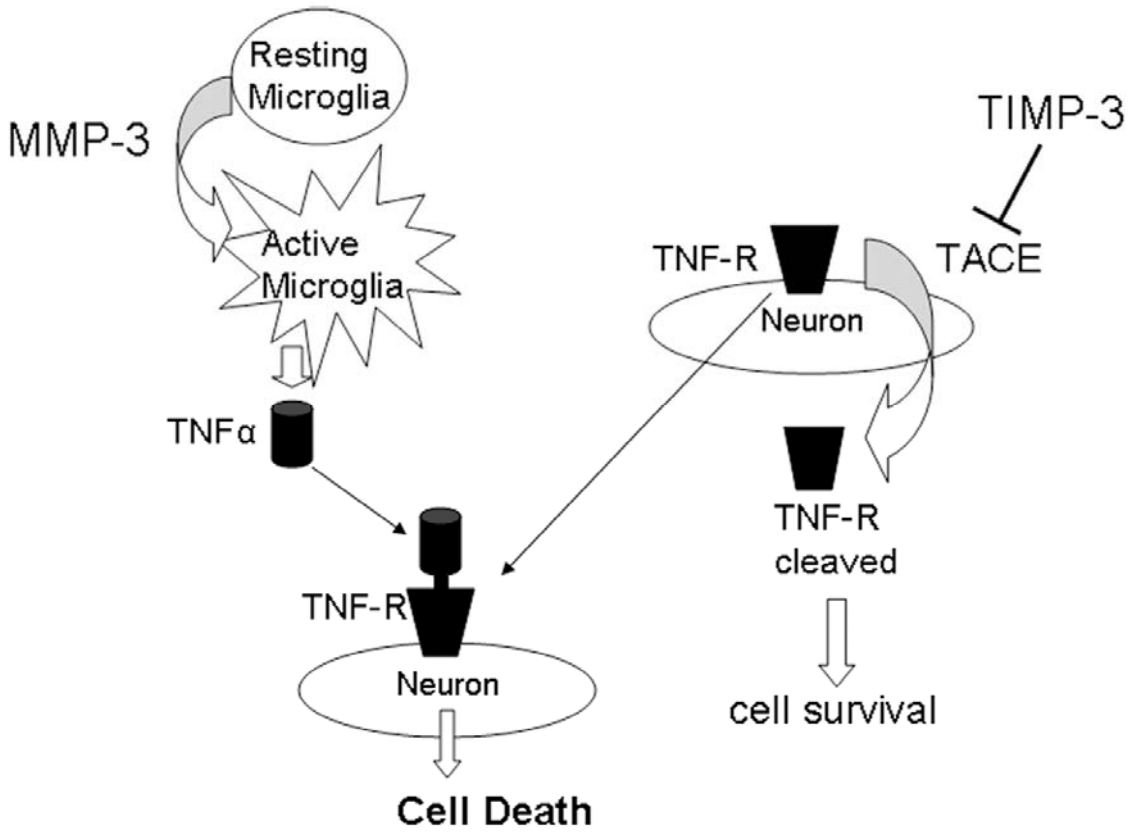

Figure 3.9: Proposed mechanism of MMP-3 and TIMP-3 induced neuronal death.

CHAPTER 4:

Stereological Quantification of Oligodendrocytes by Morphological Analysis and Multiple Antibody Immunohistochemistry of Rodent Brain

Espen J. Walker [a,b], Jeffrey F. Thompson [a], R. Ross Reichard [d] and Gary A. Rosenberg [a,b,c*]

Departments of Neurology [a], Neurosciences [b], Cell Biology and Physiology [c], and Neuropathology [d] University of New Mexico Health Sciences Center, Albuquerque, NM 87131

Paper to be submitted. J. Neuroscience Methods 2009

4.1 Abstract

The accurate quantification of mature, myelinating oligodendrocytes (OLGs) in the white matter of the central nervous system is essential when comparing healthy and injured tissue. We propose a novel technique to quantify OLGs using stereological counting of cresyl violet stained cells and multiple primary antibody staining. As an injury model, we used models of focal and global ischemia in the mouse to demonstrate application of the technique. Brain tissue sections were stained with a combination of GFAP for astrocytes and Iba-1 or OX-42 for microglia, and then counterstained with cresyl violet to label cell bodies. Morphological identification of OLG nuclei and exclusion of DAB-stained astrocytes and microglia allowed for an accurate count of OLGs in the white matter external capsule and corpus callosum. We propose this method to be used for stereological quantification of OLGs in the white matter and may be applied experimentally in the analysis of OLG loss.

4.2 Introduction

Identification of mature oligodendrocytes (OLGs) in the brain remains an experimental challenge in the literature today (Dewar, et al., 2003, Irving, et al., 2001, Kuhlmann, et al., 2007, Valeriani, et al., 2000). Originally described by Cajal in 1896 as a "third element" in the nervous system and characterized by del Rio Hortega by using morphological analysis (Ramon y Cajal, 1896, Rio-Hortega, 1921, Rio-Hortega, 1942) as cited in (Garcia-Marin, et al., 2007), there remains a controversy in the classification of OLG markers (Barradas and Cavalcante, 1998, Dewar, et al., 2003). It is crucial to

identify these cells to assess their survival or loss in various injury models. The current availability of antibodies does not clearly distinguish between the nuclei and processes. Cellular markers for OLGs can also have altered expression during injury processes, such as increased tau expression following ischemia, leading to complications in the identification of injured vs. healthy OLGs (Dewar and Dawson, 1995, Irving, et al., 2001, Irving, et al., 1997). CNPase and RIP label the myelin processes well, but it is difficult to identify the cell bodies (Friedman, et al., 1989). The CC-1 antibody to the adenomatous polyposis coli (APC) tumor suppressor protein labels a percentage of OLG nuclei (Bhat, et al., 1996, Foote and Blakemore, 2005), but has also been shown to label reactive astrocytes in Alzheimer disease and other diseases (Leroy, et al., 2001). Nogo-A has been tested as a mature, OLG cytoplasm marker in various injury models, with staining and *in-situ* hybridization patterns similar to CC-1 and PLP (proteolipid protein) (Kuhlmann, et al., 2007), but had strong labeling of OLGs in a multiple sclerosis model, with only weak labeling in normal tissue (Satoh, et al., 2005). From these experimental data, we conclude there currently is no comprehensive immunoreactive marker for OLGs.

The morphology of OLGs in the white matter is distinct *in vivo* with round nuclei typically arranged in rows. The cellular composition of the white matter is comprised of >90% OLGs (Bongarzone, et al., 1998) with fascicular, dark rows of nuclei (Mills, 2007) appearing like “pearls on a string” (Dewar, et al., 2003, Peters, et al., 1991). The processes radiate from a spherical cell body, extending across the white matter and into the gray matter (Peters, et al., 1991). *In vitro*, OLGs display different architecture with a

more expansive cytoplasm as they are not clustered with astrocytes and neurons (Behar, 2001, Dewar, et al., 2003).

The labeling of cells with a Nissl substance stain, such as cresyl violet acetate (CVA), allows for identification of all cells and a more complete assessment of normal cellular density that could be compared to changes after injury. The aim of our study was to correctly enumerate OLGs using stereological methods to ascertain loss of OLGs in ischemia / reperfusion injury of the external capsule and corpus callosum. To exclude other main cell types of the white matter we stained for astrocytes (GFAP) and microglia (Iba-1 for mouse, OX-42 for rat) to exclude them from the stereological counts. Neutrophils and endothelial cells were identified morphologically and not counted. Using our morphological criteria, only the round CVA-positive cells with nuclei less than 20μm in diameter were identified as OLGs and counted using the optical fractionator function of StereoInvestigator. We compared this method with direct immunohistochemical staining of OLGs and found a statistical correlation. We propose this operational technique may be used for stereological counting of OLGs in the white matter and may be applied experimentally in the analysis of OLG loss in a pathological context.

Materials and Methods

Focal and Global Ischemia Injury Models

All experiments performed for this study were approved by the University of New Mexico Animal Care Committee in accordance with the guidelines of the National

Institute of Health Guide for the Care and Use of Animals. Focal ischemic injury was achieved in male, spontaneously hypertensive rats weighing 250-300 grams using a 90 minute middle cerebral artery occlusion (MCAO) as described previously (Longa, et al., 1989). 90 minute transient MCAO was also conducted in mice weighing 20-30 grams as described previously (Kokovay, et al., 2006). Animals were reperfused for 72 h. Transient bilateral common carotid artery occlusion (BCAO) was conducted on the C57BL/6 mouse as described previously (Walker and Rosenberg '09). Briefly, both common carotid arteries were exposed, isolated, and clipped with metal aneurysm clips for 30 minutes. Animals were reperfused for 1, 3, or 7 days.

Tissue Preparation

Following reperfusion, animals were anesthetized with pentobarbital (50 mg/kg; i.p.), and perfused transcardially with 2% PLP (2% paraformaldehyde, 0.1 M sodium periodate, 0.075 M lysine in 100 mM phosphate buffer at pH 7.4). Brains were removed and immersed in 2% PLP overnight. The brains were cryoprotected in 30% sucrose in PLP, and frozen in O.C.T. embedding compound (Sakura Finetek USA, Inc., Torrance, CA) with 2-methylbutane cooled in liquid nitrogen. They were stored at -80^{o} C until sectioned. Tissue was cryosectioned at 10µm for immunohistochemistry (IHC) and 20 µm for stereology (Richard-Allan Scientific, Kalamazoo, MI), and mounted. Slides were stored with dessicant at -80^{o} C before staining.

Immunohistochemistry

Sections were rehydrated through a series of EtOH concentrations and phosphate buffered saline, containing 0.1% Tween-20 (PBT). Nonspecific binding sites were blocked with PBT containing 1% bovine serum albumin (BSA) and 5% normal goat serum. Sections were stained for several immunoreactive markers of OLGs; RIP (1:200,000; Chemicon Inc., Temecula, CA), CNPase (15 μg/ml; Chemicon), and CC-1 (APC) (10 μg/ml; Calbiochem, San Diego, CA). For stereology, sections were incubated two nights in GFAP (1:400; Sigma-Aldrich, St Louis, MO) for astrocytes and either Iba-1 (1:200; Wako Pure Chemical Industries, Ltd., Richmond, VA) or OX-42 (1:100; Accurate Chemical Corp., Westbury, NY) for microglia. Other cell types in the white matter were identified with von Willebrand Factor (vWF) (10 μg/ml; Chemicon) for endothelial cells and myeloperoxidase (MPO) (1:250; Santa Cruz Biotechnology, Inc.) for neutrophils. After PBT rinse and blocking, biotin conjugated goat anti-rabbit and goat anti-mouse secondaries (1:500 Jackson ImmunoResearch Laboratories, Inc., West Grove, PA) were applied for 90 min. Slides were rinsed, peroxidases quenched with 0.3% H2O2 in methanol and incubated with the Vector Elite ABC solution (PK-6100, Vector Laboratories, Burlingame, CA) for 30 min at room temperature. The reaction was visualized using 3,3'-diaminobenzidine (DAB) (K3466, Dako North America, Inc., Carpinteria, CA). Sections were then counterstained with cresyl violet acetate (CVA) to identify Nissl substance. Slides were dehydrated through alcohols and xylene and coverslipped using DPX (Sigma-Aldrich). Negative controls were incubated without the primary antibody or with normal (non-immune) IgGs from the species of the host of the primary antibodies and failed to exhibit specific immunolabelling.

Oligodendrocyte Stereology

Stereology was performed using StereoInvestigator (Version 6, MicroBrightField Inc., Williston, VT) software controlling a motorized stage equipped Olympus BX-51 microscope. Employing the optical fractionator function of StereoInvestigator, we counted the oligodendrocytes in the medial corpus callosum and external capsule regions of white matter over a total distance of 3.0 mm rostral and caudal to bregma. The region of interest was delineated and overlaid with a grid size of 130 x 130 µm and the counting frame set at 50 x 50 µm for stereological quantification of cells. Slides for analysis were blinded to the investigator as to animal identity and reperfusion time. To ensure reliability of the count, an inter-rater reliability study was performed on a subset of the stereology slides. Three investigators counted the same slides using agreed upon morphological criteria and the same operating parameters in StereoInvestigator (Table 4.1).

Fluorescence Intensity Analysis

To compare various reperfusion time points and regions of interest, slides stained with IHC were analyzed for fluorescence staining intensity. All slides to be compared were stained together. Images were taken at the same exposure time for each section and changed to grayscale. Using NIH Image J software, the region of interest was outlined and the total mean fluorescence intensity of each region was recorded and compared to control staining and other reperfusion time points. Values are reported as fluorescence intensity.

Statistical Analysis

Data are expressed as standard error of the mean using Prizm 4.0 (Graph Pad, San Diego, CA). One-way ANOVA and post-hoc analyses were used to obtain p values. Statistical significance was set at $p < 0.05$.

4.4 Results

Oligodendrocyte Staining

The currently available antibodies used for OLG identification often label immature and *in vitro* OLGs, with inconsistent staining in mature, myelinating OLGs of *in vivo* tissue. CNPase, RIP, and CC-1 (APC) were used in both immunofluorescent and DAB staining to label OLGs. As seen in Fig. 4.1A, some but not all putative OLGs are stained using these antibodies, coinciding with findings from other laboratories (Barradas and Cavalcante, 1998, Dewar, et al., 2003, Foote and Blakemore, 2005). Other antibodies, including GST, O4, and MBP have also been tested in our lab with inconsistent staining of the OLG.

White Matter Cell Population

Besides OLGs, astrocytes, and microglia, the white matter tracts of the brain also contain neutrophils and endothelial cells. To exclude neutrophils or endothelial cells from the stereological OLG counts, we stained sections for neutrophils with MPO, and endothelial cells with vWF. These cells were excluded from the stereological counts due to their distinct morphological and population parameters (Fig. 4.1B).

Multiple Primary Immunohistochemistry

Using any of the above antibodies alone would have resulted in an underestimation of total numbers of OLGs. In order to get a more accurate reflection of the total number of OLGs in both normal and injured tissue, we used a combination of multiple antibody exclusion staining and morphometric identification of the OLGs in the white matter regions examined. Primary antibodies for astrocytes (GFAP) and microglia (OX-42 in rat and Iba-1 in mouse) were added together to exclude them from the stereological counts. With the OLGs stained with CVA, they could be distinguished from the DAB-positive astrocytes and microglia (Fig. 4.2). OLGs were classified as being CVA positive, DAB negative, and rounded cells less than 20 μm in cross sectional diameter.

Oligodendrocyte Stereology

Application of our method was conducted in healthy and ischemia injured mice and rats. To verify that our technique was reproducible, three investigators performed OLG stereology on six separate animals using optical fractionator (screen capture Fig. 4.3). Using morphological characteristics and excluding DAB-positive astrocytes and microglia, there was little variability among the results. In six regions of mouse tissue, OLG counts had a maximum coefficient of variation of 0.069 in all 6 areas. (coefficient of variation = standard deviation / mean).

To further demonstrate the efficacy of our technique, we compared stereological counts from CC-1 stained tissue with our combined morphological and multiple primary exclusion technique. Only a small percentage of the OLGs identified with CV

morphology were also identified with CC-1 IHC. With a linear regression slope of 0.07, this indicates approximately 7/100 OLGs identified with CV morphology were also labeled with the CC-1 antibody. Similarities were found in the decreased OLG counts with both methods, with the injured tissue having decreased cell counts in both methods, leading to a positive slope (Fig. 4.4). Spearman correlation value of $p=0.0078$ indicates a significant correlation between CC-1 stereology counts and our CV morphological stereology.

To demonstrate the applicability of our method in an injury model, we compared injured white matter with normal white matter in both global and focal ischemia in the mouse. We were able to see a significant reduction in the number of OLGs in the focal ischemia mouse external capsule white matter at 72 hours ($p<0.01$) with no changes in the sham operated animals (Fig. 4.5). In addition, following global ischemia there was a reduction in OLG counts at 3 and 7 days reperfusion ($p<0.05$) as compared to sham (Fig. 4.6A). Also, CC-1 fluorescence staining intensity shows decreased CC-1 immunoreactivity following 3 days reperfusion (Fig. 4.6B), correlating with stereological findings.

4.5 Discussion

The quantitation of total OLGs in the white matter is an invaluable technique that may be applied to various injury models in both animals and humans, including periventricular leukomalacia (PVL) (Kadhim, et al., 2006), perinatal white matter injury (PWMI) (Back, et al., 2007), vascular dementia (Rosenberg, et al., 2001), and multiple sclerosis (MS)

(Hauser and Oksenberg, 2006, Wolswijk, 2000). We have developed and experimentally tested a method of combining multiple primary IHC with morphological identification of cell bodies for OLG quantification in the white matter. This method proved to be reliable in tissue analysis of both focal and global ischemic white matter in the rodent. With the variability in the antibody specificity to OLGs, cell death quantitation in injury models has been a challenge. By using the Nissl CVA stain, we were able to visualize all of the cells in the healthy and injured tissue. With DAB immunostaining, we were able to label and thereby exclude both astrocytes and microglia, leaving the OLGs to count with stereology.

There has been a great deal of work in the analysis of OLG death and injury in the field of MS research. Many of the potential markers for OLGs have been tested and stain a population of the mature OLGs (Foote and Blakemore, 2005, Hauser and Oksenberg, 2006, Rinaldi and Gallo, 2005), with *in vitro* and developing OLGs staining more robustly. To get a clear idea of the injury pathways of OLGs, a morphological stain has shown to be effective in the MS literature. It is important to take into account the changing morphology of the OLG nucleus following injury to appropriately identify the mature, myelinating OLG. Immature OLGs and OLGs in a lesion typically present with a large, pale nucleus, while the mature healthy OLG has a small, dense nuclei (Wolswijk, 2000).

There are many antibodies currently available from various vendors to stain for OLGs with IHC. However, they are often specific to only certain components of these cells. For

example, the anti-MBP antibody stains a protein in the myelin sheath, but obscures the soma of the OLG. In some models of injury, including MS, there is a significant amount of demyelination without OLG cell body loss as characterized by relapse and recovery states of the disease (Hauser and Oksenberg, 2006). By staining the myelin, we would not get the appropriate analysis of cell death. CC-1 stains a percentage of the OLG nuclei in both injured and healthy tissue, but to get an accurate count of cell loss, all OLG nuclei should be identified. *In vitro* and immature OLGs have greater immunoreactivity and a higher percentage of OLG labeling. Their different morphology and immunostaining makes them distinct from mature, myelinating OLGs (Back, et al., 2007). Identifying these mature stage cells to measure their loss in injury pathways is essential.

The identification of most cell types within the white matter can be accomplished by a trained histologist using morphological characteristics to distinguish cells. However, immunologically differentiating between astrocytes, microglia, and OLGs can be difficult as the shape and protein expression of these cells can change following injury. IHC is an established method of cell identification and has been tested in healthy and injured tissue. By combining these two methods into one comprehensive cell quantitation technique, we are able to more correctly characterize OLG populations in healthy and injured white matter.

In conclusion, we propose an operational method for stereological quantification of OLGs in healthy and injured rodent brain white matter. We have applied this method in both focal and global ischemic injuries and shown significant changes in OLG numbers

in the external capsule white matter. This technique may also be applied to other models of injury to the white matter where a more accurate determination of OLG death is required.

Acknowledgements:

The authors would like to thank Dr. Yi Yang for technical assistance. Funding for this project was provided by the National Institutes of Health (5R01NS04547).

4.6 Figures and Legends

A CC-1 (APC) (40x) CNPase (40x) RIP (40x)

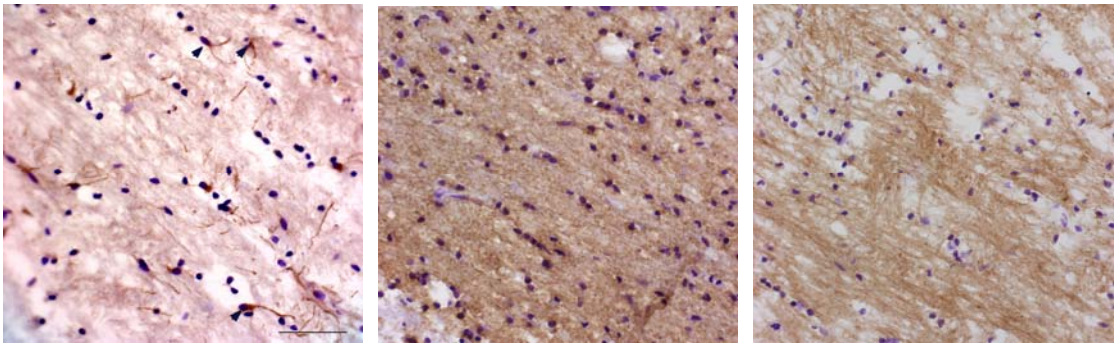

B

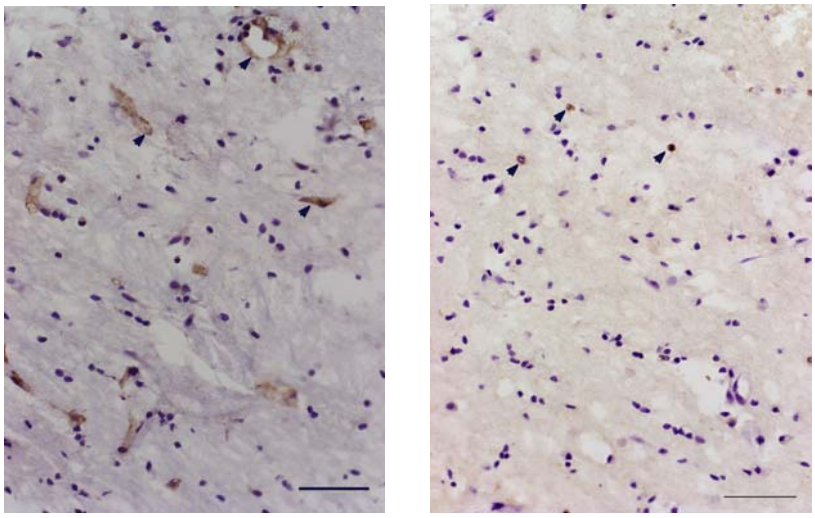

Endothelial Cells (VWF) Neutrophils (MPO)

Figure 4.1: A. OLG antibodies label various components of the OLG. CC-1(APC) labels some of the OLG cell bodies (40x), RIP and CNPase labels OLG processes (40x). All pictures were taken from 90min MCAO mice with 72h reperfusion. B. Morphology of endothelial cells and neutrophils in the white matter. VWF labels endothelial cells surrounding the blood vessels and only a few multinucleated neutrophils (MPO) are labeled (arrowheads). These cells can be excluded from OLG stereology. Scale Bars = 50μm.

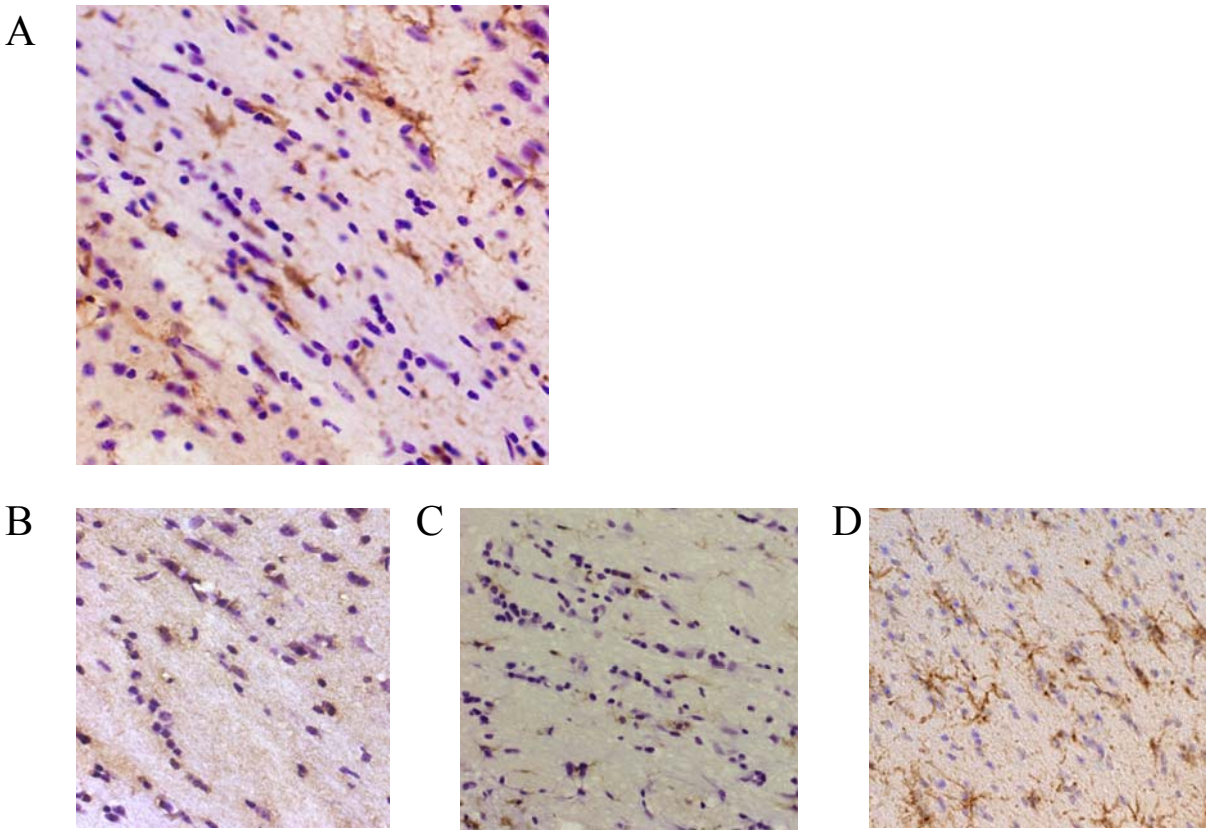

Figure 4.2: Stereology staining method for OLG identification in the white matter. A: GFAP/ Iba-1 multiple IHC staining with cresyl violet acetate (CVA) counterstain to exclude DAB-positive cells and count CVA-positive cells as OLGs. B: Mouse MCAO tissue labeled with Iba-1 for microglia/ macrophages. C: Rat tissue labeled with OX-42 to identify microglia/ macrophages. D: Mouse tissue labeled with GFAP for astrocytes.

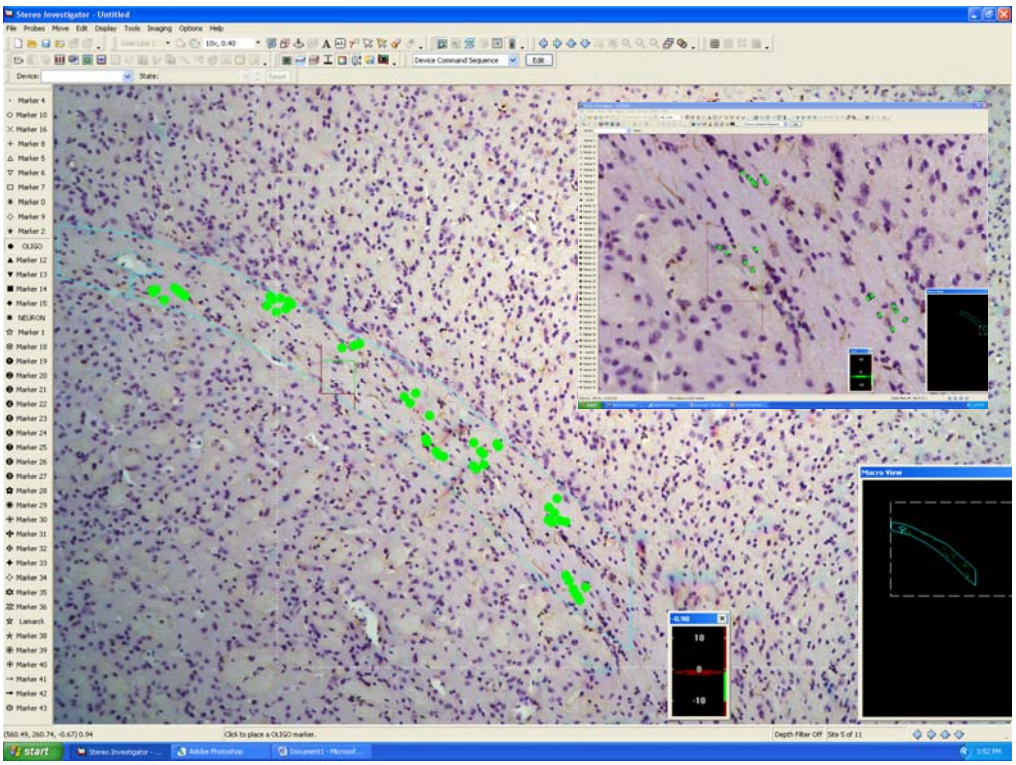

Figure 4.3: StereoInvestigator optical fractionator screen capture. Region of interest at 10x is outlined and OLGs labeled in counting frame with green. 40x inlay shows OLG counting.

Animal #	Investigator 1	Investigator 2	Investigator 3	Mean ± SD
1	231	219	244	231 ± 12.5
2	264	257	274	265 ± 8.5
3	83	89	88	87 ± 3.2
4	301	292	271	288 ± 15.4
5	237	258	232	242 ± 13.8
6	222	200	195	206 ± 14.4

Table 4.1: Inter- rater reliability of stereological counts from three investigators. Counts were done in the external capsule of mice with varying degrees of injury. Values are expressed as number of OLGs/mm^3 X 10^3.

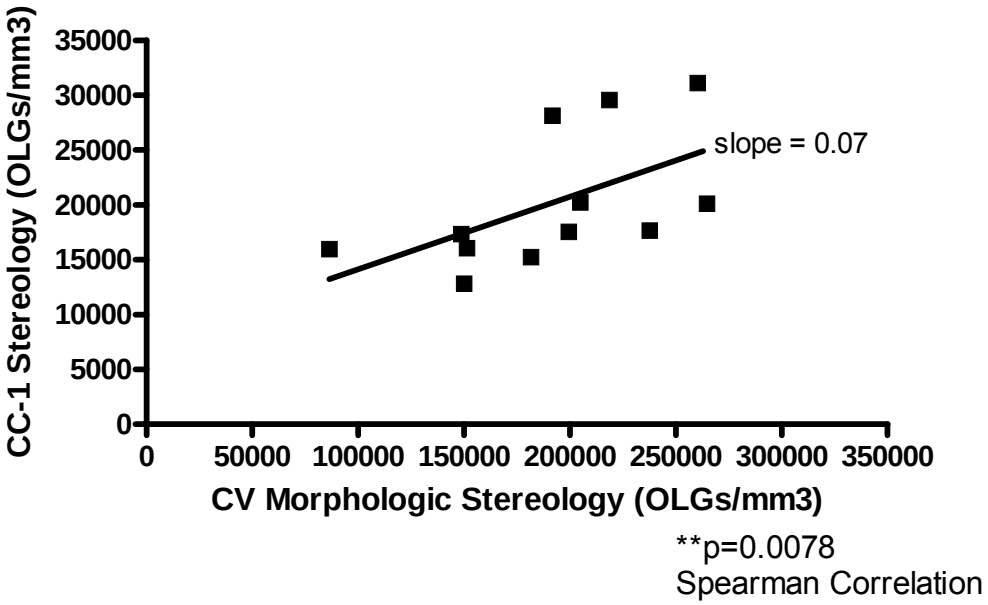

Figure 4.4: Comparison of CVA morphological analysis with CC-1 IHC identification of OLGs with quantification by stereology. CC-1 IHC vs. combined morphological and multiple primary exclusion technique (CV). Slope = 0.07 indicating 7/100 OLGs labeled with CV were labeled with CC-1. Spearman correlation **p=0.0078.

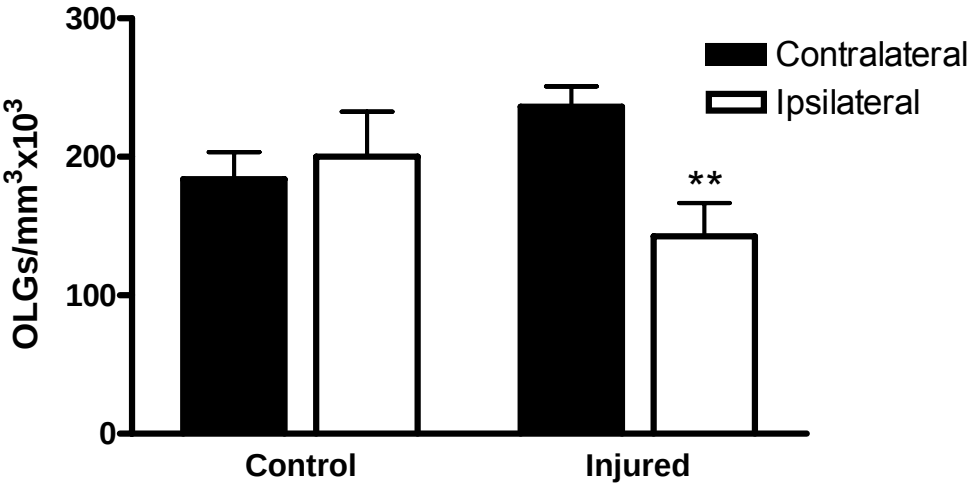

Figure 4.5: Oligodendrocyte stereology of injured mouse external capsule (EC) by MCAO with 72 h reperfusion demonstrating application of stereological morphology counting method. There was a significant loss of OLGs in the ipsilateral ischemic EC.

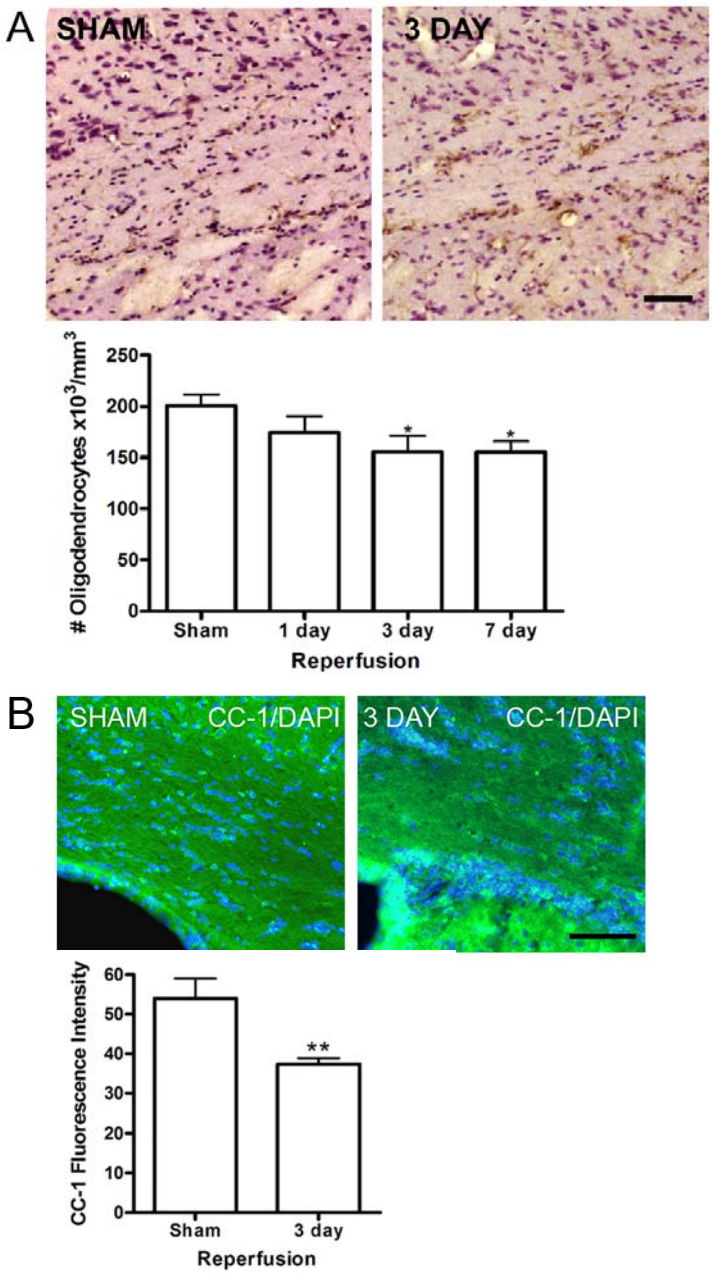

Figure 4.6: (from Chapter 5-Fig.5.5) Demonstration of OLG Stereology technique in a mouse model of transient global ischemia. A) OLG staining technique applied to Sham and 3 day reperfusion tissue. GFAP and Iba-1 (DAB, brown) with CVA counterstain for OLG identification. B) CC-1 (green) IHC staining with DAPI nuclear counterstain. Fluorescence intensity analysis demonstrates decreased CC-1 staining following 3 days reperfusion.

CHAPTER 5:

Divergent role for MMP-2 in myelin breakdown and oligodendrocyte death following transient global ischemia

Espen J. Walker [a,b] and Gary A. Rosenberg [a,b,c*]

Departments of Neurology [a], Neurosciences [b], and Cell Biology and Physiology [c],

University of New Mexico Health Sciences Center, Albuquerque, NM 87131

Walker, E.J. and Rosenberg, G.A., Journal of Neuroscience Research

submitted March 2009

5.1 Abstract

Delayed white matter injury to the brain consists of oligodendrocyte (OLG) death and myelin breakdown. In multiple sclerosis, stroke, and vascular dementia, there is increased expression and activity of matrix metalloproteinases (MMPs). With MMP gelatinase activity involved in various ischemic and white matter injury models, we hypothesized a role for MMP-2 (gelatinase A) in OLG death and myelin breakdown following transient global ischemia in the mouse. We found increased reactivity of astrocytes and microglia, MMP-2 localization in astrocytes, and increased protein expression and activity of MMP-2 in the white matter at 3 days of reperfusion. Loss of myelin basic protein (MBP) expression and caspase-3 mediated OLG death occurred following 3 days of reperfusion. Treatment with the MMP inhibitor, BB-94, decreased astrocyte reactivity, decreased MMP-2 activity, and reduced MBP breakdown. MMP inhibition had no effect on OLG loss. These results implicate MMP-mediated myelin breakdown and an MMP independent mechanism of OLG death following transient global ischemia.

5.2 Introduction

The white matter contains oligodendrocytes (OLGs) and myelin which are essential to the conduction of axonal signals throughout the brain. In the human, the white matter comprises almost half of the cortical volume (Miller, et al., 1980) and is sensitive to various injuries including stroke (Pantoni, et al., 1996), multiple sclerosis (MS) (Barnett and Prineas, 2004), and spinal cord injury (SCI) (Park, et al., 2004). Ischemic models of *in vivo* white matter injury to the rodent have demonstrated various damaging pathways

including glutamate excitotoxicity (Tekkok, et al., 2007), inflammatory cytokines (Schmitz and Chew, 2008) and protease activation (Rosenberg, et al., 2001). Following transient global ischemia in the mouse, there is evidence for a role of matrix metalloproteinases (MMPs) in delayed neuronal death (Lee, et al., 2004, Walker and Rosenberg, 2009). In addition, MMP-2 and MMP-9 have delayed expression in the glial cells following global ischemia (Magnoni, et al., 2004).

The gelatinases, MMP-2 and MMP-9, are increased in various models of ischemia. In focal ischemia, MMP-9 increases rapidly and has been shown to be involved in neuronal and white matter injury to the mouse (Asahi, et al., 2000, Asahi, et al., 2001), with MMP-2 not involved in this acute injury (Asahi, et al., 2001). In global ischemia, MMP-9 is involved in acute hippocampal neuronal injury (Lee, et al., 2004) but does not get expressed in the microglia or vascular epithelium of the white matter (Ihara, et al., 2001). MMP-2 and MMP-9 also contribute to caspase-mediated brain endothelial cell death following hypoxia-reoxygenation *in vitro* (Lee and Lo, 2004). With glial expression of MMP-2 and neuronal expression of MMP-9 in vivo (Magnoni, et al., 2004), the roles of these two gelatinases in global ischemia appear to be distinct.

MMPs are involved in the breakdown of myelin basic protein (MBP) and myelin associated glycoprotein (MAG) in various models of MS (D'Souza and Moscarello, 2006, Gijbels, et al., 1993). In an *in vitro* assay, MMP-2 was determined the most active enzyme in the degradation of MBP, followed by MMP-3 and MMP-9 (Chandler, et al.,

1995). MMP inhibition has been shown to reduce MMP-9 mediated MBP breakdown, glial activation, and cell death following spinal cord injury (Kobayashi, et al., 2008).

OLGs are sensitive to both *in vitro* and *in vivo* ischemia models (Petito, et al., 1998, Yoshioka, et al., 2000). There is evidence for an apoptotic mechanism of OLG death with caspase-3 positive cells in the white matter following SCI (Terayama, et al., 2007) and in MS (Hisahara, et al., 2003). The rat model of permanent global ischemia demonstrates white matter vulnerability (Tomimoto, et al., 2003) and there are implications for a role for MMP-2 in white matter damage and blood brain barrier (BBB) breakdown following chronic hypoperfusion in the mouse (Nakaji, et al., 2006). However, in the mouse model of transient global ischemia, the mechanisms of white matter damage are not understood.

Transient global ischemia leads to hypoxic hypoperfusion and has a delayed effect on the components of the white matter. We hypothesized that MMPs contributed to myelin breakdown and oligodendrocyte loss following transient global ischemia in the mouse. To test this hypothesis, we analyzed cell loss and expression of MMP-2. We measured MMP-2 activity, MBP expression and OLG cell bodies at 3 days reperfusion. We used MMP inhibition to reduce MBP loss, and stereological counting to assess OLG loss. We report a divergent role for MMPs in myelin and OLG cell body injury. Myelin breakdown was associated with MMP-2 activity. However, OLG cell death by a caspase-3 mechanism was independent of MMPs.

5.3 Materials and Methods

Transient Global Cerebral Ischemia and Tissue Processing

All experiments were approved by the University of New Mexico (UNM) Animal Care Committee and conformed to the National Institutes of Health Guide for the Care and Use of Animals in research. Transient bilateral common carotid artery occlusion (BCAO) was performed on the C57BL/6 mouse as described previously (Walker and Rosenberg, 2009). Briefly, both common carotid arteries were exposed, isolated, and clipped with metal aneurysm clips for 30 minutes. Cerebral blood flow was measured before, during, and after surgery with a Laser Doppler blood flow monitor (Moore Instruments Limited, Devon, UK) 3 mm caudal and 3 mm lateral to Bregma. Drug treated animals were administered 50 mg/kg BB-94 intraperitoneally as a suspension of 3 mg/ml in saline 30 minutes prior to surgery, 2 hours following surgery, and once daily on the second and third day. Controls received saline injections. Perfusion with PBS/0.1% Procaine followed by 2% PLP (2% paraformaldehyde, 0.1 M sodium periodate, 0.075 M lysine in 100 mM phosphate buffer at pH 7.4) was conducted intracardially. Brains were removed and immersed in 2% PLP overnight. The brains were cryoprotected with 30% sucrose in PBS, and frozen in OCT. They were stored at -80^{o} C until sectioned. For activity assays and immunoblotting, animals were perfused with PBS/0.1% Procaine, brains were removed and quickly frozen in 2-methylbutane.

Immunohistochemistry (IHC)

For fluorescence IHC, 10 μm sections were rehydrated through alcohols and PBS containing 0.1% Tween-20 (PBT). Nonspecific binding sites were blocked with PBT

containing 1% bovine serum albumin (BSA), and 5% normal serum. Slides were incubated overnight at 4°C with primary antibodies. Slides were washed in PBT and incubated for 90 min at room temperature with secondary antibodies conjugated with FITC and Cy-3 (1:500; Alexafluor 546 and Alexaflour 488, Invitrogen, Carlsbad, CA). Slides were incubated with 4'-6-diamidino-2-phenylinidole (DAPI) (Molecular Probes, Inc., Carlsbad, CA) prior to coverslipping to label cell nuclei. Slides were dehydrated through alcohols and xylene and coverslipped using DPX (Sigma-Aldrich). All IHC slides were viewed on an Olympus BX-51 bright field and fluorescence microscope (Olympus America Inc., Center Valley, PA) equipped with an Optronics digital camera and Picture Frame image capture software (Optronics, Goleta, CA). Primary antibodies used for IHC included glial fibrillary acidic protein (GFAP) for astrocytes (1:400; Sigma-Aldrich, St. Louis, MO), Iba-1 for microglia/ macrophages (1:400; Wako Pure Chemical Industries, Richmond, VA), MMP-2 (1:200; Chemicon, Temecula, CA), MMP-9 (1:200; Santa Cruz Biotechnology, Santa Cruz, CA), MBP (1:1000; Chemicon), CC-1 (APC) (1:20; Calbiochem, Gibbstown, NJ), and caspase-3 (1:100; Cell Signalling Technology, Danvers, MA).

Fluorescence Intensity Analysis

To compare various reperfusion time points and regions of interest, slides stained with IHC were analyzed for fluorescence staining intensity. All slides to be compared were stained together. Images were taken at the same exposure time for each section and changed to grayscale. Using NIH Image J software, the region of interest was outlined and the total mean fluorescence intensity of each region was recorded and compared to

control staining and other reperfusion time points. Values are reported as fluorescence intensity.

Oligodendrocyte Stereology

To assess OLG injury following transient global ischemia, 20 µm sections taken every 100 µm were rehydrated, rinsed, blocked, and incubated with primary antibodies for GFAP and Iba-1 for two nights at 4°C. Slides were then rinsed, blocked, and incubated with biotin conjugated secondary antibodies (1:500; Jackson ImmunoResearch Laboratories Inc., West Grove, PA) for 90 min at room temperature. Slides were rinsed in PBT, quenched in 0.3% H_2O_2 in methanol, rinsed, and exposed to the Vector Elite ABC solution. Slides were then rinsed, exposed to 3,3'-diaminobenzidine (DAB) for one minute, rinsed and counterstained with cresyl violet acetate (CVA). Slides were then rinsed, dehydrated through alcohols and xylene, and coverslipped with DPX (Sigma-Aldrich Chemicals, St. Louis, MO). Stereology of DAB-negative, CVA-positive round OLG cell bodies ≤10 µm in diameter (Pantoni, et al., 1996) was performed in the external capsule over a total distance of 3.0 mm using the optical fractionator function of StereoInvestigator software (Version 6, MicroBrightField Inc., Williston, VT) controlling a motorized stage equipped Olympus BX-51 microscope. The region of interest was delineated and overlaid with a grid size of 130 x 130 µm and counting frame set at 50 x 50 µm for stereological quantification of cells. Histological sections were blinded to the investigator as to animal identity and reperfusion time.

Gelatin Zymography

White matter regions of freshly isolated non-fixed tissue were collected by punch biopsy at -20°C and were homogenized in a lysis buffer containing 50 mM Tris-HCl pH 7.6, 150 mM NaCl, 5 mM $CaCl_2$, 0.05% Brij-35, 0.02% NaN_3, and 1% Triton X-100. MMP-2 and -9 present in the homogenates were concentrated with gelatin-sepharose 4B beads (Amersham Biosciences, Sweden). 500 µg of total protein in 500 µL buffer was incubated with 50 µL Gelatin-Sepharose 4B beads for 1 h at 4ºC with gentle rotation. The beads were collected and the gelatinases eluted by incubating with 50 µL elution buffer (10% DMSO in PBS) for 30 min at 4ºC with gentle rotation. Equal amount of samples (20 µL containing 200 µg of protein) were electrophoretically separated on 10% SDS-polyacrylamide gels co-polymerized with 1 mg/ml gelatin (Sigma-Aldrich) under non-reducing conditions. Gels were washed in 2.5% Triton X-100 for 20 min and then incubated for 72 hours with a developing buffer containing 50 mM Tris pH 7.6, 5 mM $CaCl_2$, 0.2 mM NaCl, and 0.02% Brij-35 at 37ºC. The gels were then stained with 0.125% Coomassie Blue R-250 for 1 hour in 10% acetic acid and 50% methanol. Gels were destained with 10% acetic acid until clear bands of gelatinolysis appeared on a dark blue background (2 days). The gels were dried and scanned for densitometry (Alpha Imager™ 2200; Alpha Innotech, San Leandro, CA). Molecular weights were determined by both protein standards (Bio-Rad Laboratories, Hercules, CA), and conditioned media from HT1080 human fibrosarcoma cells, a well-known source of MMP-2 and -9. Data is expressed as relative lysis units per microgram protein.

Immunoblotting

White matter tissue punches were collected by punch biopsy at -20°C and homogenized in lysis buffer described above. Protease inhibitors were added and samples were analyzed for protein expression by Western blot. Fifty μg of total protein was separated on 10% (12% for MBP) acrylamide gels. Proteins were transferred to polyvinylidene fluoride (PVDF) membranes, blocked, and incubated overnight at 4°C with primary antibodies against MMP-2 (1:500; Santa Cruz Biotechnology), MBP (1:500; Chemicon), and caspase-3 (1:1000; Cell Signalling). Membranes were incubated with HRP conjugated secondary antibodies (1:2000; Cell Signalling) and blots developed using chemiluminescent detection with the West Pico Kit (Pierce Biotechnology, Inc., Rockford, IL). Protein bands were visualized on X-ray film and densitometric analysis was used for semiquantitation of band intensities with AlphaEase image software (Alpha Innotech Corp.). Actin staining (1:7500 Sigma-Aldrich) on the same PVDF membranes was used to normalize protein loading and transfer. Results are reported as normalized band intensity for quantifying relative protein expression.

MMP-2 Activity Assay

MMP-2 enzymatic activity was measured with a fluorimetric assay using a 5-FAM/QXL™520 FRET peptide (Anaspec, San Jose, CA). In the intact FRET peptide, the fluorescence of 5-FAM was quenched by QXL™ 520. Upon cleavage into two separate fragments by the MMP-2 present in the sample, the fluorescence of 5-FAM was recovered and monitored at excitation / emission = 490 nm / 520 nm at 60 min in room temperature using a luminescence spectrometer (PerkinElmer LS55). Homogenized white

matter tissue samples with 100 µg protein were mixed with assay buffer (50 mM Tris-HCl, pH 7.6, 200 mM NaCl, 5 mM $CaCl_2$, 20 µM $ZnSO_4$, and 0.05% Brij-35) and fluorogenic substrate (1 µM final concentration) to a final volume of 200 µl. FL WinLab software was used to express data as relative fluorescence units.

Statistical Analysis

Statistical comparisons among groups were done using ANOVA with post-hoc analysis for multiple *t*- tests (Prism 4.0, GraphPad Software Incorporated). All data were presented as mean ± standard error of the mean (SEM). Statistical significance was set at $p<0.05$.

5.4 Results

Glial Inflammation following Transient Global Ischemia

Cerebral blood flow was reduced during transient global ischemia to 11.2 $\pm$ 1.1% of original flow and returned to 44.9 $\pm$ 6.3% following clip removal. To investigate the change in astrocyte and microglial expression in the hypoxic white matter following global ischemia, we stained coronal sections with GFAP or Iba-1 at various reperfusion time points and analyzed the stained tissue for fluorescence intensity. Astrocytosis increased in the white matter region at 1 day ($p<0.05$), 3 days ($p<0.01$), and 7 days ($p<0.01$) of reperfusion as compared to sham animals (Fig. 5.1A). In addition, the Iba-1 microglial staining increased in the white matter at both 3 days ($p<0.01$) and 7 days ($p<0.05$) reperfusion as compared to sham animals (Fig. 5.1B).

MMP Activity in Astrocytes

Immunohistochemistry demonstrated constitutive expression of MMP-2 in the astrocytes of the sham animals, which increased in the reactive astrocytes at 3 days of reperfusion (Fig. 5.2A). MMP-9 was rarely seen in the sham animals with some co-localization in the astrocytes following 3 days of reperfusion (Fig. 5.2B).

Gelatin zymography of white matter tissue punches demonstrated an increase in MMP-9 (98 kDa) expression, which was not significance following 3 days of reperfusion, while MMP-2 (72 kDa) had a significant increase ($p<0.05$) in expression at that time. We confirmed the expression of MMP-2 protein with Western blots, which demonstrated a significant increase in MMP-2 expression at 1 day ($p<0.01$), 3 days ($p<0.001$), and 7 days ($p<0.01$) of reperfusion (Fig. 5.3A). In addition, we performed a fluorimetric enzyme activity assay and found a significant increase ($p<0.05$) in MMP-2 activity at 3 days of reperfusion (Fig. 5.3B). A similar fluorimetric assay for MMP-3 showed no change in activity at all time points (data not shown).

Myelin Basic Protein Breakdown

MBP is a critical component of the myelin sheath produced by OLGs. As other models of white matter injury have shown a vulnerability of this protein to increased protease activity, we decided to investigate the changes in MBP following transient global ischemia. Immunohistochemistry for MBP shows a decrease in the staining of the white matter tract following 3 days of reperfusion (Fig. 5.4A). To quantify the change in MBP expression, we performed Western blots on white matter tissue punches. We found a

significant decrease in MBP expression at 3 days ($p<0.01$) and 7 days ($p<0.01$) of reperfusion for both the 21.5 kDa and 18 kDa isoforms of MBP (Fig. 5.4B), which corresponded with increased MMP-2 activity at 3 days of reperfusion.

Oligodendrocyte Death

Since MBP degradation occurred in our model, we investigated the effect of transient global ischemia on the OLG cell body. Stereological quantification of OLGs in the white matter demonstrated a significant reduction in the CVA-positive cell bodies at 3 days ($p<0.05$) and 7 days ($p<0.05$) of reperfusion (Fig. 5.5A). To confirm the morphological analysis, we also performed immunostaining of the mature oligodendrocyte marker, CC-1, in the white matter. Quantification of the mean fluorescence intensity of CC-1 confirmed the reduction in OLGs at 3 days of reperfusion ($p<0.01$) (Fig. 5.5B).

Caspases have been implicated in OLG death. Immunohistochemistry showed co-localization of the executioner caspase-3 with CC-1 following 3 days reperfusion, with minimal caspase-3 staining in the sham animals (Fig. 5.6A). This implicated an apoptotic mechanism of cell death in the OLGs. Quantification of caspase-3 with Western blots demonstrated a significant increase at 3 days ($p<0.05$) and 7 days ($p<0.05$) of reperfusion as compared to the sham (Fig.5.6B).

MMP Inhibition Protects Myelin Breakdown, not Oligodendrocyte Death

MMP inhibition has demonstrated protective effects in various models, including MS, SCI, permanent global ischemia, as well as transient global ischemia. We have previously

shown that treatment with the broad-spectrum MMP inhibitor, BB-94, protects hippocampal neuronal death following transient global ischemia in the mouse. Following treatment with BB-94 in our model, we found reduced astrocytosis and less MMP-2 activity in the white matter punches as compared to vehicle treated animals at 3 days of reperfusion (Fig. 5.7A). Immunohistochemistry of the white matter tissue shows an increase in MBP staining following BB-94 treatment as compared to vehicle (Fig. 5.7B). In addition, Western blots show reduced breakdown of the 21.5kDa isoform of MBP following BB-94 treatment as compared to vehicle ($p<0.05$) (Fig. 5.7C). With myelin protection, we proposed a reduction in OLG loss. However, following BB-94 treatment, there was no change in the immunostaining of CC-1 as compared to vehicle (Fig. 5.8A). In addition, caspase-3 Western blots of the white matter punches failed to show a significant change in caspase-3 expression following BB-94 treatment (Fig. 5.8B), suggesting that MMP inhibition had no effect on OLG death following 3 days of reperfusion.

5.5 Discussion

White matter damage is a component of various diseases and injury pathways. With the majority of research in transient global ischemia focused on neuronal loss, understanding the mechanisms of white matter injury to OLGs and myelin is important. Our data demonstrate delayed OLG death independent of MMPs and myelin breakdown that was associated with increased MMP-2 activity after 3 days of reperfusion. Inhibition of

MMPs resulted in myelin protection with no effect on OLG loss, implicating an MMP-mediated mechanism of myelin breakdown in transient global ischemia.

Comparison of various models of white matter injury shows some distinct differences between species, strain, and insult (Farkas, et al., 2007, Hagberg, et al., 2002). Specifically in global ischemia, the permanent carotid occlusion model in the rat leads to white matter damage after 7-14 days (Tomimoto, et al., 2003) lasting up to 13 weeks following injury (Farkas, et al., 2004). Permanent occlusion of both carotid arteries causes hypoxic hypoperfusion, which simulates chronic vascular disease in an aging population. In contrast, the mouse model of transient global ischemia represents acute brain injury as would occur following hypotension with cardiac arrest (Harukuni and Bhardwaj, 2006).

The physiological differences between the OLG cell body and myelin processes may be one of the reasons for our findings of differential effects of MMP activity on OLG death and myelin breakdown. NMDA receptor subunits are primarily found on the processes of the OLG and AMPA/kainate receptor subunits are found on the cell body (Salter and Fern, 2005). Blockage of AMPA/kainate receptors with antagonists in the *in vitro* optic nerve prevented white matter damage (Tekkok, et al., 2007), but is was essential to block both the NMDA and AMPA receptors to improve conduction in the myelinated axon following *in vitro* ischemia (Bakiri, et al., 2008). Distinguishing between the receptors found on the cell body and the process with OLG loss and myelin breakdown is crucial to understanding mechanisms of white matter injury.

MMPs are important in white matter injury (Kiaei, et al., 2007, Kobayashi, et al., 2008, Rosenberg, 2002). We found a significant increase in MMP-2 in tissue samples from the ischemic white matter, and an insignificant increase in MMP-9. Our findings are similar to those of others with MMP-2 emerging as the main candidate for white matter damage (Ihara, et al., 2001, Magnoni, et al., 2004, Nakaji, et al., 2006). A recent study suggested that MMP-9 was not involved in glial scarring following mild focal ischemia (Copin and Gasche, 2007).

We confirmed the increase in MMP-2 in the zymograms with Western blot and immunohistochemistry. Furthermore, we used a fluorogenic assay to demonstrate a significant increase in MMP-2 activity in the white matter. Inhibition of MBP breakdown with BB-94 supported the role for MMP-2 in white matter injury. Although MMP-9 was not significantly increased, we cannot rule out a role for MMP-9 in white matter injury since BB-94 is a broad-spectrum MMP inhibitor. Our studies are consistent with the earlier demonstration of reduced myelin damage in the MMP-2 knockout mouse (Nakaji, et al., 2006).

The ischemic injury led to expression of caspase-3 in the OLGs. This apoptotic cell death was shown to be independent of the myelin damage by MMP-2 with the use of an MMP inhibitor. Our findings show an effect on myelin breakdown, but not OLG death following treatment with BB-94. Separating myelin injury by MMP-2 from OLG death processes was a novel finding in our study (Fig. 5.9). Several other pathways of OLG death could be occurring in our model including oxidative stress (Scott, et al., 2003),

inflammation (Barnett, et al., 2006), or glutamate toxicity (Goldberg and Ransom, 2003). Independent mechanisms and timing of OLG death vs. demyelination have been proposed in other models (Jamin, et al., 2001, Merrill and Scolding, 1999), with our data supporting a distinction in this regional specific injury.

In conclusion, our data provide evidence for hypoxia-induced delayed OLG death and MMP-mediated MBP breakdown at 3 days of reperfusion in transient global ischemia in the mouse. There was increased reactivity of astrocytes and microglia, implicating an inflammatory pathway. MMP inhibition reduced astrocytosis, myelin breakdown and MMP-2 activity, suggesting involvement of MMPs in myelin disruption. On the contrary, caspase-mediated OLG apoptosis was unaffected by MMP inhibition, suggesting MMP-independent mechanisms.

5.6 Figure Legends

Figure 5.1: Inflammation of astrocytes and microglia in the white matter. A) GFAP-positive astrocytes (FITC, green) increased at 3 days as compared to sham in white matter tract. DAPI (blue) counter stain for nuclei. Quantification of fluorescence intensity demonstrates increased GFAP reactivity at 1 day (*$p<0.05$), 3 days (**$p<0.01$) and 7 days (**$p<0.01$) of reperfusion (n=10 for 3d; n=8 for Sham, 1d, and 7d). B) Iba-1 positive microglia/macrophages increased at 3 days as compared to sham. Quantification of fluorescence intensity demonstrates increased Iba-1 reactivity at 3 days (**$p<0.01$) and 7 days (*$p<0.05$) of reperfusion (n=8/group). Scale Bars: 50 µm.

Figure 5.2: MMP expression in astrocytes and gelatin zymography. A) MMP-2 (Cy3 red) co-localizes with GFAP-positive astrocytes (green) at sham and 3 days of reperfusion. B) No MMP-9 (red) expression in sham and minimal MMP-9 expression at 3 days of reperfusion in GFAP-positive astrocytes (green). DAPI (blue) counter stain for nuclei. Scale Bars: 50 µm. C) Gelatin zymography shows increased expression of MMP-9 (98 kDa), with a significant increase in MMP-2 (72 kDa) expression following 3 days of reperfusion (n=6/group).

Figure 5.3: MMP-2 expression and activity in white matter tissue punches. A) Western blot quantification of 72 kDa MMP-2 protein demonstrates increased expression at 1 day (**$p<0.01$), 3 days (***$p<0.001$), and 7 days (**$p<0.01$) of reperfusion. Protein loading normalized with actin (n=5 for Sham; n=4 for 1d, 3d, 7d). B) MMP-2 activity assessed

with a fluorometric assay shows increased activity at 3 days reperfusion (*p<0.05) (n=10 for Sham, 7d; n=7 for 1d, 3d).

Figure 5.4: MBP staining and protein expression. A) Immunohistochemistry for MBP decreases following 3 days reperfusion. Scale Bar: 50 µm. B) Western blotting quantification of 21.5 kDa and 18 kDa MBP isoforms shows loss of myelin at 3 days (**p<0.01) and 7 days (**p<0.01) of reperfusion in both bands. Protein loading normalized with actin (n=9 for Sham, 3d; n=8 for 1d; n=6 for 7d).

Figure 5.5: OLG stereology and staining analysis. A) White matter tracts stained with GFAP and Iba-1 (DAB, brown) and counterstained with nuclear stain CVA (purple) for histological analysis shows a decrease in OLG cell bodies at 3 days of reperfusion. Stereology of CVA-positive OLGs was reduced at 3 days (*p<0.05) and 7 days (*p<0.05) of reperfusion as compared to sham animals (n=14 for Sham; n=10 for 1d; n=12 for 3d, 7d). B) Confirmation of morphological analysis with immunohistochemistry and fluorescence intensity analysis shows decreased CC-1 positive cells (green) in the white matter and reduced fluorescence intensity at 3 days of reperfusion (**p<0.01) as compared to sham (n=8/group). DAPI (blue) counter stain for nuclei. Scale Bars: 50 µm.

Figure 5.6: Caspase-3 staining and protein expression. A) Co-localization of caspase-3 (red) with CC-1 (green) positive cells increased following 3 days of reperfusion. DAPI (blue) counter stain for nuclei. Scale Bar: 50 µm. B) Western blot quantification of 34kDa caspase-3 band in white matter punches shows increased expression at 3 days

(*p<0.05) and 7 days (*p<0.05) of reperfusion as compared to sham. Protein loading normalized with actin (n=9 for Sham, 1d; n=6 for 3d, n=8 for 7d).

Figure 5.7: MMP inhibition reduces astrocytosis and protects myelin following 3 days of reperfusion. A) GFAP-positive astrocytes (green) decreased following BB-94 treatment as compared to vehicle. DAPI (blue) counter stain for nuclei. Fluorescence intensity analysis confirms significant reduction in GFAP intensity (***p<0.001) (n=8/group). MMP-2 activity was also reduced following BB-94 treatment (n=8/group). B) Immunohistochemistry for MBP shows increased staining following BB-94 treatment. C) Western blot quantification of MBP expression shows a significant increase in the 21.5 kDa band (*p<0.05), with a non-significant increase in the 18 kDa band (n=8/group). Scale Bars: 50 µm.

Figure 5.8: MMP inhibition does not affect OLG death. A) Immunohistochemistry of CC-1 positive cells (green) in the white matter shows no difference following BB-94 treatment as compared to vehicle. DAPI (blue) counter stain for nuclei. Scale Bar: 50 µm. Fluorescence intensity analysis confirms no significant difference between BB-94 and vehicle treated mice following 3 days reperfusion (n=8/group). B) Western blot quantification of 34kDa caspase-3 band in white matter punches also shows no significant difference between BB-94 and vehicle treated mice. Protein loading normalized with actin (n=8/group).

Figure 5.9: Proposed model of white matter injury. Following global ischemia induced hypoxia, astrocytes become reactive and express MMP-2. MMP-2 activity leads to loss of MBP. BB-94 treatment inhibits MMP-2 and reduces myelin loss. OLGs express caspase-3 following hypoxia leading to cell death. BB-94 treatment does not appear to affect caspase-3 expression or CC-1 staining in the white matter following 3 days of reperfusion.

5.7 Figures

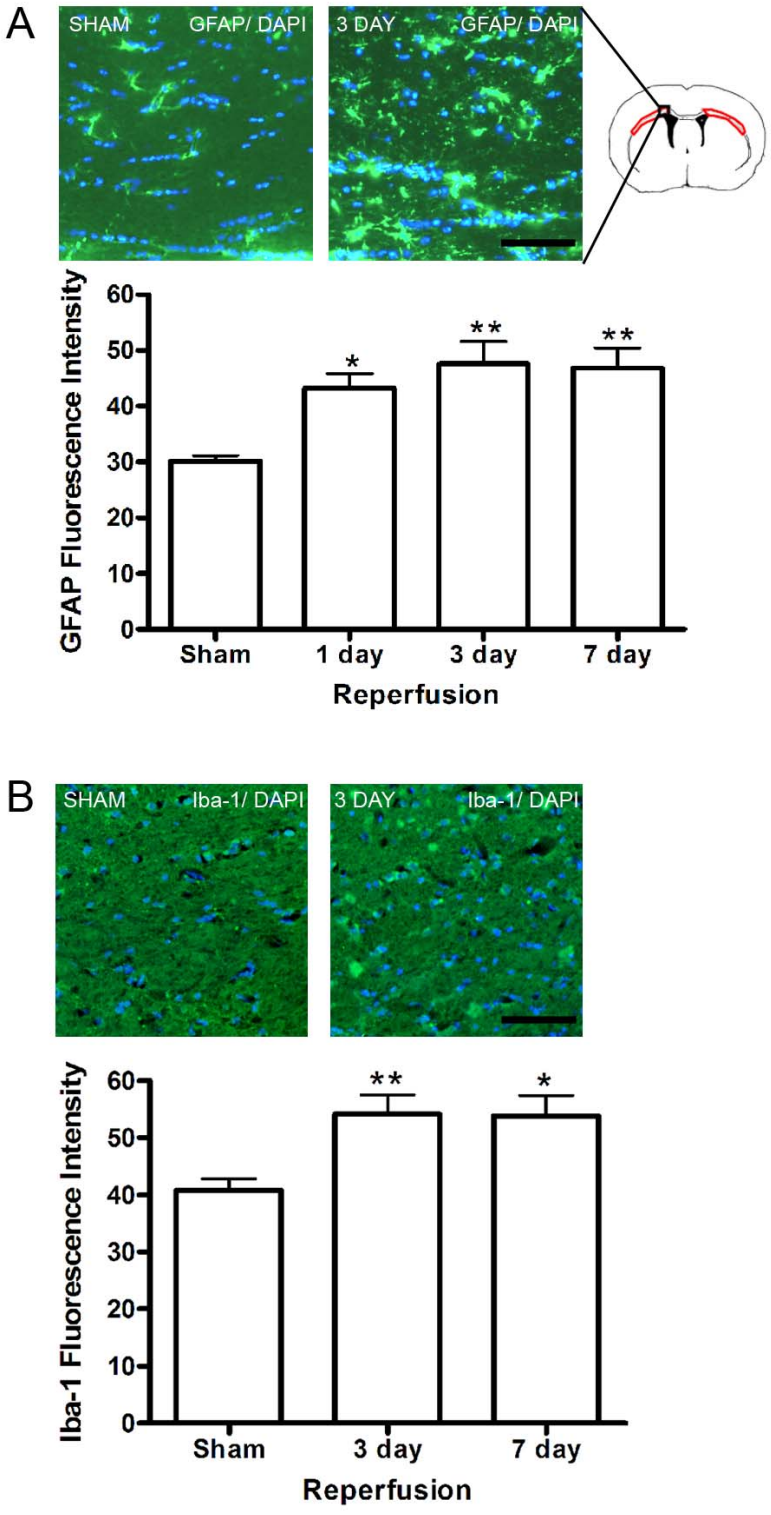

Figure 5.1: Inflammation of astrocytes and microglia in the white matter.

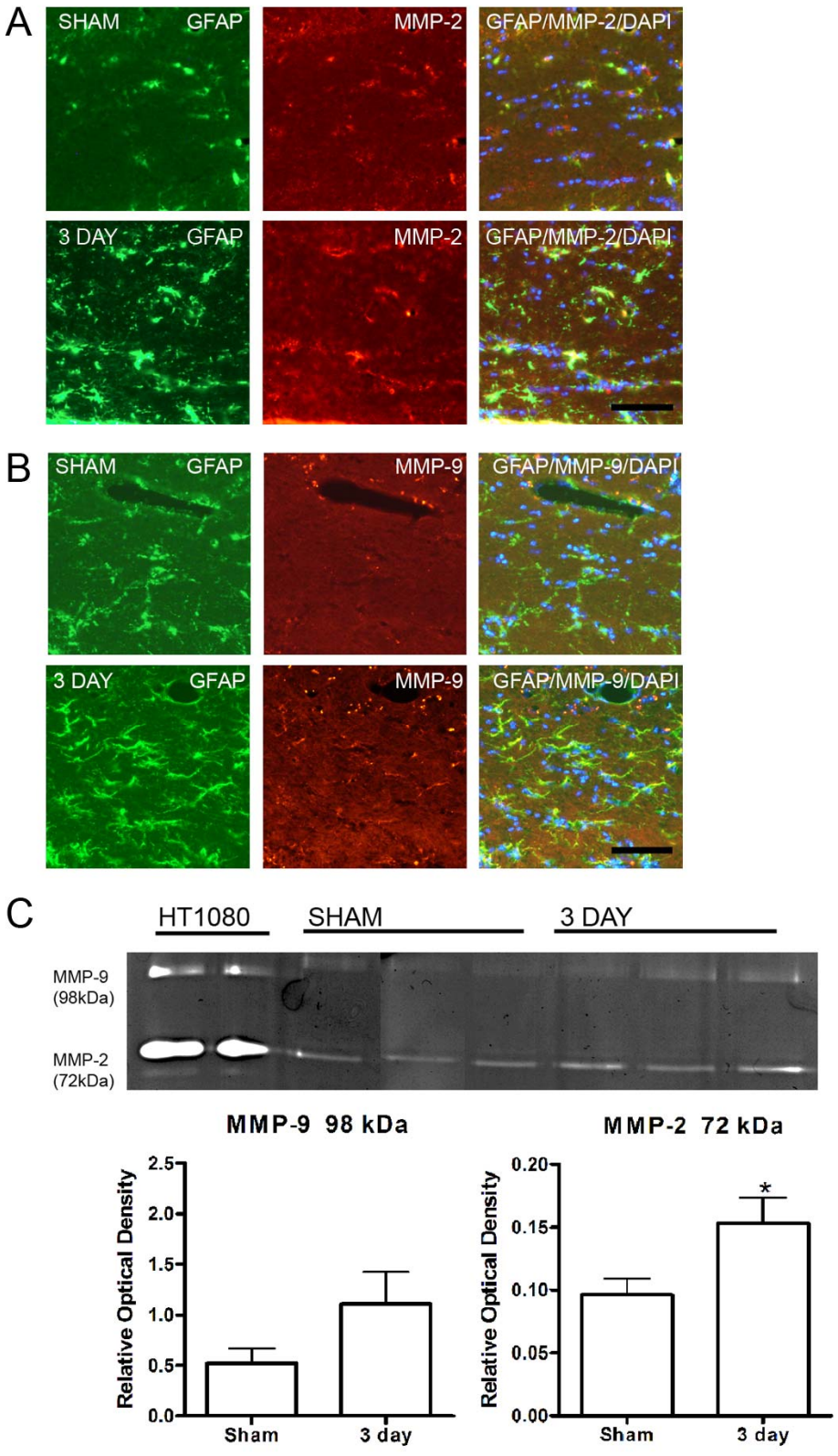

Figure 5.2: MMP expression in astrocytes and gelatin zymography.

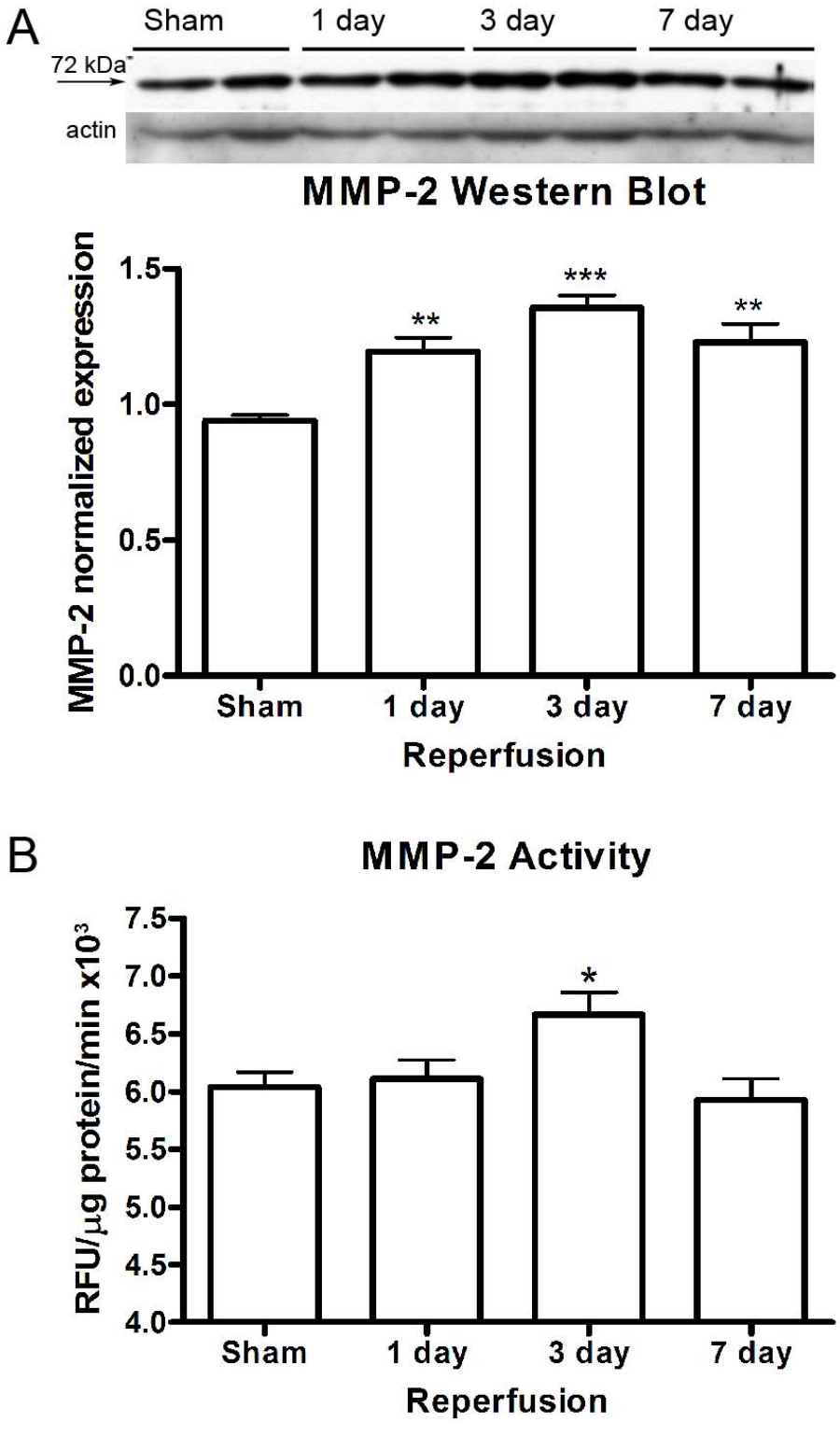

Figure 5.3: MMP-2 expression and activity in white matter tissue punches.

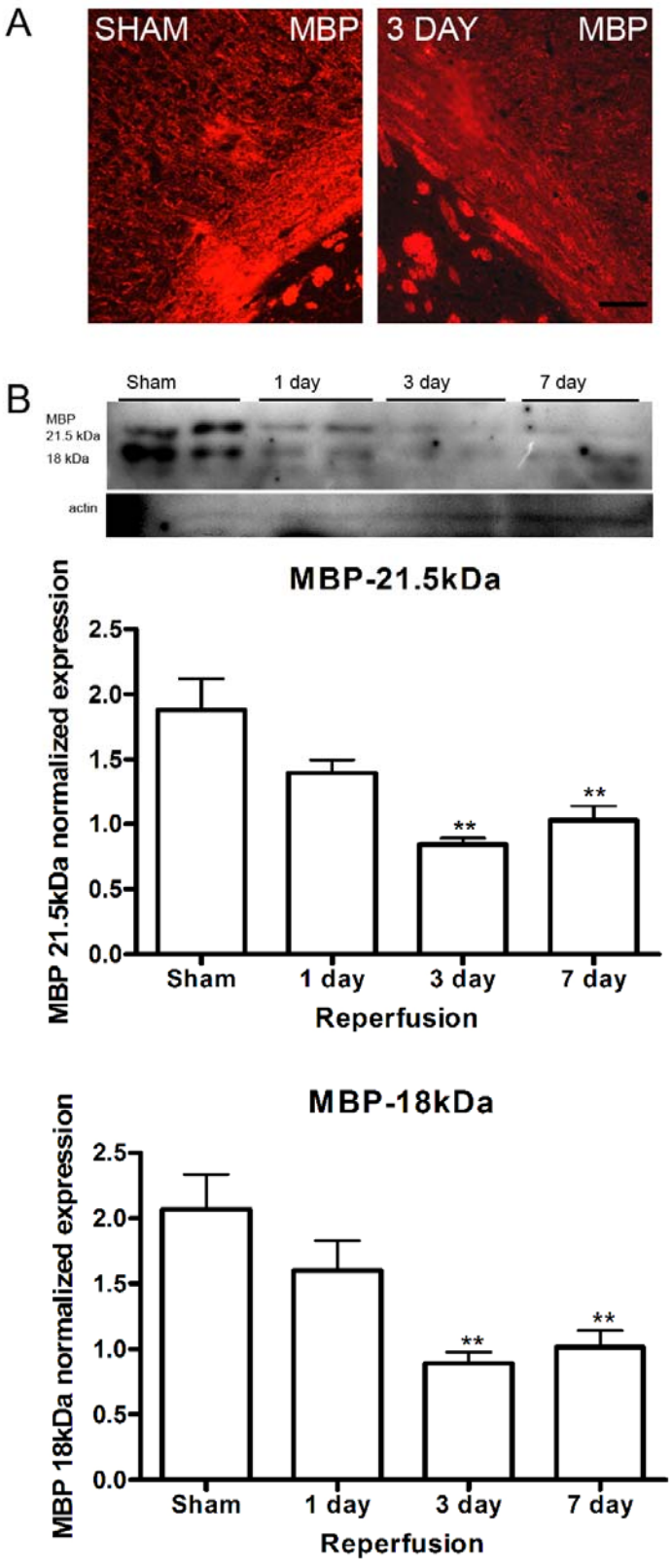

Figure 5.4: MBP staining and protein expression.

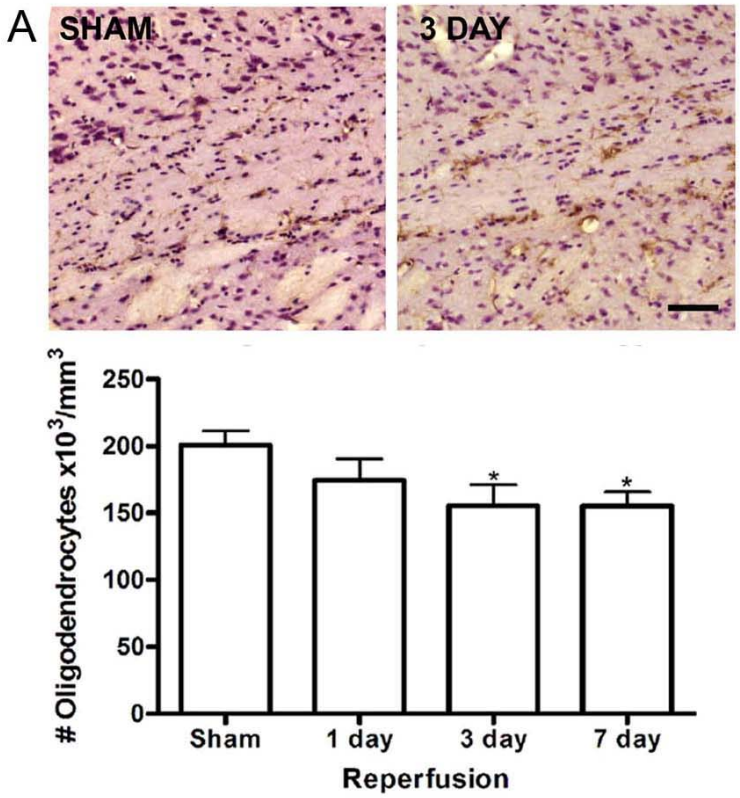

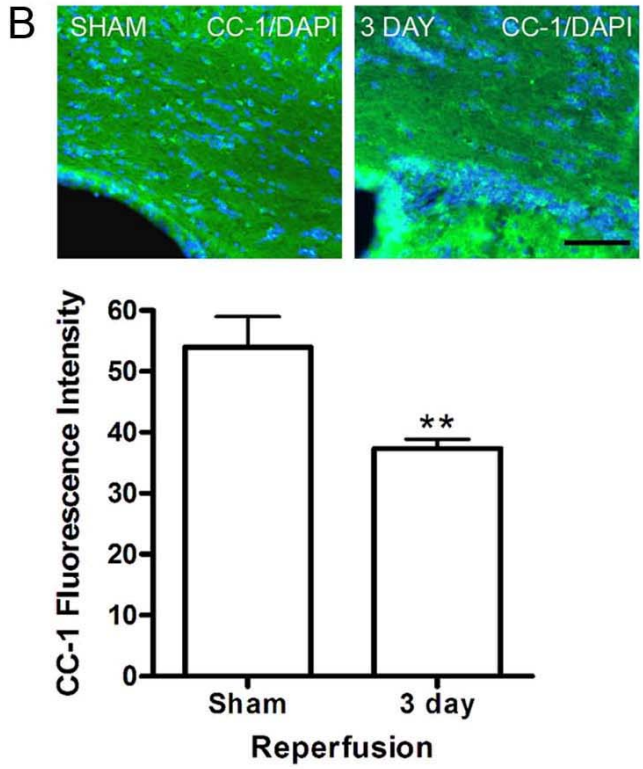

Figure 5.5: OLG stereology and staining analysis.

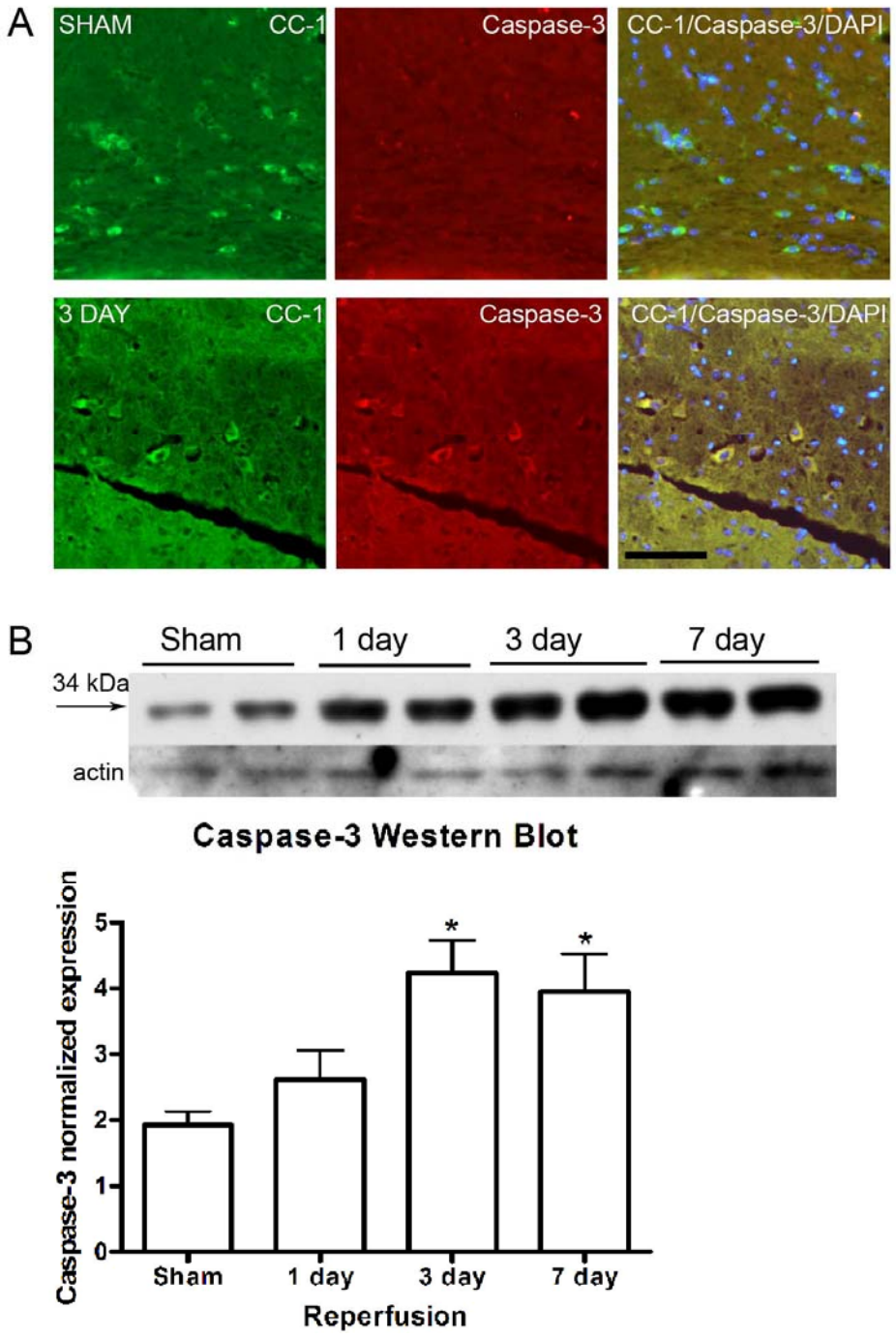

Figure 5.6: Caspase-3 staining and protein expression.

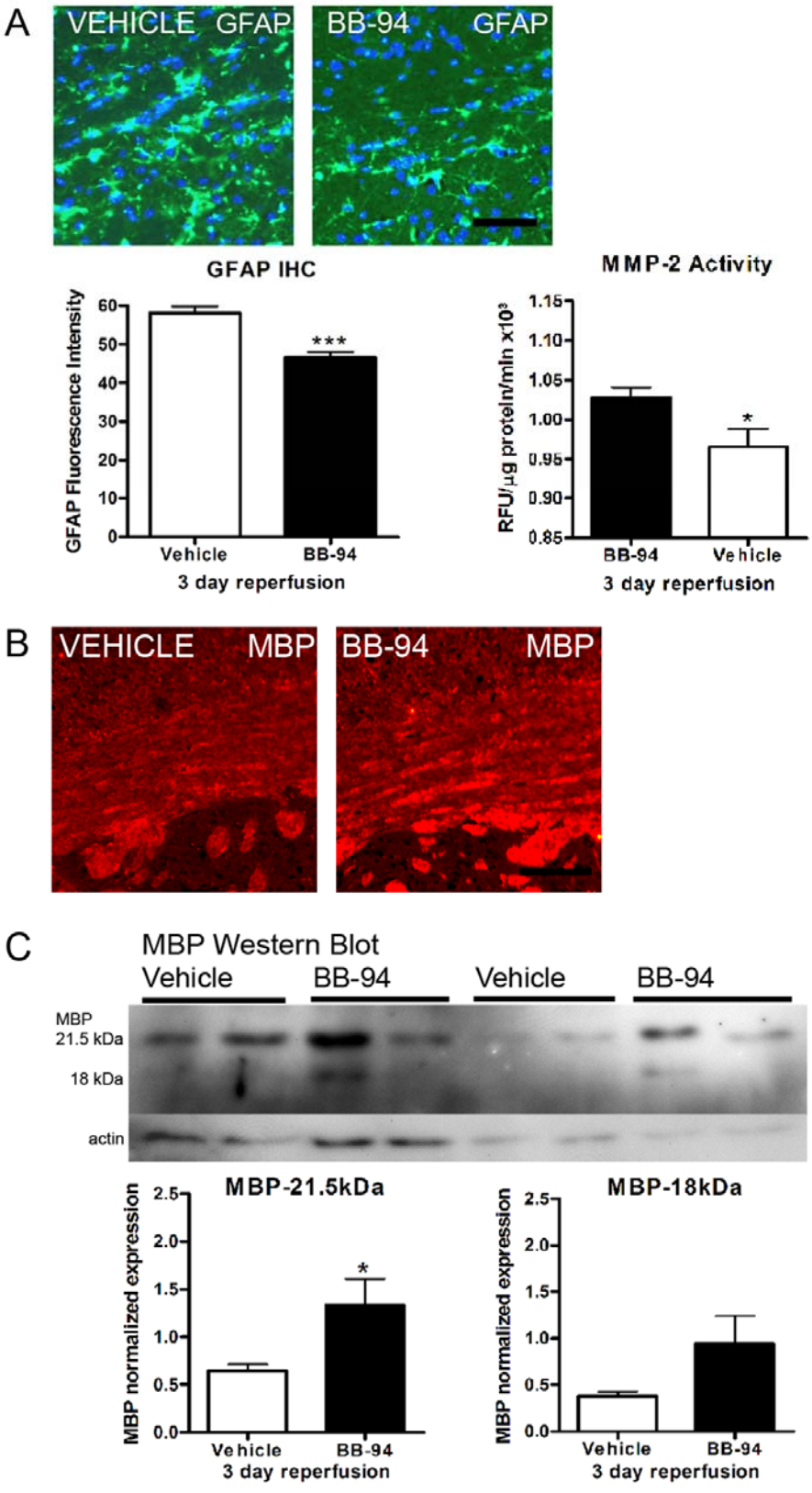

Figure 5.7: MMP inhibition reduces astrocytosis and protects myelin loss.

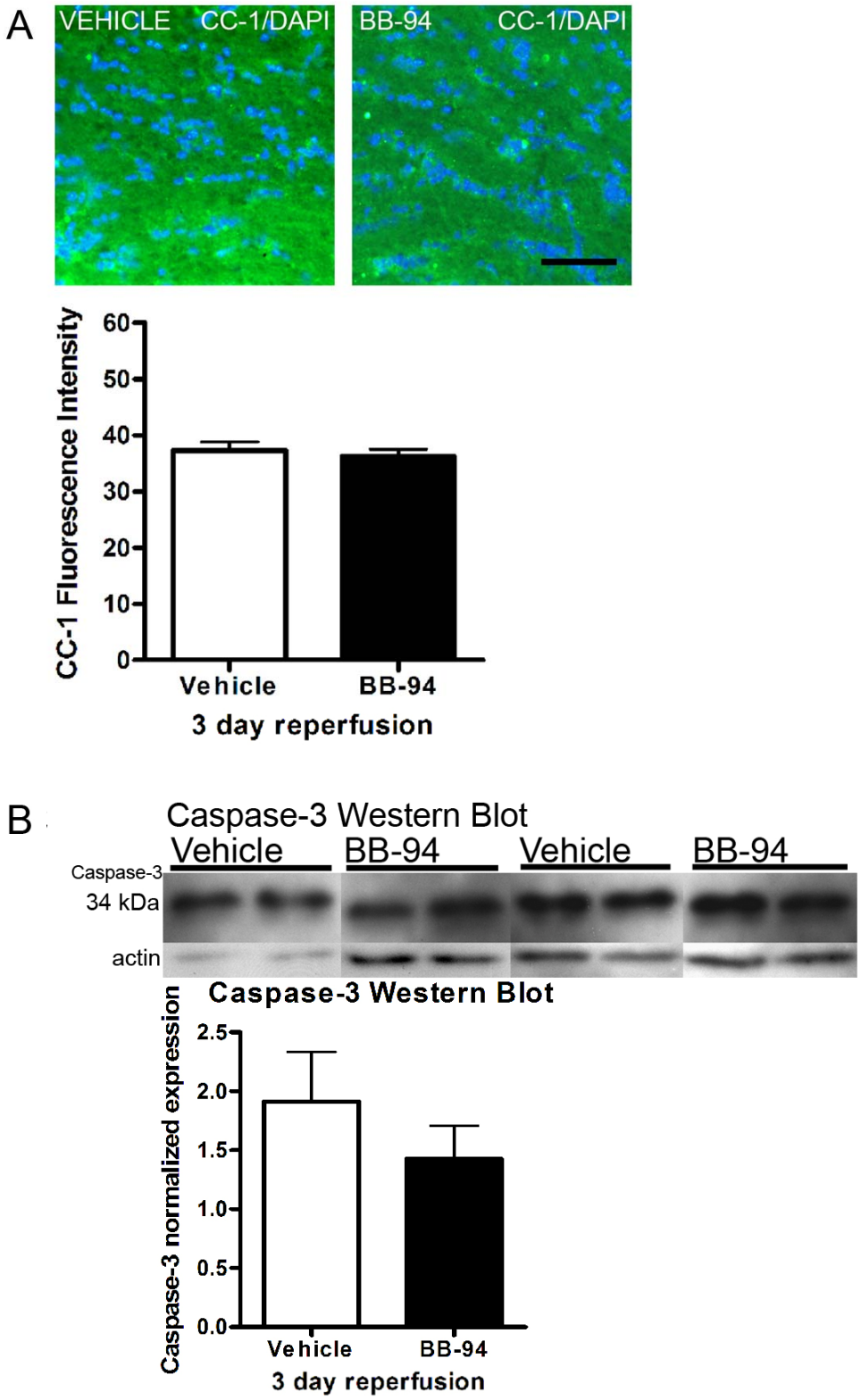

Figure 5.8: MMP inhibition does not affect OLG death.

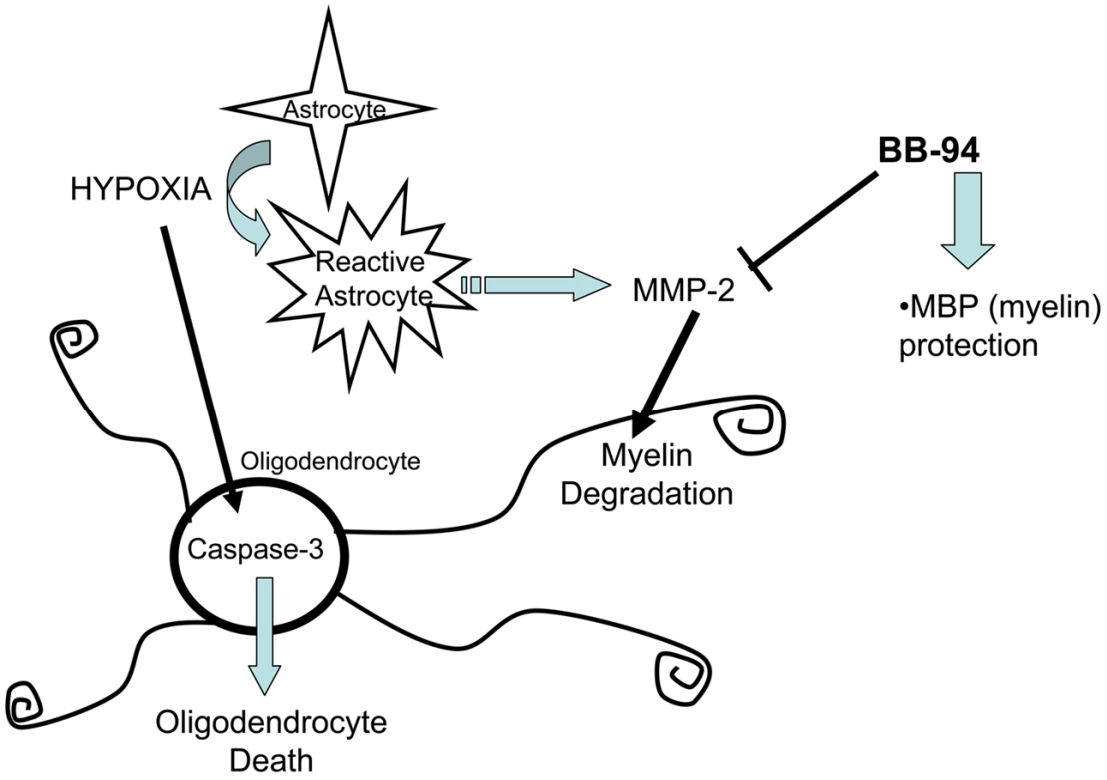

Figure 5.9: Proposed model of white matter injury.

CHAPTER 6:

Discussion

Following characterization of a novel model of transient global cerebral ischemia in the mouse, we describe a role for MMPs and TIMP-3 in delayed neuronal and white matter injury. As this was a new model for our lab, there was a great deal of preliminary investigations needed to confirm that the injury was consistent. Once the model was developed, we used it to test various hypotheses about the role of MMPs and their inhibitors in delayed cell death.

We studied the role of TIMP-3 and MMP-3 in transient global ischemia using knockout mice. In the hippocampus, we demonstrate inflammatory pathways marked by increased reactivity of astrocytes and microglia. Knockout of the *Timp-3* gene showed that it was a mediator of death receptor regulation, while knockout of MMP-3 resulted in reduced activation of microglia and less TNFα expression. These two pathways converged on the neuron, leading to delayed death following 7 days of reperfusion.

With a need for more detailed analysis of OLG cell loss in the white matter, we developed and verified a technique to quantify OLGs in the white matter using a combination of morphological and IHC techniques for stereological counting. With these tools we were able to perform quantification of the white matter and hypothesize a role for MMP-2 in white matter injury to both the myelin and OLG. Our data supported a role

for MMP-2 in myelin loss, and inhibition of MMPs with BB-94 further demonstrated an MMP-mediated MBP loss, with no effect on the observed OLG death.

6.1 Gray and White Matter Injury

These two studies of the hippocampus and white matter were done in parallel, with two regions of the same animal used for separate studies. This was useful to allow for reduced animal use, but it also had another benefit. By studying two pathways within the same animal, correlations and implications can be made as to the interactions between these two regions. In addition, with disparate mechanisms and timing of reperfusion injury it appears there are indeed separate mechanisms of injury occurring in these two locations within the brain.

We provide evidence for regional specific injury to the hippocampus and white matter following transient global cerebral ischemia in the mouse. With delayed myelin breakdown and oligodendrocyte loss at 3 days of reperfusion and neuronal loss following 7 days of reperfusion there appears to be distinct characteristics of these regions in the brain. Different strains of mice have shown variable sensitivity to 20 minutes of transient global ischemia, with the C57BL/6 mice having the greatest sensitivity (Yang, et al., 1997). Another group described that variability in the patency of the posterior communicating artery was a contributing factor in determining sensitivity to transient occlusion of the carotid arteries, with the C57BL/6 mice being more sensitive to BCAO than MF1 mice (Kelly, et al., 2001). With vasculature clearly playing a role in injury

sensitivity, this could be a reason for the regional sensitivity of both the hippocampus and white matter regions.

6.2 BCAO Model of Injury

The transient global ischemia model in the mouse has been described and used as a model for hypoxic hypoperfusion and reperfusion injury for many years. However, studies using the model have great variability in the choice of time of occlusion and reperfusion. One group has described a period of 15 minutes of occlusion leading to significant neuronal injury (Terashima, et al., 1998), with another study on strain differences using 20 minutes of occlusion (Yang, et al., 1997). Other groups have determined 17 minutes of occlusion led to a consistent neuronal injury (Magnoni, et al., 2004). Some labs, including our own, decided to test various occlusion time points of occlusion up to 40 minutes to obtain the most consistent injury (Kelly, et al., 2001, Lee, et al., 2004, Walker and Rosenberg, 2009). It is important that the injury is extensive and consistent, without increased mortality rates that can occur after approximately 1 hour of occlusion.

The appropriate reperfusion time is also a factor to consider when trying to determine maximal injury. As we and others have demonstrated, there is regional sensitivity following BCAO. There is regional specificity within the CA regions of the hippocampus. The CA1 has been the more commonly described sensitive region in both mouse and rat models of global ischemia (Lee, et al., 2004, Rivera, et al., 2002), but the CA2 region has also emerged as a region with even greater sensitivity in our own lab

(Walker and Rosenberg, 2009), as well as others (Magnoni, et al., 2004). The variability of reperfusion timing to achieve neuronal injury has varied from 8 hours (Terashima, et al., 1998) to 7 days of reperfusion (Oguro, et al., 2001). Clearly there is variability in occlusion and reperfusion timing to produce hippocampal injury and care must be taken when using this model.

Within the white matter, there is less literature describing the timing of injury. In the rat, global ischemia has led to glial reactivity from 3 days (Sugawara, et al., 2002), up to 30 days (Lee, et al., 2006). In the mouse, glial reactivity has been described starting around 1 day (Walker and Rosenberg unpublished findings) to around 3 days of reperfusion (Magnoni, et al., 2004). Determining the appropriate timing to analyze white matter injury may vary between labs as hippocampal injury has. Complete timeline studies will help target when and where the injury of interest is occurring.

6.3 MMP Inhibition

Use of the MMP inhibitor at a delayed time point in our studies of the hippocampus allowed for isolation of the delayed MMP mechanisms. We are proposing in Chapter 3 that through delayed MMP-3 inhibition, there is a decrease in cell death to the neurons and oligodendrocytes, respectively. However, other groups have demonstrated MMP-9 to be involved in neuronal death at 3 days. By inhibiting all MMPs with a broad-spectrum inhibitor such as BB-94, the inhibition of MMP-9 will also occur and we therefore cannot rule out the effects of MMP-9.

A more specific MMP inhibitor could be used to isolate the separate MMP pathways. One potential inhibitor is SB-3CT, a MMP-2 and MMP-9 specific inhibitor, which could be administered to inhibit gelatinolytic activity, while still allowing the effects of other MMPs. Overall, there are many pathways involved in this neuronal death. By inhibiting one pathway, there may be an increase in another. By isolating these mechanisms as best we can, we can start to getter a better understanding of why these cells die.

From Chapter 5, we provide evidence of OLG death and myelin injury following BCAO-induced global ischemia. We propose this to be due to the effects of MMP-2 as both the expression and activity of MMP-2 are increased at the same time as the observed myelin breakdown and OLG death. However, the connection between these events is only correlative and we cannot rule out other mechanisms involved in this observed injury. As there is not a lot of literature describing this injury to the mouse white matter, further studies may be able to shed light onto these delayed white matter effects.

Other potential mechanisms may include an effect of MMP-9 on the myelin damage as it also is involved in MBP degradation (Chandler, et al., 1995). In the white matter tissue collected however, there were no significant increases in MMP-9 analysis by gelatin zymography.

Also, as MMP-9 seems to be involved in neuronal injury in this model (Lee, et al., 2004, Magnoni, et al., 2004), it could be involved in the oligodendrocyte death as well. Further

studies into the role of the MMP-2 and MMP-9, including MMP knockout animals would help clarify the role for these gelatinases in white matter damage.

6.4 Significance

Looking at the role of MMPs and TIMP-3 in gray and white matter ischemia in the rodent has helped us get a better understanding of the mechanisms of cell death in this model. Each of these findings, from model development and hippocampal injury to OLG loss and myelin breakdown, provides insight into the potential pathways of cellular damage that occur following transient global ischemia in the mouse. Ideally, these findings can be applied to human studies and develop treatments for patients affected by this injury. However, this is only one study in an animal model that is still under investigation by the scientific community.

If these studies are verified, the next potential step would be to take the results obtained and apply them to cell death in the human brain following cardiac arrest or hypotension in a surgical procedure. Analyzing human tissue for MMPs, TNFα, and TIMP-3 will determine if the animal and culture models are a good representation of human injury models. Eventually, drugs can be tested in animals and humans to inhibit the detrimental or enhance the beneficial pathways implied by our findings.

The data collected for this project has described some interesting potential pathways of cell injury to both the gray and white matter following global cerebral ischemia in the mouse. We provide novel findings of both TIMP-3 and MMP-3 involved in delayed

inflammation and hippocampal neuronal death. We also provide evidence implicating MMP-2 in the breakdown of myelin, but not involved in OLG cell loss. These two primary studies are intended to build upon the current knowledge of global ischemic mechanisms and contribute to the broader understanding of how to eventually reduce the cell death that occurs following this injury.

Appendix: Additional Supporting Data

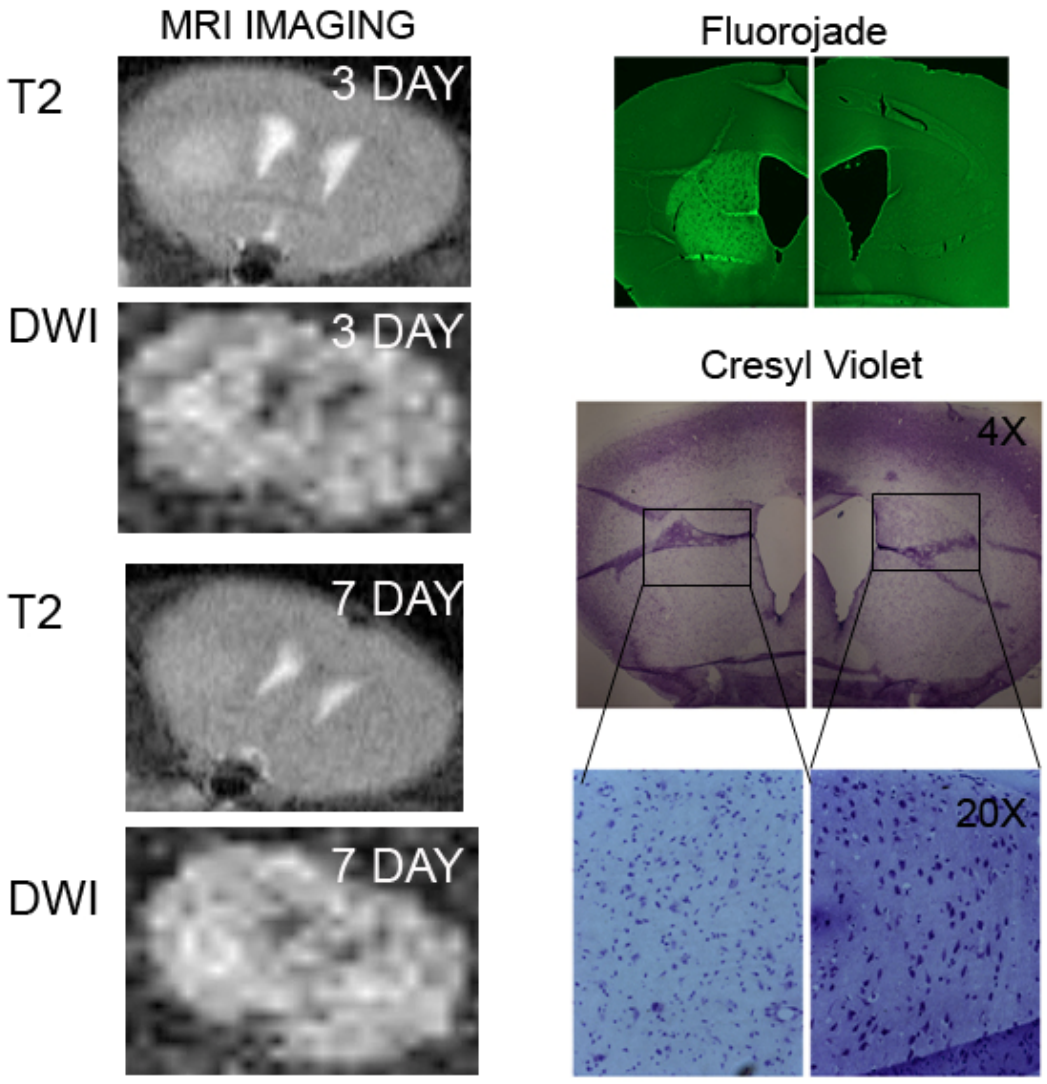

Figure A.1: Representative MRI images of the same BCAO mouse brain showing a decrease in anatomical injury from 3-7 days with T2 scanning. DWI images show increased edema at 3 days reperfusion. At 7 days reperfusion, Fluorojade staining correlates with the region of MRI injury, as well as Cresyl Violet staining identifying cell loss.

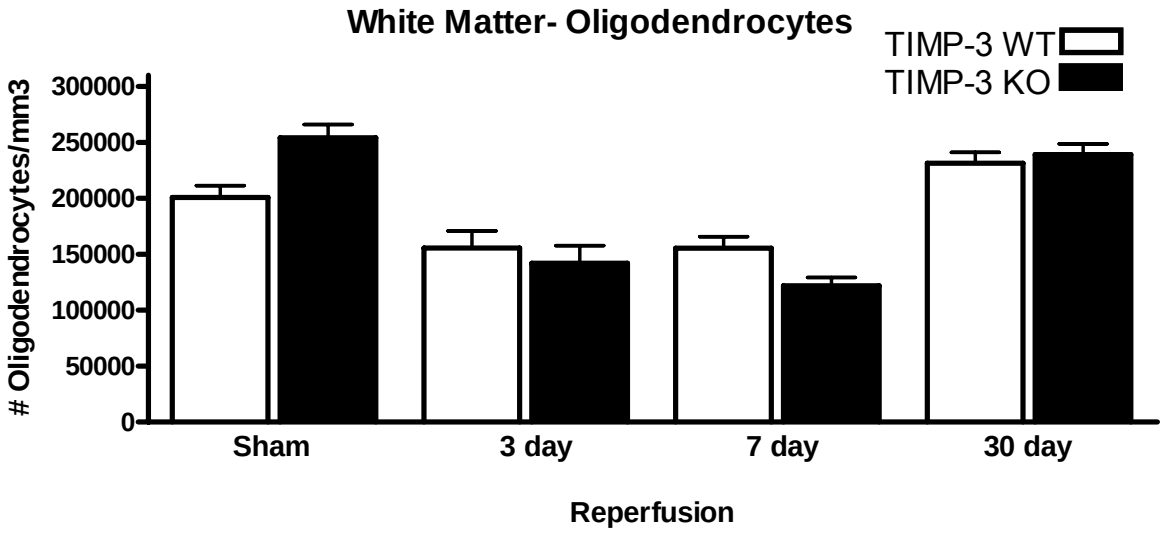

Figure A.2: Oligodendrocyte Stereology of the external capsule in the TIMP-3 WT and TIMP-3 KO mice. There was loss of oligodendrocytes at 3 and 7 days reperfusion in both TIMP-3 WT and TIMP-3 KO mice. Comparison of both strains showed no significant difference at each time point (n=10 to 14).

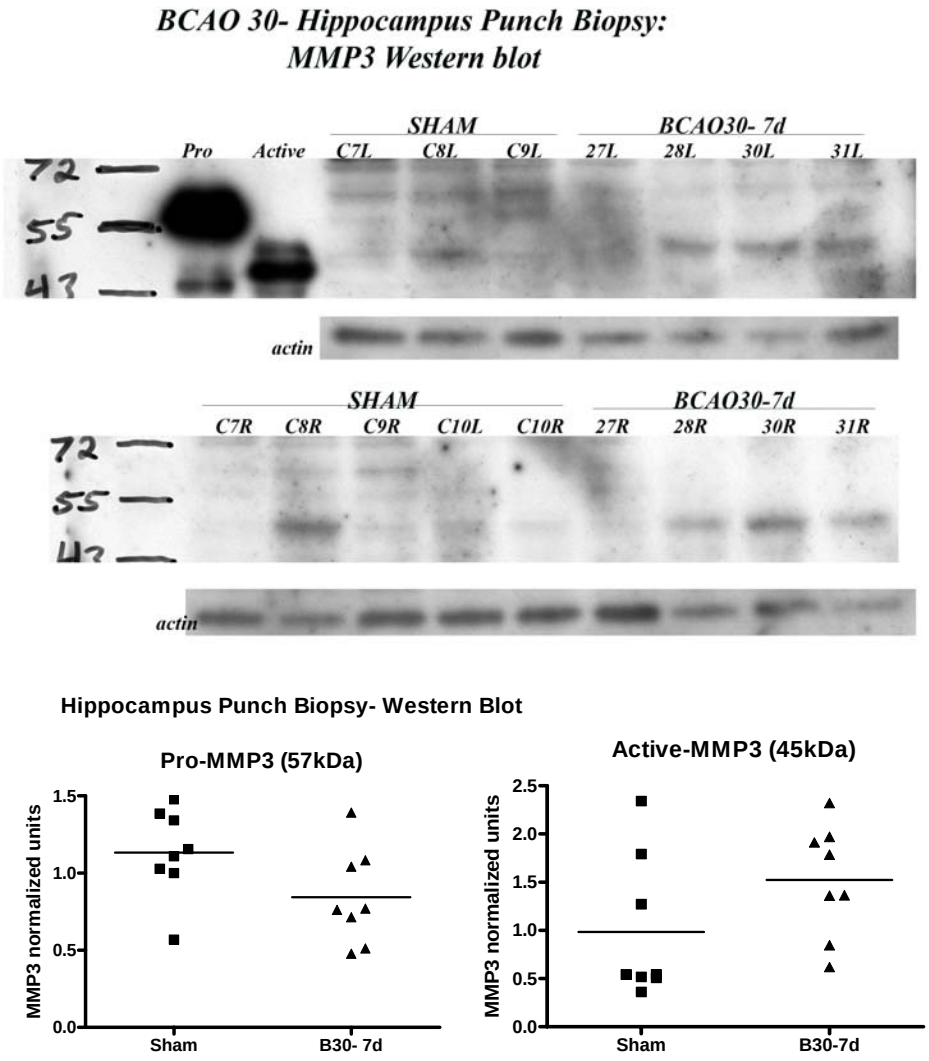

Figure A.3: MMP-3 Western blot of hippocampal tissue demonstrates a non-significant change from pro-MMP-3 (57 kDa) to active MMP-3 (45 kDa). This correlates with the increase in MMP-3 Activity demonstrated in Figure 3.6.

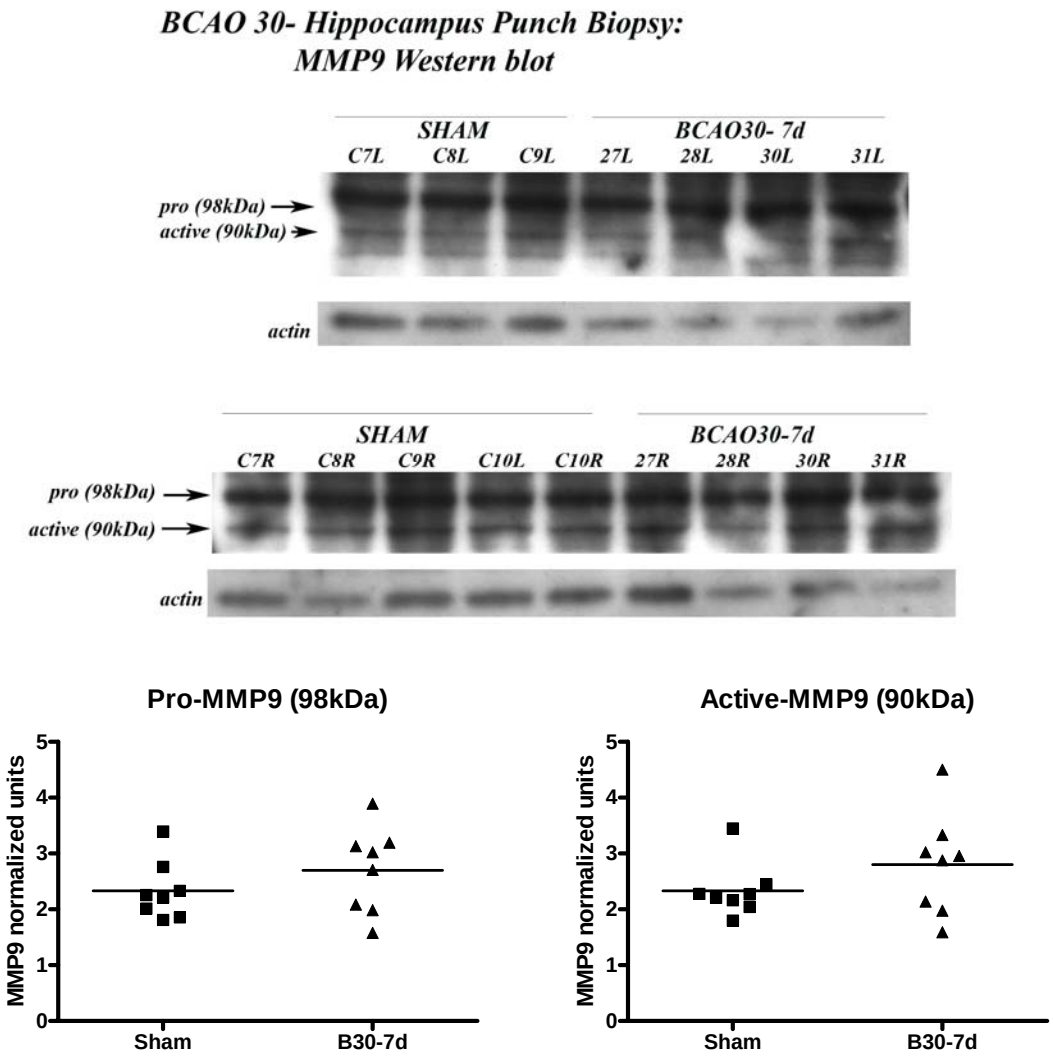

Figure A.4: MMP-9 Western blot of hippocampal tissue demonstrating no difference between Sham and 7 days of reperfusion in both pro MMP-9 (98 kDa) and active MMP-9 (90 kDa).

Hippocampal Injury MMP Inhibition

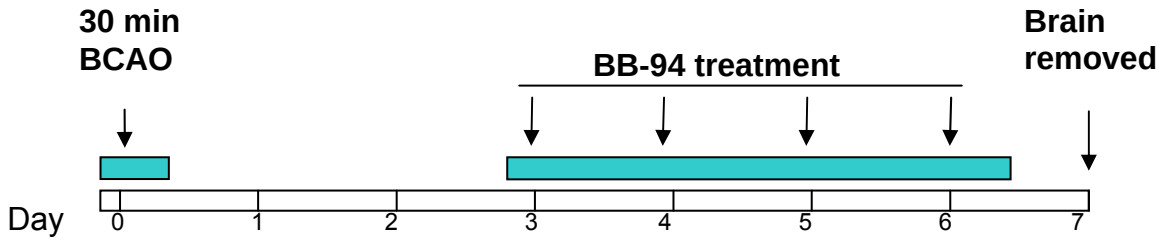

Figure A.5: Delayed MMP inhibition with BB-94 used to protect neuronal loss. 50 mg/kg was administered IP on days 3-6. Treatment timeline for neuronal protection is described in Chapter 3.

White Matter Injury MMP Inhibition

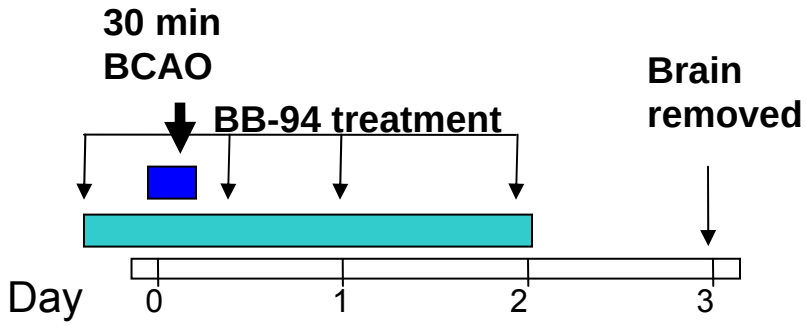

Figure A.6: MMP Inhibition with BB-94 was used to protect myelin loss. 50 mg/kg was administered IP 30 minutes before, 2 hours after, and once daily up to day 3. Treatment timeline for white matter injury is described in Chapter 5.

REFERENCES

1. Amour, A., Slocombe, P. M., Webster, A., Butler, M., Knight, C. G., Smith, B. J., Stephens, P. E., Shelley, C., Hutton, M., Knauper, V., Docherty, A. J., and Murphy, G., 1998. TNF-alpha converting enzyme (TACE) is inhibited by TIMP-3. FEBS Letters 435**,** 39-44.
2. Asahi, M., Asahi, K., Jung, J. C., del Zoppo, G. J., Fini, M. E., and Lo, E. H., 2000. Role for matrix metalloproteinase 9 after focal cerebral ischemia: effects of gene knockout and enzyme inhibition with BB-94. J. Cereb. Blood Flow Metab. 20**,** 1681-1689.
3. Asahi, M., Sumii, T., Fini, M. E., Itohara, S., and Lo, E. H., 2001. Matrix metalloproteinase 2 gene knockout has no effect on acute brain injury after focal ischemia. Neuroreport 12**,** 3003-3007.
4. Asahi, M., Wang, X., Mori, T., Sumii, T., Jung, J. C., Moskowitz, M. A., Fini, M. E., and Lo, E. H., 2001. Effects of matrix metalloproteinase-9 gene knock-out on the proteolysis of blood-brain barrier and white matter components after cerebral ischemia. J.Neurosci. 21**,** 7724-7732.
5. Back, S. A., Riddle, A., and McClure, M. M., 2007. Maturation-dependent vulnerability of perinatal white matter in premature birth. Stroke 38**,** 724-730.
6. Back, T., Hemmen, T., and Schuler, O. G., 2004. Lesion evolution in cerebral ischemia. J. Neurol. 251**,** 388-397.
7. Bakiri, Y., Hamilton, N. B., Karadottir, R., and Attwell, D., 2008. Testing NMDA receptor block as a therapeutic strategy for reducing ischaemic damage to CNS white matter. Glia 56**,** 233-240.
8. Barnett, M. H., Henderson, A. P., and Prineas, J. W., 2006. The macrophage in MS: just a scavenger after all? Pathology and pathogenesis of the acute MS lesion. Mult Scler 12**,** 121-132.
9. Barnett, M. H., and Prineas, J. W., 2004. Relapsing and remitting multiple sclerosis: pathology of the newly forming lesion. Ann.Neurol. 55**,** 458-468.
10. Barradas, P. C., and Cavalcante, L. A., 1998. Proliferation of differentiated glial cells in the brain stem. Braz J Med Biol Res 31**,** 257-270.
11. Behar, T. N., 2001. Analysis of fractal dimension of O2A glial cells differentiating in vitro. Methods 24**,** 331-339.
12. Bhat, R. V., Axt, K. J., Fosnaugh, J. S., Smith, K. J., Johnson, K. A., Hill, D. E., Kinzler, K. W., and Baraban, J. M., 1996. Expression of the APC tumor suppressor protein in oligodendroglia. Glia 17**,** 169-174.
13. Bongarzone, E. R., Howard, S. G., Schonmann, V., and Campagnoni, A. T., 1998. Identification of the dopamine D3 receptor in oligodendrocyte precursors: potential role in regulating differentiation and myelin formation. J Neurosci 18**,** 5344-5353.
14. Bottiger, B. W., Schmitz, B., Wiessner, C., Vogel, P., and Hossmann, K. A., 1998. Neuronal stress response and neuronal cell damage after cardiocirculatory arrest in rats. J Cereb Blood Flow Metab 18**,** 1077-1087.
15. Brew, K., Dinakarpandian, D., and Nagase, H., 2000. Tissue inhibitors of metalloproteinases: evolution, structure and function. Biochim.Biophys.Acta 1477**,** 267-283.

16. Cauwe, B., Van den Steen, P. E., and Opdenakker, G., 2007. The biochemical, biological, and pathological kaleidoscope of cell surface substrates processed by matrix metalloproteinases. Crit Rev Biochem Mol Biol 42**,** 113-185.
17. Chandler, S., Coates, R., Gearing, A., Lury, J., Wells, G., and Bone, E., 1995. Matrix metalloproteinases degrade myelin basic protein. Neuroscience Letters 201**,** 223-226.
18. Chen, J., Nagayama, T., Jin, K., Stetler, R. A., Zhu, R. L., Graham, S. H., and Simon, R. P., 1998. Induction of caspase-3-like protease may mediate delayed neuronal death in the hippocampus after transient cerebral ischemia. J. Neurosci. 18**,** 4914-4928.
19. Cho, J. Y., Kim, I. S., Jang, Y. H., Kim, A. R., and Lee, S. R., 2006. Protective effect of quercetin, a natural flavonoid against neuronal damage after transient global cerebral ischemia. Neurosci. Lett. 404**,** 330-335.
20. Choi, D. H., Kim, E. M., Son, H. J., Joh, T. H., Kim, Y. S., Kim, D., Flint Beal, M., and Hwang, O., 2008. A novel intracellular role of matrix metalloproteinase-3 during apoptosis of dopaminergic cells. J. Neurochem. 106**,** 405-415.
21. Copin, J. C., and Gasche, Y., 2007. Matrix metalloproteinase-9 deficiency has no effect on glial scar formation after transient focal cerebral ischemia in mouse. Brain Res 1150**,** 167-173.
22. Crocker, S. J., Milner, R., Pham-Mitchell, N., and Campbell, I. L., 2006. Cell and agonist-specific regulation of genes for matrix metalloproteinases and their tissue inhibitors by primary glial cells. J. Neurochem. 98**,** 812-823.
23. Crocker, S. J., Pagenstecher, A., and Campbell, I. L., 2004. The TIMPs tango with MMPs and more in the central nervous system. J. Neurosci. Res. 75**,** 1-11.
24. Cunningham, L. A., Wetzel, M., and Rosenberg, G. A., 2005. Multiple roles for MMPs and TIMPs in cerebral ischemia. Glia 50**,** 329-339.
25. D'Souza, C. A., Mak, B., and Moscarello, M. A., 2002. The up-regulation of stromelysin-1 (MMP-3) in a spontaneously demyelinating transgenic mouse precedes onset of disease. J. Biol. Chem. 277**,** 13589-13596.
26. D'Souza, C. A., and Moscarello, M. A., 2006. Differences in susceptibility of MBP charge isomers to digestion by stromelysin-1 (MMP-3) and release of an immunodominant epitope. Neurochem Res 31**,** 1045-1054.
27. Deierborg, T., Wieloch, T., Diano, S., Warden, C. H., Horvath, T. L., and Mattiasson, G., 2008. Overexpression of UCP2 protects thalamic neurons following global ischemia in the mouse. J. Cereb. Blood Flow Metab. 28**,** 1186–1195.
28. Dewar, D., and Dawson, D., 1995. Tau protein is altered by focal cerebral ischaemia in the rat: an immunohistochemical and immunoblotting study. Brain Res 684**,** 70-78.
29. Dewar, D., Underhill, S. M., and Goldberg, M. P., 2003. Oligodendrocytes and ischemic brain injury. J Cereb Blood Flow Metab 23**,** 263-274.
30. Drynda, A., Quax, P. H., Neumann, M., van der Laan, W. H., Pap, G., Drynda, S., Meinecke, I., Kekow, J., Neumann, W., Huizinga, T. W., Naumann, M., Konig, W., and Pap, T., 2005. Gene transfer of tissue inhibitor of metalloproteinases-3 reverses the inhibitory effects of TNF-alpha on Fas-induced apoptosis in rheumatoid arthritis synovial fibroblasts. J. Immunol. 174**,** 6524-6531.

31. Farkas, E., Donka, G., de Vos, R. A., Mihaly, A., Bari, F., and Luiten, P. G., 2004. Experimental cerebral hypoperfusion induces white matter injury and microglial activation in the rat brain. Acta Neuropathol (Berl). 108**,** 57-64.
32. Farkas, E., Luiten, P. G., and Bari, F., 2007. Permanent, bilateral common carotid artery occlusion in the rat: A model for chronic cerebral hypoperfusion-related neurodegenerative diseases. Brain Res.Brain Res.Rev.
33. Foote, A. K., and Blakemore, W. F., 2005. Inflammation stimulates remyelination in areas of chronic demyelination. Brain 128**,** 528-539.
34. Friedman, B., Hockfield, S., Black, J. A., Woodruff, K. A., and Waxman, S. G., 1989. In situ demonstration of mature oligodendrocytes and their processes: an immunocytochemical study with a new monoclonal antibody, rip. Glia 2**,** 380-390.
35. Garcia-Marin, V., Garcia-Lopez, P., and Freire, M., 2007. Cajal's contributions to glia research. Trends Neurosci 30**,** 479-487.
36. Gearing, A. J., Beckett, P., Christodoulou, M., Churchill, M., Clements, J., Davidson, A. H., Drummond, A. H., Galloway, W. A., Gilbert, R., Gordon, J. L., and et al., 1994. Processing of tumour necrosis factor-alpha precursor by metalloproteinases. Nature 370**,** 555-557.
37. Gijbels, K., Proost, P., Masure, S., Carton, H., Billiau, A., and Opdenakker, G., 1993. Gelatinase B is present in the cerebrospinal fluid during experimental autoimmune encephalomyelitis and cleaves myelin basic protein. J.Neurosci.Res. 36**,** 432-440.
38. Ginsberg, M. D., and Busto, R., 1989. Rodent models of cerebral ischemia. Stroke 20**,** 1627-1642.
39. Goldberg, M. P., and Ransom, B. R., 2003. New light on white matter. Stroke 34**,** 330-332.
40. Gu, Z., Kaul, M., Yan, B., Kridel, S. J., Cui, J., Strongin, A., Smith, J. W., Liddington, R. C., and Lipton, S. A., 2002. S-nitrosylation of matrix metalloproteinases: signaling pathway to neuronal cell death. Science 297**,** 1186-1190.
41. Gurney, K. J., Estrada, E. Y., and Rosenberg, G. A., 2006. Blood-brain barrier disruption by stromelysin-1 facilitates neutrophil infiltration in neuroinflammation. Neurobiol. Dis. 23**,** 87-96.
42. Hagberg, H., Peebles, D., and Mallard, C., 2002. Models of white matter injury: comparison of infectious, hypoxic-ischemic, and excitotoxic insults. Ment Retard Dev Disabil Res Rev 8**,** 30-38.
43. Harukuni, I., and Bhardwaj, A., 2006. Mechanisms of brain injury after global cerebral ischemia. Neurol. Clin. 24**,** 1-21.
44. Hauser, S. L., and Oksenberg, J. R., 2006. The neurobiology of multiple sclerosis: genes, inflammation, and neurodegeneration. Neuron 52**,** 61-76.
45. Hisahara, S., Okano, H., and Miura, M., 2003. Caspase-mediated oligodendrocyte cell death in the pathogenesis of autoimmune demyelination. Neurosci Res. 46**,** 387-397.
46. Ihara, M., Tomimoto, H., Kinoshita, M., Oh, J., Noda, M., Wakita, H., Akiguchi, I., and Shibasaki, H., 2001. Chronic cerebral hypoperfusion induces MMP-2 but

not MMP-9 expression in the microglia and vascular endothelium of white matter. J.Cereb.Blood Flow Metab 21, 828-834.
47. Irving, E. A., Bentley, D. L., and Parsons, A. A., 2001. Assessment of white matter injury following prolonged focal cerebral ischaemia in the rat. Acta Neuropathol 102, 627-635.
48. Irving, E. A., Yatsushiro, K., McCulloch, J., and Dewar, D., 1997. Rapid alteration of tau in oligodendrocytes after focal ischemic injury in the rat: involvement of free radicals. J Cereb Blood Flow Metab 17, 612-622.
49. Jamin, N., Junier, M. P., Grannec, G., and Cadusseau, J., 2001. Two temporal stages of oligodendroglial response to excitotoxic lesion in the gray matter of the adult rat brain. Exp Neurol 172, 17-28.
50. Kadhim, H., Khalifa, M., Deltenre, P., Casimir, G., and Sebire, G., 2006. Molecular mechanisms of cell death in periventricular leukomalacia. Neurology. 67, 293-299.
51. Kelly, S., McCulloch, J., and Horsburgh, K., 2001. Minimal ischaemic neuronal damage and HSP70 expression in MF1 strain mice following bilateral common carotid artery occlusion. Brain Res 914, 185-195.
52. Kiaei, M., Kipiani, K., Calingasan, N. Y., Wille, E., Chen, J., Heissig, B., Rafii, S., Lorenzl, S., and Beal, M. F., 2007. Matrix metalloproteinase-9 regulates TNF-alpha and FasL expression in neuronal, glial cells and its absence extends life in a transgenic mouse model of amyotrophic lateral sclerosis. Exp Neurol 205, 74-81.
53. Kim, Y. S., Kim, S. S., Cho, J. J., Choi, D. H., Hwang, O., Shin, D. H., Chun, H. S., Beal, M. F., and Joh, T. H., 2005. Matrix metalloproteinase-3: a novel signaling proteinase from apoptotic neuronal cells that activates microglia. J. Neurosci. 25, 3701-3711.
54. Kobayashi, H., Chattopadhyay, S., Kato, K., Dolkas, J., Kikuchi, S., Myers, R. R., and Shubayev, V. I., 2008. MMPs initiate Schwann cell-mediated MBP degradation and mechanical nociception after nerve damage. Mol Cell Neurosci 39, 619-627.
55. Kokovay, E., Li, L., and Cunningham, L. A., 2006. Angiogenic recruitment of pericytes from bone marrow after stroke. J Cereb.Blood Flow Metab 26, 545-555.
56. Kuhlmann, T., Remington, L., Maruschak, B., Owens, T., and Bruck, W., 2007. Nogo-A is a reliable oligodendroglial marker in adult human and mouse CNS and in demyelinated lesions. J Neuropathol Exp Neurol 66, 238-246.
57. Kumaran, D., Udayabanu, M., Nair, R. U., R, A., and Katyal, A., 2008. Benzamide protects delayed neuronal death and behavioural impairment in a mouse model of global cerebral ischemia. Behav. Brain Res. 192, 178-184.
58. Larsen, P. H., DaSilva, A. G., Conant, K., and Yong, V. W., 2006. Myelin formation during development of the CNS is delayed in matrix metalloproteinase-9 and -12 null mice. J Neurosci 26, 2207-2214.
59. Lee, J. H., Park, S. Y., Shin, Y. W., Hong, K. W., Kim, C. D., Sung, S. M., Kim, K. Y., and Lee, W. S., 2006. Neuroprotection by cilostazol, a phosphodiesterase type 3 inhibitor, against apoptotic white matter changes in rat after chronic cerebral hypoperfusion. Brain Res. 1082, 182-191.
60. Lee, J. K., Shin, J. H., Suh, J., Choi, I. S., Ryu, K. S., and Gwag, B. J., 2008. Tissue inhibitor of metalloproteinases-3 (TIMP-3) expression is increased during

serum deprivation-induced neuronal apoptosis in vitro and in the G93A mouse model of amyotrophic lateral sclerosis: a potential modulator of Fas-mediated apoptosis. Neurobiol. Dis. 30, 174-185.

61. Lee, S. R., and Lo, E. H., 2004. Induction of caspase-mediated cell death by matrix metalloproteinases in cerebral endothelial cells after hypoxia-reoxygenation. J Cereb Blood Flow Metab 24, 720-727.
62. Lee, S. R., Lok, J., Rosell, A., Kim, H. Y., Murata, Y., Atochin, D., Huang, P. L., Wang, X., Ayata, C., Moskowitz, M. A., and Lo, E. H., 2007. Reduction of hippocampal cell death and proteolytic responses in tissue plasminogen activator knockout mice after transient global cerebral ischemia. Neuroscience 150, 50-57.
63. Lee, S. R., Tsuji, K., Lee, S. R., and Lo, E. H., 2004. Role of matrix metalloproteinases in delayed neuronal damage after transient global cerebral ischemia. J. Neurosci. 24, 671-678.
64. Leroy, K., Duyckaerts, C., Bovekamp, L., Muller, O., Anderton, B. H., and Brion, J. P., 2001. Increase of adenomatous polyposis coli immunoreactivity is a marker of reactive astrocytes in Alzheimer's disease and in other pathological conditions. Acta Neuropathol 102, 1-10.
65. Liu, W., Furuichi, T., Miyake, M., Rosenberg, G. A., and Liu, K. J., 2007. Differential expression of tissue inhibitor of metalloproteinases-3 in cultured astrocytes and neurons regulates the activation of matrix metalloproteinase-2. J. Neurosci. Res. 85, 829-836.
66. Lo, E. H., Dalkara, T., and Moskowitz, M. A., 2003. Mechanisms, challenges and opportunities in stroke. Nat. Rev. Neurosci. 4, 399-415.
67. Longa, E. Z., Weinstein, P. R., Carlson, S., and Cummins, R., 1989. Reversible middle cerebral artery occlusion without craniectomy in rats. Stroke 20, 84-91.
68. Magnoni, S., Baker, A., George, S. J., Duncan, W. C., Kerr, L. E., McCulloch, J., and Horsburgh, K., 2004. Differential alterations in the expression and activity of matrix metalloproteinases 2 and 9 after transient cerebral ischemia in mice. Neurobiol. Dis. 17, 188-197.
69. Masumura, M., Hata, R., Nagai, Y., and Sawada, T., 2001. Oligodendroglial cell death with DNA fragmentation in the white matter under chronic cerebral hypoperfusion: comparison between normotensive and spontaneously hypertensive rats. Neurosci.Res. 39, 401-412.
70. Merrill, J. E., and Scolding, N. J., 1999. Mechanisms of damage to myelin and oligodendrocytes and their relevance to disease. Neuropathol Appl Neurobiol 25, 435-458.
71. Miller, A. K., Alston, R. L., and Corsellis, J. A., 1980. Variation with age in the volumes of grey and white matter in the cerebral hemispheres of man: measurements with an image analyser. Neuropathol Appl Neurobiol 6, 119-132.
72. Mills, S. E., 2007. Histology for Pathologists. Lippincott Williams and Wilkins, Philadelphia, PA.
73. Mun-Bryce, S., Lukes, A., Wallace, J., Lukes-Marx, M., and Rosenberg, G. A., 2002. Stromelysin-1 and gelatinase A are upregulated before TNF-alpha in LPS-stimulated neuroinflammation. Brain Res. 933, 42-49.
74. Nagase, H., 1997. Activation mechanisms of matrix metalloproteinases. [Review]. Biological Chemistry 378, 151-160.

75. Nagase, H., and Woessner, J. F., Jr., 1999. Matrix metalloproteinases. [Review]. Journal of Biological Chemistry 274**,** 21491-21494.
76. Nakaji, K., Ihara, M., Takahashi, C., Itohara, S., Noda, M., Takahashi, R., and Tomimoto, H., 2006. Matrix metalloproteinase-2 plays a critical role in the pathogenesis of white matter lesions after chronic cerebral hypoperfusion in rodents. Stroke. 37**,** 2816-2823.
77. Oguro, K., Jover, T., Tanaka, H., Lin, Y., Kojima, T., Oguro, N., Grooms, S. Y., Bennett, M. V., and Zukin, R. S., 2001. Global ischemia-induced increases in the gap junctional proteins connexin 32 (Cx32) and Cx36 in hippocampus and enhanced vulnerability of Cx32 knock-out mice. J. Neurosci. 21**,** 7534-7542.
78. Oh, L. Y., Larsen, P. H., Krekoski, C. A., Edwards, D. R., Donovan, F., Werb, Z., and Yong, V. W., 1999. Matrix metalloproteinase-9/gelatinase B is required for process outgrowth by oligodendrocytes. J Neurosci 19**,** 8464-8475.
79. Pantoni, L., Garcia, J. H., and Gutierrez, J. A., 1996. Cerebral white matter is highly vulnerable to ischemia. Stroke 27**,** 1641-1646.
80. Park, E., Velumian, A. A., and Fehlings, M. G., 2004. The role of excitotoxicity in secondary mechanisms of spinal cord injury: a review with an emphasis on the implications for white matter degeneration. J Neurotrauma 21**,** 754-774.
81. Peters, A., Palay, S. L., and Webster, H. D., 1991. The Fine Structure of the Nervous System: Neurons and their Supporting Cells. Oxford University Press, New York.
82. Petito, C. K., Olarte, J. P., Roberts, B., Nowak, T. S., Jr., and Pulsinelli, W. A., 1998. Selective glial vulnerability following transient global ischemia in rat brain. J Neuropathol Exp Neurol 57**,** 231-238.
83. Petty, M. A., and Wettstein, J. G., 1999. White matter ischaemia. Brain Res Brain Res Rev 31**,** 58-64.
84. Pulsinelli, W. A., 1985. Selective neuronal vulnerability: morphological and molecular characteristics. Prog Brain Res 63**,** 29-37.
85. Pulsinelli, W. A., and Brierley, J. B., 1979. A new model of bilateral hemispheric ischemia in the unanesthetized rat. Stroke. 10**,** 267-272.
86. Ramon y Cajal, S., 1896. Sobre las relaciones de las celulas nerviosas con las neuroglicas. Revista Trimestral Micrografica 1**,** 38-41.
87. Rinaldi, L., and Gallo, P., 2005. Immunological markers in multiple sclerosis: tackling the missing elements. Neurol Sci 26 Suppl 4**,** S215-217.
88. Rio-Hortega, P. d., 1921. Estudios sobre la neuroglia. La glia de escasas radiacciones (oligodendroglia). Bol. Soc. Esp. Hist. Nat. 10**,** 63-92.
89. Rio-Hortega, P. d., 1942. La neuroglia normal- Conceptos de angiogliona y neurogliona. Archivos de Histologia Normal y Patologica 1**,** 5-72.
90. Rivera, S., Ogier, C., Jourquin, J., Timsit, S., Szklarczyk, A. W., Miller, K., Gearing, A. J., Kaczmarek, L., and Khrestchatisky, M., 2002. Gelatinase B and TIMP-1 are regulated in a cell- and time-dependent manner in association with neuronal death and glial reactivity after global forebrain ischemia. Eur.J.Neurosci. 15**,** 19-32.
91. Rosenberg, G. A., 2002. Matrix metalloproteinases and neuroinflammation in multiple sclerosis. Neuroscientist. 8**,** 586-595.

92. Rosenberg, G. A., 2002. Matrix metalloproteinases in neuroinflammation. Glia 39, 279-291.
93. Rosenberg, G. A., 2009. Matrix metalloproteinases and their multiple roles in neurodegenerative diseases. Lancet Neurol 8, 205-216.
94. Rosenberg, G. A., Cunningham, L. A., Wallace, J., Alexander, S., Estrada, E. Y., Grossetete, M., Razhagi, A., Miller, K., and Gearing, A., 2001. Immunohistochemistry of matrix metalloproteinases in reperfusion injury to rat brain: activation of MMP-9 linked to stromelysin-1 and microglia in cell cultures. Brain Res. 893, 104-112.
95. Rosenberg, G. A., Sullivan, N., and Esiri, M. M., 2001. White matter damage is assoiciated with matrix metalloproteinases in vascular dementia. Stroke 32, 1162-1168.
96. Salter, M. G., and Fern, R., 2005. NMDA receptors are expressed in developing oligodendrocyte processes and mediate injury. Nature 438, 1167-1171.
97. Satoh, J., Onoue, H., Arima, K., and Yamamura, T., 2005. Nogo-A and nogo receptor expression in demyelinating lesions of multiple sclerosis. J Neuropathol Exp Neurol 64, 129-138.
98. Schmidt-Kastner, R., Aguirre-Chen, C., Saul, I., Yick, L., Hamasaki, D., Busto, R., and Ginsberg, M. D., 2005. Astrocytes react to oligemia in the forebrain induced by chronic bilateral common carotid artery occlusion in rats. Brain Res 1052, 28-39.
99. Schmitz, T., and Chew, L. J., 2008. Cytokines and myelination in the central nervous system. ScientificWorldJournal 8, 1119-1147.
100. Scott, G. S., Virag, L., Szabo, C., and Hooper, D. C., 2003. Peroxynitrite-induced oligodendrocyte toxicity is not dependent on poly(ADP-ribose) polymerase activation. Glia 41, 105-116.
101. Shibata, M., Ohtani, R., Ihara, M., and Tomimoto, H., 2004. White matter lesions and glial activation in a novel mouse model of chronic cerebral hypoperfusion. Stroke 35, 2598-2603.
102. Smith, M. R., Kung, H., Durum, S. K., Colburn, N. H., and Sun, Y., 1997. TIMP-3 induces cell death by stabilizing TNF-alpha receptors on the surface of human colon carcinoma cells. Cytokine 9, 770-780.
103. Smookler, D. S., Mohammed, F. F., Kassiri, Z., Duncan, G. S., Mak, T. W., and Khokha, R., 2006. Tissue inhibitor of metalloproteinase 3 regulates TNF-dependent systemic inflammation. J. Immunol. 176, 721-725.
104. Sugawara, T., Lewen, A., Noshita, N., Gasche, Y., and Chan, P. H., 2002. Effects of global ischemia duration on neuronal, astroglial, oligodendroglial, and microglial reactions in the vulnerable hippocampal CA1 subregion in rats. J Neurotrauma 19, 85-98.
105. Tekkok, S. B., Ye, Z., and Ransom, B. R., 2007. Excitotoxic mechanisms of ischemic injury in myelinated white matter. J Cereb Blood Flow Metab 27, 1540-1552.
106. Terashima, T., Namura, S., Hoshimaru, M., Uemura, Y., Kikuchi, H., and Hashimoto, N., 1998. Consistent injury in the striatum of C57BL/6 mice after transient bilateral common carotid artery occlusion. Neurosurgery 43, 900-907; discussion 907-908.

107. Terayama, R., Bando, Y., Murakami, K., Kato, K., Kishibe, M., and Yoshida, S., 2007. Neuropsin promotes oligodendrocyte death, demyelination and axonal degeneration after spinal cord injury. Neuroscience 148**,** 175-187.
108. Tomimoto, H., Ihara, M., Wakita, H., Ohtani, R., Lin, J. X., Akiguchi, I., Kinoshita, M., and Shibasaki, H., 2003. Chronic cerebral hypoperfusion induces white matter lesions and loss of oligodendroglia with DNA fragmentation in the rat. Acta Neuropathol (Berl) 106**,** 527-534.
109. Traystman, R. J., 2003. Animal models of focal and global cerebral ischemia. ILAR J 44**,** 85-95.
110. Valeriani, V., Dewar, D., and McCulloch, J., 2000. Quantitative assessment of ischemic pathology in axons, oligodendrocytes, and neurons: attenuation of damage after transient ischemia. J Cereb Blood Flow Metab 20**,** 765-771.
111. Wakita, H., Tomimoto, H., Akiguchi, I., Matsuo, A., Lin, J. X., Ihara, M., and McGeer, P. L., 2002. Axonal damage and demyelination in the white matter after chronic cerebral hypoperfusion in the rat. Brain Res. 924**,** 63-70.
112. Walker, E. J., and Rosenberg, G. A., 2009. TIMP-3 and MMP-3 contribute to delayed inflammation and hippocampal neuronal death following global ischemia. Exp Neurol.
113. Wallace, J. A., Alexander, S., Estrada, E. Y., Hines, C., Cunningham, L. A., and Rosenberg, G. A., 2002. Tissue inhibitor of metalloproteinase-3 is associated with neuronal death in reperfusion injury. J. Cereb. Blood Flow Metab. 22**,** 1303-1310.
114. Wei, S., Kashiwagi, M., Kota, S., Xie, Z., Nagase, H., and Brew, K., 2005. Reactive site mutations in tissue inhibitor of metalloproteinase-3 disrupt inhibition of matrix metalloproteinases but not tumor necrosis factor-alpha-converting enzyme. J. Biol. Chem. 280**,** 32877-32882.
115. Wetzel, M., Li, L., Harms, K. M., Roitbak, T., Ventura, P. B., Rosenberg, G. A., Khokha, R., and Cunningham, L. A., 2007. Tissue inhibitor of metalloproteinases-3 facilitates Fas-mediated neuronal cell death following mild ischemia. Cell Death Differ.
116. Wetzel, M., Li, L., Harms, K. M., Roitbak, T., Ventura, P. B., Rosenberg, G. A., Khokha, R., and Cunningham, L. A., 2008. Tissue inhibitor of metalloproteinases-3 facilitates Fas-mediated neuronal cell death following mild ischemia. Cell Death Differ. 15**,** 143-151.
117. Wetzel, M., Rosenberg, G. A., and Cunningham, L. A., 2003. Tissue inhibitor of metalloproteinases-3 and matrix metalloproteinase-3 regulate neuronal sensitivity to doxorubicin-induced apoptosis. Eur. J. Neurosci. 18**,** 1050-1060.
118. Wetzel, M., Tibbitts, J., Rosenberg, G. A., and Cunningham, L. A., 2004. Vulnerability of mouse cortical neurons to doxorubicin-induced apoptosis is strain-dependent and is correlated with mRNAs encoding Fas, Fas-Ligand, and metalloproteinases. Apoptosis. 9**,** 649-656.
119. Will, H., Atkinson, S. J., Butler, G. S., Smith, B., and Murphy, G., 1996. The soluble catalytic domain of membrane type 1 matrix metalloproteinase cleaves the propeptide of progelatinase A and initiates autoproteolytic activation. Regulation by TIMP-2 and TIMP-3. J. Biol. Chem. 271**,** 17119-17123.
120. Wolswijk, G., 2000. Oligodendrocyte survival, loss and birth in lesions of chronic-stage multiple sclerosis. Brain 123 (Pt 1)**,** 105-115.

121. Xanthoulea, S., Pasparakis, M., Kousteni, S., Brakebusch, C., Wallach, D., Bauer, J., Lassmann, H., and Kollias, G., 2004. Tumor necrosis factor (TNF) receptor shedding controls thresholds of innate immune activation that balance opposing TNF functions in infectious and inflammatory diseases. J. Exp. Med. 200**,** 367-376.
122. Yang, G., Kitagawa, K., Matsushita, K., Mabuchi, T., Yagita, Y., Yanagihara, T., and Matsumoto, M., 1997. C57BL/6 strain is most susceptible to cerebral ischemia following bilateral common carotid occlusion among seven mouse strains: selective neuronal death in the murine transient forebrain ischemia. Brain Res 752**,** 209-218.
123. Yong, V. W., 2005. Metalloproteinases: mediators of pathology and regeneration in the CNS. Nat.Rev.Neurosci 6**,** 931-944.
124. Yong, V. W., Power, C., Forsyth, P., and Edwards, D. R., 2001. Metalloproteinases in biology and pathology of the nervous system. Nat.Rev.Neurosci. 2**,** 502-511.
125. Yoshioka, A., Yamaya, Y., Saiki, S., Kanemoto, M., Hirose, G., Beesley, J., and Pleasure, D., 2000. Non-N-methyl-D-aspartate glutamate receptors mediate oxygen--glucose deprivation-induced oligodendroglial injury. Brain Res 854**,** 207-215.
126. Zalewska, T., Ziemka-Nalecz, M., Sarnowska, A., and Domanska-Janik, K., 2002. Involvement of MMPs in delayed neuronal death after global ischemia. Acta Neurobiol. Exp. (Wars) 62**,** 53-61.
127. Zhao, B. Q., Wang, S., Kim, H. Y., Storrie, H., Rosen, B. R., Mooney, D. J., Wang, X., and Lo, E. H., 2006. Role of matrix metalloproteinases in delayed cortical responses after stroke. Nat. Med. 12**,** 441-445.